

**KINETIC AND DYNAMIC EFFECTS OF INTESTINAL PEPT1 ON THE
BACTERIALLY-PRODUCED CHEMOTACTIC PEPTIDE FMET-LEU-PHE
AND THE ANTI-INFLAMMATORY PEPTIDE LYS-PRO-VAL**

by

Shu-Pei Wu

A dissertation submitted in partial fulfillment
of the requirements for the degree of
Doctor of Philosophy
(Pharmaceutical Sciences)
in The University of Michigan
2011

Doctoral Committee:

Professor David E. Smith, Chair
Professor Gordon L. Amidon
Associate Professor Duxin Sun
Associate Professor Ellen M. Zimmermann

© Shu-Pei Wu
2011

DEDICATION

To my parents

Mrs. Mei-Hsiu Lee Wu

Mr. Sho-Fu Wu

To my beloved wife Szu-Yuan Chen

For all of your support and love

ACKNOWLEDGEMENTS

First, I would like to thank my advisor, Dr. David E. Smith, for his mentoring in scientific research and in helping me to learn how to perform science independently. I also want to thank all my committee members: Dr. Gordon L. Amidon, Dr. Duxin Sun, and Dr. Ellen M. Zimmermann for their suggestions and comments on my research, and for allowing me to view and think about science from different angles. In addition, I appreciate Dr. Rose Feng for her kindness and instruction in computational modeling, and in providing me an extension of my research.

I want to thank all the members in Dr. Smith's laboratory: Yongjun Hu, Maria M. Posada, Bei Yang, Yeamin Huh, Yehua Xie, Dr. Ke Ma, Dr. Naoki Nishio, and Dr. Huidi Jiang for all their help in the laboratory. Especially, I would like to thank Judy Opp in Dr. Vincent Young's laboratory for her generous help in providing animal samples and experimental advice.

I want to express my sincere gratitude to my friends and all the staff in the College of Pharmacy: Jason Baik, Juhee Lee, Nan Zheng, Lindsay White, Cara Hartz Nelson, and Chinmay Maheshwari for their friendship during the long journey of Ph.D.; Lynn Alexander, Terri Azar, Jeanne Getty, Maria Herbel, Pat Greeley, L.D. Hieber for all their support and help in things that are harder than scientific research, the things of regular basis, thereby allowing me to focus more on my studies. Also, I appreciate the many types of financial support that allowed me to fulfill my Ph.D. journey.

Last, but not least, I would like to thank my parents for their love and support from Taiwan. To my lovely wife, Szu-Yuan Chen, and my angel-like son, Max P. Wu, you are always my strength to face all difficulties. Without you, I could not make it by myself.

TABLE OF CONTENTS

DEDICATION	ii
ACKNOWLEDGEMENTS.....	iii
LIST OF FIGURES	vii
LIST OF TABLES	xii
LIST OF APPENDICES	xiii
ABSTRACT	xiv
Chapter 1.....	1
RESEARCH OBJECTIVES.....	1
Chapter 2.....	5
BACKGROUND AND LITERATURE REVIEW.....	5
PROTON-COUPLED OLIGOPEPTIDE TRANSPORTERS 1	5
INFLAMMATORY BOWEL DISEASE.....	34
REFERENCES.....	44
Chapter 3.....	62
IMPACT OF INTESTINAL PEPT1 ON THE KINETICS AND DYNAMICS OF N-FORMYL- METHIONYL-LEUCYL-PHENYLALANINE (FMET-LEU-PHE), A BACTERIALLY-PRODUCED CHEMOTACTIC PEPTIDE	62
ABSTRACT	62
INTRODUCTION	64
MATERIALS AND METHODS.....	67
RESULTS	74
DISCUSSION	78
FIGURES	83

REFERENCES	93
Chapter 4.....	97
IMPACT OF INTESTINAL PEPT1 ON THE REGIONAL PERMEABILITY OF LYS-PRO-VAL, AN ANTI-INFLAMMATORY TRIPEPTIDE DERIVED FROM α -MELANOCYTE-STIMULATING HORMONE	97
ABSTRACT	97
INTRODUCTION	99
MATERIALS AND METHODS	102
RESULTS	109
DISCUSSION	113
FIGURES	119
REFERENCES	128
APPENDIX A	131
COMPARISON OF THE SUSCEPTIBILITY TO DEXTRAN SODIUM SULFATE BETWEEN WILD-TYPE AND <i>PEPT1</i> KNOCKOUT MICE	131
OBJECTIVE.....	131
MATERIALS AND METHODS.....	131
RESULTS	132
DISCUSSION	135
FIGURES	136
REFERENCES.....	152
APPENDIX B	153
UP-REGULATION OF COLONIC PEPT1 EXPRESSION BY OTHER ALTERNATIVE COLITIS MODELS	153
OBJECTIVE.....	153
MATERIALS AND METHODS	153
RESULTS	153
DISCUSSION	154
FIGURES	155
REFERENCES	157

LIST OF FIGURES

Figure 2.1. Structure template for PEPT1 (Adopted from Bailey et al., 2006).	40
Figure 2.2. Pathway of peptide absorption (Adopted from Daniel et al., 2004).	41
Figure 2.3. Model of the involvement of hPEPT1 in IBD (Adopted from Charrier et al., 2006). ...	42
Figure 3.1. Chromatogram of metabolites of fMet-Leu-Phe after incubation with 1 cm intestinal segments of wild-type mice for 5 min at 37°C and metabolites in the portal vein plasma after <i>in situ</i> perfusion for 90 mins. (A) duodenum (B) jejunum (C) ileum (D) colon (E) portal vein plasma. Phe: phenylalanine, f-Met: formyl-methionine, f-Met-Leu: formyl-methionyl-leucine, fMet-Leu-Phe: N-formyl-methionyl-leucyl-phenylalanine.	83
Figure 3.2. Effective permeability of fMet-Leu-Phe in jejunum of wild-type mice in the presence of phenylalanine at different concentrations (Mean \pm SE, n=3). Groups with different letters represented statistical difference which performed by one-way ANOVA with Tukey's comparison.	84
Figure 3.3. Effective permeability of fMet-Leu-Phe in different intestinal segments of wild-type mice and <i>Pept1</i> knockout mice in the presence of 100 mM phenylalanine (Mean \pm SE, n=6). Groups with different letters represented statistical difference which performed by one-way ANOVA with Tukey's comparison for the same genotype and by t-test between different genotypes for each intestinal segment.	85
Figure 3.4. Gly-Pro (50 mM) inhibited the effective permeability of fMet-Leu-Phe in the jejunum of wild-type mice (A) but not in that of <i>Pept1</i> knockout mice (B) (Mean \pm SE, n=4). L-histidine (50 mM) showed no inhibitory effects in the jejunum of both wild-type and <i>Pept1</i> knockout mice (Mean \pm SE, n=4). Statistical analysis was performed by one-way ANOVA with Dunnett's analysis as compared to control. * p < 0.05.	86

Figure 3.5. Concentration dependency of fMet-Leu-Phe uptake in the jejunum of wild-type mice (Mean \pm SE, n=4). fMet-Leu-Phe _w was referenced to the estimated concentration at intestinal wall.....	87
Figure 3.6. (A) fMet-Leu-Phe induced the MPO activity and Gly-Gly (50 mM) reversed the fMet-Leu-Phe-induced MPO activity in the jejunum of wild-type mice (Mean \pm SE, n=5). (B) fMet-Leu-Phe-induced MPO activity was not observed in the jejunum of <i>Pept1</i> knockout mice (Mean \pm SE, n=5). (C) fMet-Leu-Phe showed no effects in the colon of both wild-type and <i>Pept1</i> knockout mice (Mean \pm SE, n=5). Groups with different letters represented statistical difference which performed by one-way ANOVA with Tukey's comparison.	88
Figure 3.7. fMet-Leu-Phe hydrolysis kinetics by jejunal homogenates of wild-type and <i>Pept1</i> knockout mice (Mean \pm SE, n=4). The data were fitted to Michaelis-Menten equation.	89
Figure 3.8. Effective permeability of Gly-Sar were affected in the presence of the inhibitor of carboxypeptidase BzS and EDTA (Mean \pm SE, n=3).	90
Figure 3.9. Representative photomicrographs of jejunum of experimental groups. A. wild-type control. B, F. <i>Pept1</i> knockout control. C. wild-type + fMet-Leu-Phe. D. <i>Pept1</i> knockout + fMet-Leu-Phe . E. wild-type + fMet-Leu-Phe + Gly-Gly) . A-E: original magnification (x200), bars = 100 μ m. Insets (x1800). F. original magnification (x600), bar = 20 μ m.	91
Figure 4.1. The hydrolysis of Lys-Pro-Val by intestinal homogenates (Mean \pm SE, n=3).....	119
Figure 4.2. (A) Co-perfusion of peptidase inhibitors (5 mM Phe-pyrrolidide and 0.25 mM o-phenathroline) demonstrated completely inhibition of hydrolysis of Lys-Pro-Val during perfusion in the <i>Pept1</i> knockout mice (Mean \pm SE, n=3). (B) Regional permeability of Lys-Pro-Val in wild-type mice and <i>Pept1</i> knockout mice (Mean \pm SE, n=6). * < 0.05, ** < 0.01,*** <0.001 as compared to each wild-type segment by student's t-test.	120
Figure 4.3. PEPT1 substrates (Gly-Pro and Cefadroxil) inhibited the effective permeability of Lys-Pro-Val in three small intestinal segments, but not in colon. Substrate of PHT1/2, L-	

histidine, substrate of organic cation transporter, TEA, and substrate of PAT1 transporter, L-Proline showed no inhibition in all intestinal segments (Mean \pm SE, n=4). The concentration of all inhibitors was 25 mM. Statistical analyses were performed by one-way ANOVA with Dunnett's comparison against control within each segment..... 121

Figure 4.4. Concentration dependency of Lys-Pro-Val uptake in the jejunum of wild-type mice (Mean \pm SE, n=3-4). (A) as referenced to the inlet concentration which modeled by a single Michaelis-Menten equation. (B) as referenced to the estimated concentration at intestinal wall which modeled by a single Michaelis-Menten plus a linear term. 122

Figure 4.5. mRNA expression of DPPIV and APP in the intestinal segments in both genotypes (Mean \pm SE, n=6)..... 123

Figure 4.6. Effective permeability of GlySar was influence by peptidase inhibitors at high concentrations (Mean \pm SE, n=4-6). Statistical analyses were performed by one-way ANOVA with Dunnett's comparison against control within each segment (* <0.05, ** < 0.01). 124

Figure 4.7. (A-D) pH dependency of Lys-Pro-Val transport in different intestinal segments (Mean \pm SE, n=4). (E) Influence of DMA to the transport of Lys-Pro-Val in the jejunum of wild-type mice (Mean \pm SE, n=4). 125

Figure 4.8. Chromatogram of [3 H-Pro]Lys-Pro-Val during the perfusion of jejunum in wild-type mice. (A) Control, (B) Outlet perfusate without peptidase inhibitors, (C) Outlet perfusate with peptidase inhibitors. 126

Figure 4.9. Chromatogram of [3 H-Pro]Lys-Pro-Val in portal vein plasma during the perfusion of jejunum in wild-type mice. 127

Figure A.1. Percentage of weight loss after 3% DSS treatment in wild-type and *Pept1* knockout mice over time (Mean \pm SE, n=6). Statistical analyses were performed by student's t-test. (* denoted DSS vs. control of wild-type; # denoted DSS vs. control of *Pept1* knockout mice; + denoted DSS between genotypes; * p< 0.05, ** p< 0.01, *** p < 0.001, etc.) 136

Figure A.2. The disease activity index (DAI) after treatment of 3% DSS in wild-type and <i>Pept1</i> knockout mice over time (Mean \pm SE, n=6). Statistical analyses were performed by student's t-test. (++) $p < 0.01$; (+++) $p < 0.001$ between genotypes).	137
Figure A.3. The myeloperoxidase (MPO) activity after 3% DSS treatment for 8 days in wild-type mice and <i>Pept1</i> knockout mice (Mean \pm SE, n=5). Statistical analyses were performed by student's t-test. (* denoted DSS vs. control of wild-type; # denoted DSS vs. control of <i>Pept1</i> knockout mice).....	138
Figure A.4. mRNA expression of different cytokines in wild-type and <i>Pept1</i> knockout mice treated with 3% DSS for 8 days (Mean \pm SE, n=3-6). Statistical analyses were performed by student's t-test. (A) TNF- α , (B) IL-1 β , (C) IL-6, (D) IL-12B, (E) IFN- γ (* denoted DSS vs. control of wild-type; # denoted DSS vs. control of <i>Pept1</i> knockout mice).	139
Figure A.5. mRNA expression of different chemokines between wild-type and <i>Pept1</i> knockout mice after treatment of 3% DSS for 8 days (Mean \pm SE, n=3-6). Statistical analyses were performed by student's t-test. (A) Cxcl2, (B) KC (* denoted DSS vs. control of wild-type; # denoted DSS vs. control of <i>Pept1</i> knockout mice).	140
Figure A.6. mRNA expression of different anti-inflammatory cytokines between wild-type and <i>Pept1</i> knockout mice after treatment of 3% DSS for 8 days (Mean \pm SE, n=3-6). Statistical analyses were performed by student's t-test. (A) IL-10, (B) TGF- β (* denoted DSS vs. control of wild-type; # denoted DSS vs. control of <i>Pept1</i> knockout mice).	141
Figure A.7. Percentage of weight loss after 5-day 3% DSS treatment and recovered for 1 or 2 weeks in wild-type mice (solid circle: control, slide triangle: DSS) and <i>Pept1</i> knockout mice (open circle: control, open triangle: DSS) (Mean \pm SE, n=6-12 in each group). 142	
Figure A.8. The MPO activity of mice treated with 3% DSS for 5 days and recovered for 1 or 2 weeks (Mean \pm SE, n=5-6). Statistical analyses were performed by one-way ANOVA with Dunnett's comparison against each genotype control (# denoted DSS vs. control of <i>Pept1</i> knockout mice; + denoted DSS between genotypes).	143
Figure A.9. mRNA expression of different cytokines in wild-type and <i>Pept1</i> knockout mice at the recovery phase after treated with 3% DSS for 5 days and recovered for 1 or 2 weeks	

(Mean \pm SE, n=6). Statistical analyses were performed by one-way ANOVA with Dunnett's comparison against each genotype control. (A) TNF- α , (B) IL-1 β , (C) IL-6, (D) IL-12B, (E) IFN- γ (* denoted DSS vs. control of wild-type mice).....	144
Figure A.10. mRNA expression of different chemokines in wild-type and <i>Pept1</i> knockout mice at the recovery phase after treated with 3% DSS for 5 days and recovered for 1 or 2 weeks (Mean \pm SE, n=6). Statistical analyses were performed by one-way ANOVA with Dunnett's comparison against each genotype control. (A) Cxcl2, (B) KC (# denoted DSS vs. control of <i>Pept1</i> knockout mice).	145
Figure A.11. mRNA expression of different anti-inflammatory cytokines in wild-type and <i>Pept1</i> knockout mice at the recovery phase after treated with 3% DSS for 5 days and recovered for 1 or 2 weeks (Mean \pm SE, n=6). Statistical analyses were performed by one-way ANOVA with Dunnett's comparison against each genotype control (A) IL-10, (B) TGF- β . (* denoted DSS vs. control of wild-type mice; # denoted DSS vs. control of <i>Pept1</i> knockout mice).	146
Figure A.12. PEPT1 expression in colon after 3% DSS treatment for 8 days. (A) mRNA expression showed decrease after 8 days DSS treatment (Mean \pm SE, n=3-6). Statistical analyses were performed by student's t-test. (B) PEPT1 protein expression showed no increase in either proximal or distal colon after 8 days DSS treatment.....	147
Figure A.13. PEPT1 expression in colon at the recovery phase after 3% DSS treatment for 5 days. (A) mRNA expression show slight decrease at 1 week recovery, but return to normal after 2 weeks of treatment (Mean \pm SE, n=6). (B) PEPT1 protein expression showed no up-regulation at 1 or 2 weeks recovery after treatment with 5 days DSS.	148
Figure B.1. The protein expression of PEPT1 after <i>citrobacter rodentium</i> infection. (C: control, T: <i>citrobacter rodentium</i> infection, SI: small intestine).	155
Figure B.2. PEPT1 expression in wild-type and IL-10 knockout mice. (A) mRNA expression showed increase but not reached statistical difference between genotypes (Mean \pm SE, n=3). (B) Protein expression showed significantly increase in IL-10 knockout mice as compared to wild-type mice (Mean \pm SE, n=3).	156

LIST OF TABLES

Table 2.1. List of studies focusing on PEPT1 related to intestinal inflammation.	43
Table 3.1. Scores of edema and inflammation of each sample.....	92
Table A.1. The clinical criteria of scoring system for colitis progress (Adopted from Cooper HS et al., 1993).	149
Table A.2. Primers for the real-time PCR analysis of cytokines and chemokines.	150
Table A.3. Clinical signs of DSS-induced colitis and MPO activity in wild type and <i>Pept1</i> knockout mice at day 8 of DSS treatment (Mean \pm SE, n=6 in each group; Mean \pm SE, n=5 for MPO activity).	151

LIST OF APPENDIXES

APPENDIX A

COMPARISON OF THE SUSCEPTIBILITY TO DEXTRAN SODIUM SULFATE BETWEEN WILD-TYPE AND <i>PEPT1</i> KNOCKOUT MICE.....	131
---------------------------------------------------------------------------------------------------------------------	-----

APPENDIX B

UP-REGULATION OF COLONIC PEPT1 EXPRESSION BY OTHER ALTERNATIVE COLITIS MODELS.....	153
---------------------------------------------------------------------------------------	-----

ABSTRACT

The proton-coupled oligopeptide transporter PEPT1 has recently been linked to intestinal inflammation and inflammatory bowel disease (IBD) because of its ability to transport bacterial peptides (e.g., Tri-DAP, MDP, fMet-Leu-Phe) and its aberrant expression in the colon of IBD patients. Although studies have demonstrated that several bacterial peptides were substrates of PEPT1, the relative importance of this protein (as compared to other transporters and pathways) and its regional permeability have not been addressed. Therefore, the first objective of this dissertation focused on the importance of intestinal PEPT1 in transporting a bacterially-produced chemotactic peptide, fMet-Leu-Phe, using the *in situ* single-pass intestinal perfusion (SPIP) technique in wild-type and *Pept1* knockout mice. The results demonstrated that PEPT1 contributed about 80-90% of fMet-Leu-Phe transport in the small intestine and showed saturable and low-affinity kinetics ($K_m = 1.6 \text{ mM}$). The contribution of PHT1 was ruled out due to the lack of inhibition of fMet-Leu-Phe transport by L-histidine. The significance of fMet-Leu-Phe transport could be translated from kinetic to dynamic effects. Using a modified intestinal perfusion condition, the activity of myeloperoxidase (MPO), a marker for neutrophil migration, was increased by perfusing fMet-Leu-Phe in the jejunum of wild-type mice. In contrast, MPO activity showed no increase when perfusing fMet-Leu-Phe in the jejunum of *Pept1* knockout mice. These findings suggested that PEPT1 was the major transporter

for the transport of fMet-Leu-Phe in the small intestine and could influence the induction of inflammation.

Lys-Pro-Val has been suggested as a potential therapeutic agent for IBD due to its anti-inflammatory effects in mouse colitis models. However, some important properties (e.g., intestinal permeability and stability) have not been studied. Therefore, the second objective of this dissertation was to study the transport properties of the anti-inflammatory tripeptide Lys-Pro-Val using the intestinal perfusion technique in wild-type and *Pept1* knockout mice. The results showed that PEPT1 was responsible for at least 90% of Lys-Pro-Val uptake in the small intestine and exhibited saturable transport with relatively high affinity ($K_m = 0.11$ mM). The potential contribution of other transporters (e.g., PHT1, OCT, PAT1) was not evident because no inhibition of Lys-Pro-Val transport was observed by substrates of these transporters. These findings suggested that PEPT1 was the major transporter in transporting Lys-Pro-Val in small intestine. The results of intestinal stability studies suggested that Lys-Pro-Val was not enzymatically stable in the intestinal lumen and that major metabolism took place in the jejunum and ileum. Taken together, although Lys-Pro-Val may be a good candidate to treat IBD through the aberrant expression of colonic PEPT1, drug stability was a significant concern for oral administration.

In conclusion, results from this dissertation suggested that PEPT1 could transport bacterial peptides, implying that aberrant expression of PEPT1 in the colon may contribute to the progression of IBD. Although colonic PEPT1 may also serve as a drug targeting (delivery) opportunity for some bioactive peptides, such as Lys-Pro-Val to treat IBD, intestinal stability of this substrate is a realistic concern.

Chapter 1

RESEARCH OBJECTIVES

PEPT1 belongs to the proton-coupled oligopeptide transporter (POT) family. According to the HUGO Gene Nomenclature Committee (HGNC), PEPT1 is categorized under the Solute Carrier family 15 (SLC15). So far, there have been four mammalian members recognized within this family: PEPT1 (SLC15A1), PEPT2 (SLC15A2), PHT1 (SLC15A4), and PHT2 (SLC15A3). PEPT1 has been considered an important transporter because of its absorption of di/tripeptides, primarily from the breakdown products of protein in the digestive tract. In addition to its physiological importance in protein absorption, PEPT1 also has pharmacological importance because of its ability to transport a variety of peptidomimetic drugs. Due to the broad spectrum of substrate specificity and its importance in intestinal absorption, PEPT1 has been utilized as a drug delivery target in order to improve the bioavailability of poorly absorbed compounds. The impact and influence of transporters in drug absorption, disposition, elimination, drug-drug interactions, and disease-related pathogenesis have also received increasing attention. For example, PEPT1 has been shown to be regulated by several endogenous and exogenous factors (e.g., hormones, growth factor, 5-fluorouracil, and cyclosporine). More interestingly, under some disease conditions (i.e., inflammation), PEPT1 exhibited an aberrant expression and up-regulation in the colon.

Inflammatory bowel disease (IBD) was recently linked to PEPT1 for several reasons. First, in colonic biopsies of patients with IBD, it was demonstrated that PEPT1 was up-regulated in the apical membrane of colon. Second, it was shown that PEPT1 has the ability to transport some bacterially-produced peptides which can exacerbate inflammation. Third, one of the ligands of the NOD2 receptor, muramyl dipeptide (MDP), has been shown to be a substrate of PEPT1. Since the NOD2 gene was the first gene associated with an IBD phenotype, the fact that PEPT1 could transport its ligand was believed to be strong supportive evidence. Although it has been suggested that PEPT1 was associated with IBD, the true function and role of PEPT1 in the pathogenesis of IBD is still uncertain. A polymorphism study recently revealed that a SNP in the PEPT1 gene (Ser117ASN) showed association with Crohn's disease (CD) susceptibility in two populations in opposed directions (risk and protection, respectively).

Among different experimental models, the genetic knockout mouse model provides a great opportunity and tool to study the contribution and impact of PEPT1 in substrate absorption, disposition, pharmacology and, perhaps, pathology. Previously, our laboratory has successfully demonstrated the value of using *Pept2* knockout mice to study the importance of PEPT2 in renal drug reabsorption and of using *Pept1* knockout mice to study the contribution of PEPT1 in intestinal drug absorption *in vitro*, *in situ*, and *in vivo*. Although studies have demonstrated that several bacterial peptides (e.g., Tri-DAP, MDP, fMet-Leu-Phe) were substrates of PEPT1, the relative importance of this protein (as compared to other transporters and pathways) and the regional permeability have not been addressed. Therefore, the first objective of this dissertation was to use *Pept1* knockout mice to study the importance of PEPT1 in transporting a bacterial peptide,

fMet-Leu-Phe, by using the *in situ* single-pass perfusion technique. The specific aims were: 1) to study the importance of intestinal PEPT1 in transporting fMet-Leu-Phe, 2) to determine the regional permeability of fMet-Leu-Phe, and 3) to study the functional dynamics (i.e., effect on neutrophil migration) of transporting fMet-Leu-Phe into enterocytes.

Several bioactive peptides have attracted interest because of their pharmacological potential in treating intestinal inflammation. Lys-Pro-Val is one such example that has recently drawn attention. Lys-Pro-Val is a bioactive tripeptide, derived from α -melanocyte-stimulating hormone (α -MSH). Studies have demonstrated that Lys-Pro-Val exhibited promising anti-inflammatory activity in different models. Recent reports have also considered Lys-Pro-Val as a potential therapeutic opportunity for the treatment of IBD. Although Lys-Pro-Val has been shown to be a substrate of PEPT1 in Caco-2 cells, the direct measurement of its intestinal permeability in a relevant mammalian model has not been demonstrated. Furthermore, the stability of Lys-Pro-Val in the intestine has not been addressed. Therefore, the second objective of this dissertation was to study the intestinal transport of Lys-Pro-Val using an *in situ* single-pass intestinal perfusion technique in both wild-type and *Pept1* knockout mice. The specific aims were: 1) to determine the intestinal permeability of Lys-Pro-Val, 2) to study the regional permeability in the PEPT1-mediated transport of transporting Lys-Pro-Val, and 3) to study the intestinal stability of Lys-Pro-Val using intestinal homogenates.

Several important findings have been provided from this dissertation. First, the results have demonstrated that fMet-Leu-Phe has substantial permeability in the duodenum, jejunum and ileum, but not colon, of wild-type mice and that this translates

into a greater neutrophil migration in jejunum than that observed in *Pept1* knockout mice. This provides solid evidence for a role of intestinal PEPT1 in the transport of a bacterially-produced chemotactic peptide and subsequent inflammatory effects. Second, the anti-inflammatory tripeptide Lys-Pro-Val also has marked transport by intestinal PEPT1 in all regions of the small intestine (but not colon). However, its instability in the intestine precludes its use as an effective tool against inflammation in IBD patients after oral dosing.

Chapter 2

BACKGROUND AND LITERATURE REVIEW

PROTON-COUPLED OLIGOPEPTIDE TRANSPORTERS 1

Description

Proton-coupled oligopeptide transporters 1 (PEPT1) is categorized under solute carrier family 15 (SLC15) according to the HUGO Gene Nomenclature Committee (HGNC) system. Four members have been identified so far in this family, which includes PEPT1 (SLC15A1), PEPT2 (SLC15A2), PHT1 (SLC15A4), and PHT2 (SLC15A3). PEPT1 is the first peptide transporter cloned from the rabbit intestine cDNA library (Fei *et al.*, 1994) in 1994. Since then, PEPT1 have been cloned from several other mammals, including human (Liang *et al.*, 1995), monkey (Zhang *et al.*, 2004a), rat (Saito *et al.*, 1995; Miyamoto *et al.*, 1996), mouse (Fei *et al.*, 2000), pig (Klang *et al.*, 2005), and sheep (Pan *et al.*, 2001). In general, they shared high degree of sequence homology across species (~ 80% identity). Comparing to the amino acid sequence of human PEPT1, they were 92%, 83%, 83%, 82.8%, 83%, 81% identities for monkey, rat, mouse, pig, sheep, and rabbit, respectively. Indeed, PEPT1 was one of the archaic transporters recognized with high conservation from prokaryotes to eukaryotes (Daniel *et al.*, 2006). The human PEPT1 gene is located on chromosome 13q33-34 and encodes 708

amino acids. Unlike high homology across species, PEPT1 shares around 50% amino acid identity with PEPT2, another peptide transporter that cloned from human kidney cDNA library in 1995 (Liu *et al.*, 1995). PEPT2 gene is located on chromosome 3 and encodes 729 amino acids in human. PEPT1 and PEPT2 transporters share many common features, however, the major distinction between both is from the kinetic characteristic, that is, PEPT1 is considered as a low affinity and high capacity transporter, whereas PEPT2 is considered a high affinity and low capacity transporter. Two additional peptide transporters, PHT1 (Yamashita *et al.*, 1997) and PHT2 (Sakata *et al.*, 2001) were cloned from the rat brain cDNA library in 1997 and 2001, respectively. PHT1 and PHT2 genes encode 572 and 582 amino acids and they shared less than 20% amino acid identity to PEPT1 and PEPT2 and they have been demonstrated to transport not only di/tripeptides, but also a single amino acid, L-histidine, in a proton dependent fashion. Unlike PEPT1 and PEPT2, there were less studies on PHT1 and PHT2 regarding to their function, importance and substrate specificity, however, recently, studies have shown that PHT1 (SLC15A4) was important in the toll-like receptor 9 (TLR9) and NOD1 signaling and associated with inflammatory bowel diseases and systemic lupus erythematosus (Han *et al.*, 2009; Sasawatari *et al.*, 2011).

Molecular Structure

The molecular structure of PEPT1 has been demonstrated by the hydropathy analysis of the amino acid sequence. 12 putative transmembrane domains (TMD) with both N- and C- termini facing the cytosol and a large hydrophilic loop presented between TMD9 and TMD10 have been predicted. For human PEPT1, from the amino acid

sequence, 7 putative N-linked glycosylation sites, 2 protein kinase C-dependent phosphorylation sites (Ser-357, Ser-704), but none of protein kinase A-dependent phosphorylation site (Liang *et al.*, 1995). Similarly, in mouse PEPT1, 6 putative N-linked glycosylation sites, 1 protein kinase C-dependent phosphorylation site (Ser-357), and 1 protein kinase A-dependent phosphorylation site (Thr-362) has been suggested (Fei *et al.*, 2000). Regarding to the putative promoter regions, both human and mouse PEPT1 were lack of classical TATA box element presented in the -30 to -90 bp upstream position nearby the transcription start site. Instead, a TATA box-like sequence, CAATAAATA, was present at a farther upstream position of mouse PEPT1 (-813). For human PEPT1, two TATA boxes were present at unusual positions 511 bp and 571 bp upstream from the transcription start site. Therefore, the GC box was believed to be the primarily regulatory sites for PEPT1 transporter. Three GC-rich boxes (-88, -322, -352 bp) and one at -29 bp and several others within -300 bp were identified in mouse and human PEPT1, respectively (Fei *et al.*, 2000; Urtti *et al.*, 2001).

Importance

PEPT1 has an indispensable role in the absorption of protein. Before the discovery of PEPT1, it was first believed that the dietary proteins were not absorbed until hydrolysis to the form of free amino acids. However, several studies have demonstrated evidence that proteins were absorbed mainly in the form of small peptides rather than single amino acids. Adibi and Mercer found that after the subjects fed with a meal containing 50 g bovine serum albumin, the concentration of peptide-bound amino acids in the lumen of the small intestine was greater than that of amino acid in free form (Adibi

et al., 1973). Nixon and Mawer also found that after feeding test meals, the free amino acid concentrations in the intestinal lumen correlated poorly to the concentration of the free amino acid in the acid hydrolysates of test meals, which suggesting that hydrolyzed peptides might directly be absorbed from the intestine (Nixon *et al.*, 1970). Latter studies further showed that intact dipeptides could be detected in the mesenteric plasma (Boullin *et al.*, 1973) and amino acids and di/tripeptides have different mechanisms of absorption, showing different V_{max} and K_t. In general, (1) di/tripeptides showed higher absorption rate in proximal small intestine than that in distal small intestine; (2) free amino acid showed higher absorption rate in distal small intestine than that in proximal small intestine; (3) the absorption rate of di/tripeptides was higher than that of free amino acid (Matthews *et al.*, 1968; Crampton *et al.*, 1973; Matthews, 1975). After the discovery of PEPT1, more specific and extensive studies have been performed and well accepted that PEPT1 is the major transporter responsible for the absorption of dietary protein in the form of di/tripeptides. The concentration of peptide-bound amino acid could achieve as high as 80% of the total amino acids and get absorbed by PEPT1 (Ganapathy *et al.*, 2006).

The importance of PEPT1 was highlighted in some genetic disorder diseases. Hartnup disease is a recessive genetic disorder, which affects the intestinal and renal transport of neutral amino acids (alanine, serine, threonine, valine, leucine, isoleucine, histidine, glutamine, asparagines, phenylalanine, tyrosine, and tryptophan) (Leny, 2001). Recent studies identified the B⁰AT1 transporter (system B⁰) was defective in the patients of hartnup disease (Kleta *et al.*, 2004; Seow *et al.*, 2004). Cystinuria is the other genetic defect in system b^{0,+} resulted in a dysfunction of transport of cationic amino acids (arginine, lysine, and ornithine) and cystine (Palacin *et al.*, 2001b). The gene that

responsible for this defect were also recognized as rBAT (Type I) or b⁰⁺AT (Non-type I) (Palacin *et al.*, 2001a). Surprisingly, patients with these genetic defects did not exhibit any obvious symptoms or evidence of protein malnutrition. The answer was unclear until studies found out that the affected amino acids were absorbed adequately in the form of small peptides (Asatoor *et al.*, 1970; Hellier *et al.*, 1970). Hellier showed that the absorption of lysine was compromised in cystinuric patient, but the absorption of glycyl-L-lysine was similar to normal subject (Hellier *et al.*, 1970), which again supported that PEPT1 was very important in the absorption of dietary protein especially in certain genetic disorders.

PEPT1 has not only nutritional importance but also pharmacological relevance because studies have shown that some peptidomimetic drugs, such as β -lactam antibiotics (Okano *et al.*, 1986), ACE inhibitors (Thwaites *et al.*, 1995), renin inhibitors (Kramer *et al.*, 1990), anticancer drug bestatin (Tomita *et al.*, 1990), and antiviral prodrug valacyclovir (Ganapathy *et al.*, 1998), were the substrates for PEPT1. With the fact that PEPT1 transporter could accommodate compounds with various physicochemical characteristics in size, charge, polarity, and structure flexibility, a prodrug strategy targeting for PEPT1 has been widely used in the pharmaceutical industry (Rubio-Aliaga *et al.*, 2002). Successful examples were like valacyclovir, val-ganciclovir, and L-Pro-L-Phe-Alendronate. The bioavailability as supposed to their parent compounds was increased 3-5 fold, 10 fold, and 3 fold, respectively (Beauchamp *et al.*, 1992; Jung *et al.*, 1999; Ezra *et al.*, 2000).

Since PEPT1 also expressed in kidney (Lu *et al.*, 2006) (especially in rat), the importance of PEPT1 in the renal reabsorption has been studied as well. However,

PEPT1 has been shown to be less important than PEPT2 with regard to the reabsorption of the peptide-bound amino nitrogen and peptidomimetic drugs in kidney. Studies using *Pept2* knockout mice revealed that PEPT2 was more important than PEPT1 in kidney for the reabsorption of two known substrates (for Gly-Sar, PEPT2 contributed for 86% and PEPT1 accounted for 14% of total reabsorption; for cefadroxil, PEPT2 accounted for 95% and PEPT1 only contributed for 5% of total reabsorption) (Ocheltree *et al.*, 2005; Shen *et al.*, 2007).

Tissue Distribution and Cellular Localization

Although PEPT1 widely expressed in several tissues, the mRNA expression of PEPT1 primarily focused in the small intestine region of the digestive tract (Lu *et al.*, 2006). The protein expression of PEPT1 agreed with the mRNA that PEPT1 predominately expressed in the small intestine rather than in large intestine of digestive tract (Ogihara *et al.*, 1996; Jappar *et al.*, 2010). In the small intestine, PEPT1 has been shown to express mostly in the absorptive epithelial cell on the tip of the villi and very less amount in the crypt and the goblet cell. The expression of PEPT1 was limited to the apical membrane of epithelial cells (Ogihara *et al.*, 1996; Walker *et al.*, 1998; Groneberg *et al.*, 2001). The expression of PEPT1 in kidney was species dependent. PEPT1 have been shown to locate at the apical membrane of S1 segment of renal proximal tubule in rat (Shen *et al.*, 1999). However, in other species, such as rat and human, PEPT1 showed low expression level in kidney (Lu *et al.*, 2006; Hilgendorf *et al.*, 2007).

PEPT1 recently has been found to express in human macrophages isolated from human peripheral blood and a monocytic cell line, KG-1. Although the characteristic

function of PEPT1 in immune cell showed slightly different from PEPT1 expressed in epithelial cell (the maximal activity presented at physiological pH, 7.2 as opposed to epithelial cell at acidic environment, around pH 6.2), this expression might imply the importance of PEPT1 in the innate immunity (Charrier *et al.*, 2006a). Other tissues, such as liver, pancreas, lung, bile duct, ovary, placenta, testis, prostate, mammary gland, nasal epithelium, and placenta, have been shown to express some level of PEPT1 mRNA. However, because there was little information available for these tissues, less was known about the function of PEPT1 in these tissues (Herrera-Ruiz *et al.*, 2001; Knutter *et al.*, 2002; Lu *et al.*, 2006; Gilchrist *et al.*, 2010; Agu *et al.*, 2011).

Interestingly, PEPT1 has been found to express not only in the plasma membrane but also in the membrane of the subcellular organelle. The lysosomal localization of PEPT1 has been shown in renal cells and acinar cells in exocrine pancreas, which suggesting a transport phenomenon occurred to prevent the accumulation of incomplete digested peptides in lysosome (Bockman *et al.*, 1997; Zhou *et al.*, 2000).

Structure Function Relationship

Up to date, only the crystal structure of a prokaryotic homologues, PepT(So) from the bacterium *Shewanella oneidensis*, has been resolved (Newstead *et al.*, 2011). However, with the absence of the exact structure of mammalian PEPT1 transporter, many other alternative methods have been used to elucidate the structure function relationship such as epitope insertion method, site-directed mutagenesis approach, chimeric construction, substituted-cysteine accessibility method (SCAM) and computer modeling technique. Based on the hydropathy analysis of amino acid sequences, PEPT1 has been

suggested to contain 12 transmembrane domains (TMD). The membrane topology model has been confirmed and supported by an epitope insertion study (Covitz *et al.*, 1998). Doring constructed a chimeric protein consisted of PEPT2 N- terminal region (1-401) and PEPT1 C- terminal region (402-707) and found that the chimeric protein behaved more like PEPT2 than PEPT1 in terms of substrate specificity and affinity, indicating that the substrate binding region might reside in the region before TMD9 (Doring *et al.*, 1996), rather than in the large extracellular loop between TMD9 and TMD10. More chimeric proteins were made and further pointed out the putative substrate binding site was located between TMD7-9 and TMD1-6 were involved in the determination of pH dependency and the major part of substrate-binding pocket (Fei *et al.*, 1998; Terada *et al.*, 2000a).

Site-directed mutagenesis studies have revealed the essential amino residues of PEPT1. At first, three highly conserved histidyl residues of PEPT1 across species, His-57, His-121, and His-260 have been studied. Terada demonstrated that after the mutation of His-57 and His-121, the uptake of Gly-Sar and ceftibuten were abolished, suggesting that these two histidyl residues were crucial and involved in substrate recognition of rat PEPT1 (Terada *et al.*, 1996). In contrast to rat PEPT1, only His-57 residue seemed to have an obligatory role for the function of human PEPT1 (Fei *et al.*, 1997). Latter studies have suggested that His-57 residue might serve as the proton binding site for PEPT1 to initiate the transport (Chen *et al.*, 2000; Uchiyama *et al.*, 2003). A number of other mutations have been studied to demonstrate some function-related residues other than conserved histidyl residues. Tyr-56 and Tyr-64 have been shown to be indispensable for the normal function of PEPT1. The mutation of Tyr-56 and Tyr-64 resulted in a complete loss of function. Since they were both neighboring residues to His-57, one explanation

has been proposed that Tyr-56 and Tyr-64 were involved in the stabilization of positive charges within the membrane electric field (Chen *et al.*, 2000). Arg-282 and R-361 were other examples of critical residues for the function of PEPT1. After the mutation of either Arg-282 or R-361, the uptakes of D-Phe-L-Gln or GlySar were significantly compromised and Meredith and his coworkers proposed a charge pair model between Arg-282 and R-361 (Meredith, 2004; Kulkarni *et al.*, 2007; Pieri *et al.*, 2008). Another study also showed supportive data that Arg-282 and R-361 were forming a charge pair (electrostatic gate) between TMD7 and 8 of PEPT1 (Bossi *et al.*, 2011).

Substituted-cysteine accessibility method (SCAM) is another method to study the structure of transporter, especially to determine the relative orientation, functional importance, and solvent accessibility of the transmembrane segments of transporter (Liapakis *et al.*, 2001). Kulkarni has employed this method to elucidate the structural information of TMD5 (Kulkarni *et al.*, 2003a) and TMD7 (Kulkarni *et al.*, 2003b). In general, TMD5 lined slightly tilted along the putative aqueous channel with the exofacial half forming a classical amphipathic α -helix and the cytoplasmic half being highly solvent accessible. TMD7, however, is relatively solvent-accessible along most of its length, particularly on the intracellular end. Upon substrate binding, TMD7 might shift to allow the opening of channel and translocation of substrate. TMD3 has been also studied by Links using SCAM. TMD3 was proposed to slightly tilting to substrate translocation pathway similarly to TMD5 and TMD 7 and would interact with TMD5 with limited solvent accessibility in the extracellular region and relatively solvent accessible in the intracellular region (Links *et al.*, 2007). Several crucial amino acid residues have been identified as well, such as Tyr-167, Asn-171, and Ser-174 in TMD5, Phe-293, Leu-296,

and Phe-297 in TMD7, and Thr-83, Leu-87, Ser-88, Tyr-91, Gly-94 and Ser-101 in TMD3. The uptake of Gly-Sar of all of the mutations significantly reduced to < 25% of that of wild-type.

Computer modeling approach has been applied to predict the structure function relationship of PEPT1. Bolger has successfully proposed a computer simulated model for PEPT1 based on the energy minimization and molecular dynamics simulation (AMBER) algorithm. The putative model was then submitted to the substrates (Gly-Gly and Gly-Gly-Gly) interaction analysis by MIDAS and DOCK. Several hypothesized residues were proposed and confirmed by site-directed mutagenesis approach. Tyr-167, Trp-294, and Glu-595 have been shown to be important for the function of PEPT1 (Bolger *et al.*, 1998).

Structure Activity Relationship

Since PEPT1 has been shown to transport a number of peptidomimetic drug, such as β -lactam antibiotics (Okano *et al.*, 1986), ACE inhibitors (Thwaites *et al.*, 1995), renin inhibitors (Kramer *et al.*, 1990), anticancer drug bestatin (Tomita *et al.*, 1990), and antiviral prodrug valacyclovir (Ganapathy *et al.*, 1998), PEPT1 has been considered as a promising drug delivery target to increase the bioavailability of poorly absorbed drugs (Terada *et al.*, 2004). In order to develop a better candidate targeting to PEPT1 transporter, the structural requirements for transport via PEPT1 have been extensively studied (Brodin *et al.*, 2002; Brandsch *et al.*, 2004). However, most of studies performed by a traditional competition assay, which reported the inhibition (affinity) constant K_i (or IC_{50}) of a test compound to a known substrate (e.g. [^{14}C]Gly-Sar). Therefore, to interpret the affinity data should always bear in mind that they were not actual transport. Brandsch

and his group provided the criteria to classify the substrates based on the affinity constant (K_i). K_i values < 0.5 mM as high affinity, $0.5 - 5$ mM as medium affinity and $> 5 - 15$ mM as low affinity.

The actual transport of PEPT1 substrate could be monitored by two experimental methods; both were based on the characteristic of PEPT1 transport, electrogenicity. Two electrode voltage clamp technique in PEPT1 expressing *Xenopus* oocytes could measure the inward current evoked along the translocation of substrate (Fei *et al.*, 1994). The other method was developed recently by Smith and his group. The method used a membrane potential-sensitive fluorescent dye (MP) to indicate the occurrence of transport event (Faria *et al.*, 2004). Since different experimental setting and data analysis, they provided different criteria for the classification of substrate. A parameter $\%GlySar_{max}/EC_{50}$ was used and the classification as following: best substrates > 1000 , good substrates = 300-1000, intermediate substrates = 100-300, and poor substrates = 0-100 ($\% GlySar_{max}$: maximum activation relative to Gly-Sar) (Vig *et al.*, 2006).

The physicochemical properties of potential substrates were listed below:

Size: There was no common agreement for the maximal molecular weight that PEPT1 could transport. Generally speaking, candidate substrates need to be large than single amino acid and smaller than tetrapeptides. However, the distance between N- and C- termini influence more than the molecular weight. The optimal length was estimated about 5.5 \AA ($= 550 \text{ pm}$) by Li, and confirmed by Doring that the distance between N- and C- termini should fall between 5.0 to 6.35 \AA ($= 500$ to 635 pm) (Li *et al.*, 1996; Doring *et al.*, 1998b).

Stereospecificity: PEPT1 was markedly stereochemically specific in substrate transport. L-configuration of each amino acid was preferable. The rank of affinity for PEPT1 in Caco2 cell was L-Val-L-Val > D-Val-L-Val > L-Val-D-Val > D-Val-D-Val and L-Val-L-Val-L-Val > L-Val-L-Val-D-Val > D-Val-L-Val-L-Val > D-Val-D-Val-L-Val > L-Val-D-Val-L-Val > D-Val-L-Val-D-Val, L-Val-D-Val-D-Val, D-Val-D-Val-D-Val (no affinity) shown by Li (Li *et al.*, 1998). Meredith also showed similar results on tripeptide Ala-Ala-Ala by PEPT1 expressing *Xenopus* oocytes as L-Ala-L-Ala-L-Ala > L-Ala-L-Ala-D-Ala > D-Ala-L-Ala-L-Ala > L-Ala-D-Ala-L-Ala (Meredith *et al.*, 2000). Interestingly, the low affinity of D-configured peptide could be resolved by the side chain modification. D-Asp(OBzl)-Ala, a β -esterified dipeptide showed remarked affinity to PEPT1 ($IC_{50} = 2.62$ mM). It provided a solution to generate an enzymatically stable peptide while retaining a comparable affinity to PEPT1 (Taub *et al.*, 1997).

Terminal groups: Generally speaking, modification of either N- or C- terminal groups would result in the decrease of affinity to PEPT1 (Meredith *et al.*, 2000). However, both N- or C-terminal groups were not absolutely essential for affinity and transport. Dipeptides with N-methylation Sar-Pro showed decrease but still comparable affinity as compared to Gly-Pro (K_i from 0.16 to 2.5 mM) (Brandsch *et al.*, 1999). However, an exception has been demonstrated when modifying N- terminal group with fatty acid (C₄-Phe-Gly and C₆-Phe-Gly). The affinity of the compound with modification increase comparing to parent compound (Fujita *et al.*, 1997). C- terminal modification of peptide was more tolerable than N- terminal modification (Borner *et al.*, 1998; Brandsch *et al.*, 1999).

Peptide bonds: The peptide bond within a peptide structure has proved to be not essential requirement for the substrate of PEPT1. Enjoh demonstrated that arphamenine A (the peptide bond was replaced by ketomethylene bond) was transported by PEPT1 in Caco-2 cell with K_m equaled 0.14 mM (Enjoh *et al.*, 1996). δ -aminolevulinic acid (5-ALA also bearing a ketomethylene group has been shown to be transported by PEPT1 (Doring *et al.*, 1998a). A more systemic investigation was then performed by Doring, and surprisingly found that ω -amino fatty acids were substrates for PEPT1. Therefore, they suggested that the distance between N- and C- terminal groups was more important than the presence of peptide bond. The optimal distance was suggested to be 5.0 to 6.35 Å (Doring *et al.*, 1998b).

Configuration isomerism: When a peptide bond was present in di/tripeptides, there was trans- or cis- configuration. The configuration was critical for PEPT1 substrate. Brandsch demonstrated that with lower cis/trans ratio, compound Ala- ψ [CS-N]-Pro exhibited significantly higher affinity to PEPT1 (K_i = 0.3 mM for lower cis/trans ratio; K_i = 0.51 mM for higher cis/trans ratio) (Brandsch *et al.*, 1998). More Xaa-Pro dipeptides were used and confirmed that PEPT1 selectively transport only trans-configuration peptide (Brandsch *et al.*, 1999).

Charge: The influence of charge on dipeptide affinity and transport has been noticed soon after PEPT1 was cloned. The general understanding was that charged dipeptides have lower affinity as compared to structurally similar dipeptides (Brandsch *et al.*, 1999; Terada *et al.*, 2000b). More systemic investigation regarding charge was not performed until 2006, Vig used a high-throughput screening method to study several dipeptides of PEPT1 (Vig *et al.*, 2006). The conclusion they made was dipeptides with

acidic residues (negative charged) at both positions were poor substrates of PEPT1. However, dipeptides with basic amino acids (positive charged) at both positions were not substrates at all (e.g. Arg-Arg, Arg-Lys, Lys-Lys, Lys-Arg, and Orn-Orn). The rank of affinity of dipeptide to PEPT1 was suggested as follows: neutral-neutral > charged-neutral ~ neutral-charged > acidic-acidic > basic-basic. This was the first data showing that not all of the 400 dipeptides were substrate of PEPT1 (Vig *et al.*, 2006).

Substrate Template for PEPT1

By analysis over 100 substrates, Bailey proposed the first qualitative template for PEPT1 (Bailey *et al.*, 2000). There were 10 features to consider for substrate of PEPT1. Four of them were thought to be the key features, which were: 1) a strong binding site for the N-terminal NH_3^+ group; 2) a hydrogen bond to the carbonyl group of the first peptide bond; 3) a carboxylate binding site which controls the preferred stereochemistry of the adjacent chiral centre and 4) a hydrophobic pocket with a strong directional vector (Figure 2.1). Few years later, Bailey further proposed a semi-quantitative method to predict the substrate affinity for PEPT1 (Bailey *et al.*, 2006). The brief procedures are

- 1) to assign the score of each factor that contributes to the binding;
- 2) to determine the total binding parameter T, which is the sum of 10 scores at step 1;
- 3) to multiply by 2.8 (scaling factor) to convert into binding energies ΔG (kJ/mol);
- 4) to find the corresponding Log K by using the linear correlation plot.

Surprisingly, the simple semi-quantitative method worked pretty well. It successfully made prediction of the substrate affinity for PEPT1 (Bailey *et al.*, 2006). More details were listed in Figure 2.1.

Quantitative Structure Activity Relationship

Computer simulated 3D-QSAR models for dipeptide and tripeptide were developed using DISCO module for the pharmacophore construction and following by CoMFA or CoMSIA analysis (Gebauer *et al.*, 2003; Biegel *et al.*, 2005). The Q-SAR models not only successfully predicted additional substrates, but also provided more detailed explanation about the substrate requirements for PEPT1. For example, the reduced affinity of introducing D-configured amino acid was attributed to the disfavored steric hindrance. The reason why modification of C- terminal groups generally more tolerated than modification of N- terminal groups was rationalized by the fact that at C-terminus the electron density was more important than the specific negative charge end. The design of new PEPT1 targeting drug became more visualized and logical with the help of 3D-QSAR models although it might need considerable computational time and manual optimization (Foley *et al.*, 2010).

The Mode of Transport

It was well accepted now that the driving forces of PEPT1 transporter are proton electrochemical gradient and membrane potential (Fei *et al.*, 1994). From pre-steady state current analysis, a model has been proposed regarding to the transport cycle of PEPT1. The transport cycle was in an ordered, simultaneous transport model, in which H⁺ bound first to the transporter in outward facing conformation, following by a change in substrate-binding affinity. After the accommodating the substrate, PEPT1 underwent a conformational change to start the translocation process (Mackenzie *et al.*, 1996). Similar model with an extension focusing on the intracellular event was supported by Nussberger,

suggesting a symmetry H^+ binding intra- and extracellular model (Nussberger *et al.*, 1997). Since the transport via PEPT1 involved at least two binding steps, H^+ and substrate, a model focusing on the substrate binding event has been further proposed. The substrate binding affinity of PEPT1 in outward facing conformation was 5 fold higher than that of inward facing conformation, which implied that the substrate binding domain favored the intracellular releasing of substrate rather than binding of substrate. Also, at saturating substrate concentration, the direction and rate of transport were determined solely by the membrane potential (Kottra *et al.*, 2001).

Due to the fact that PEPT1 could transport charged peptide and an observation of increasing rate of transport at lower external pH for anionic substrate (Wenzel *et al.*, 1996). A different stoichiometry of proton to substrate when transporting different charged substrate was hypothesized and studied. Steel reported the stoichiometry of neutral, cationic, and anionic dipeptides as 1:1, 1:1, and 2:1 (proton : substrate) (Steel *et al.*, 1997). The additional proton for anionic peptides was thought to neutralize the charge on the dipeptide substrate to generate a net neutral species (zwitterions). By contrast, the histidyl residue of PEPT1 was thought to be deprotonated to accommodate the positively charged moiety on cationic dipeptide. Although the stoichiometry was correct for the transport of different charged dipeptides, latter study showed that for cationic dipeptide, the position of charged residue mattered. For example, Lys-Gly, the transport occurred on both positively charged and neutral form, which resulted in an extra inward current. However, for Gly-Lys, the transport was predominantly via its neutral form rather than positively charged form. For anionic dipeptides, the transport with an additional H^+ was to neutralize the side chain carboxyl group, which in agreement with the previous finding

(Kottra *et al.*, 2002). However, limited information of charged tripeptides was available so far.

The acidic microclimate has been shown to exist and be able to provide a proton gradient across the intestinal epithelium (pH 6.65, jejunum v.s. pH 7.3, intracellular) (Daniel *et al.*, 1989). Because the substrate transport via PEPT1 would result in the acidification of intracellular pH, a system to counterbalance the intracellular accumulation of H^+ was needed (Fei *et al.*, 1994). Thwaites has demonstrated that after adding Gly-Sar, the activity of Na^+/H^+ exchanger (NHE3) on the apical membrane increased, but remained the same on basolateral membrane (NHE1) in Caco-2 cell (Thwaites *et al.*, 1999). PEPT1 activity has been shown to be influenced when inhibiting the NHE3 activity as well (Kennedy *et al.*, 2002; Watanabe *et al.*, 2005). Although the NHE3-coupling peptide transport pathway has been well accepted (Figure 2.2), the possibility that other systems involved in the maintenance of pH gradient could not completely rule out. NHE2, an isoform of Na^+/H^+ exchanger has been found to express on the apical membrane of duodenum and ileum in human but the contribution to PEPT1 transporter has not been studied yet (Hoogerwerf *et al.*, 1996).

Polymorphism

Although only few genetic polymorphism studies have been performed, the overall conclusion was that PEPT1 as a conserved gene showed very low allelic frequencies of single-nucleotide polymorphisms (SNPs) (Zhang *et al.*, 2004b; Anderle *et al.*, 2006; Sala-Rabanal *et al.*, 2006). In Zhang's study, 44 ethnically diverse individuals were taken for SNP identification. Total 13 SNPs were identified and 9 out of them were nonsynonymous mutations. Using HeLa cells transfected system, 9 mutated hPEPT1 were

expressed. Although there were overall 1.6 to 2.2 fold increase in mRNA expression, only P586L (1758C>T) variant (frequency = 1.1%) showed decrease of uptake of Gly-Sar. Interestingly, the substrate specificity and substrate affinity were not affected in P586L variant. Instead, the immunoblot and immunocytochemistry results showed the reduction of protein expression of P586L. Therefore, taken together, P586L was thought to have profound effect on protein stability or protein translation (Zhang *et al.*, 2004b). Another larger study (247 individuals) was performed across different races by Anderle. 9 out of 17 were nonsynonymous mutations and 8 of them were further tested in Cos7 and CHO cells transfected systems. Only one variant F28Y showed decrease affinity to Gly-Sar but no alteration in the protein expression and capacity. One interesting finding was although the allelic frequencies of many SNPs were relatively low, some SNPs showed ethnic bias. For example, V21I, F28Y, S117R, V112M, P537S were bias to African American.

Since most allelic frequencies of SNPs of PEPT1 were relatively low, Salazar-Rabanal investigated the significance of the most frequent SNPs, S117N and G419A of PEPT1. Not surprisingly, S117N and G419A showed no change of capacity, affinity, and substrate specificity, suggesting the polymorphism of PEPT1 has low impact of oral peptidomimetic drugs. A pharmacokinetic study was performed to investigate the impact of PEPT1 on the intra- and inter-individual variabilities of valacyclovir systemic exposure. The result again supported that PEPT1 was a highly conserved gene, since no obvious contribution from SNPs was observed. The intra-individual variability was significant lower than inter-individual variability and even when concomitant administering cephalexin, the systemic exposure ($AUC_{0 \rightarrow \infty}$) was changed less than 2 fold

inter-individually (Phan *et al.*, 2003). Taken all together, PEPT1 is a conserved gene with very stable activity *in vivo*, which ensures PEPT1 as a good drug delivery target.

Regulation of PEPT1

Because PEPT1 has indispensable role in protein assimilation, the transport activity must be modulated to meet physiological needs. PEPT1 has been shown to be regulated under a variety of factors and conditions (Adibi, 2003). Although the pathways involved in the regulation of PEPT1 has not been fully understood, the general mechanisms might be categorized to:

- (1) Modification of PEPT1 protein post-translationally: Study performed in Caco-2 cell has demonstrated that phorbol esters (PMA), an activator of protein kinase C, could decrease the maximal capacity (V_{\max}) without changing affinity (K_m) of Gly-Sar uptake (Brandsch *et al.*, 1994).
- (2) Recruitment of PEPT1 protein from the intracellular vesicles to plasma membrane (cellular trafficking): Regulation has been observed when insulin was added to the Caco-2 cells. Specifically, Gly-Gln uptake was significantly increased with a change in V_{\max} but not K_m . The increasing uptake was a result of the increasing amount of PEPT1 protein at the apical membrane without increasing the mRNA level. Since the increase could be inhibited by colchicine, a depolymerizer of microtubules, the regulation mechanism of insulin was suggested to increase translocation of PEPT1 from a preformed cytoplasmic pool (Thamotharan *et al.*, 1999b).

(3) Modification of the gene expression transcriptionally or change on mRNA stability:

PEPT1 substrates (e.g. Gly-Sar or Gly-Gln) but not the single amino acid residues (e.g. Glycine, sarcosine, or glutamine) have been shown to stimulate the uptake of substrate in Caco-2 cells with a change of V_{\max} , but not K_m . The increase was attributed to the increase of mRNA expression for PEPT1 by Northern blot analysis and increase of mRNA stability. (Thamotharan *et al.*, 1998; Walker *et al.*, 1998).

(4) Modulation of the intracellular ion homeostasis: When one of the exchanger NHE3 for proton balance was influenced by inhibitors, such as vasoactive intestinal polypeptide (VIP) or NHE3 selective inhibitor S1611, the uptake of Gly-Sar was significantly affected in capacity rather than affinity (Thwaites *et al.*, 2002).

Several factors and conditions have been demonstrated to influence the PEPT1 activity via one of the mechanisms above. The factors that affected PEPT1 activity could be generally categorized as physiological, pharmacological, and pathological. (Adibi, 2003).

Physiological factors:

A number of physiological factors have been shown to influence the PEPT1 activity. First, the substrate of PEPT1 has been suggested to stimulate the PEPT1 activity through the increase of the stability of mRNA and increase of the mRNA expression (Thamotharan *et al.*, 1998; Walker *et al.*, 1998).

Insulin could promote the translocation of the preformed PEPT1 from the intracellular pool to increase the protein level of PEPT1 on membrane, which resulted in the increase of PEPT1 activity (Thamotharan *et al.*, 1999b).

Leptin, an adipocyte secreted hormone has been shown to have short-term and long-term effect on PEPT1 activity. Both *in vitro* and *in vivo*, leptin treated groups showed increase of uptake of Gly-Sar. The mechanism of increasing PEPT1 activity has been suggested to relate to the increase of translocation of PEPT1 from the cytoplasmic pool (Buyse *et al.*, 2001) and also transcriptionally stimulated the mRNA expression via cAMP-response element-binding protein (CREB) and Cdx2 transcription factors to increase protein expression (Nduati *et al.*, 2007). Interestingly, the leptin knockout mice (ob/ob) showed significant low PEPT1 protein, mRNA expression and uptake activity as compared to wild-type mice. However, after 7 days treatment of leptin via implanted mini-osmotic pump subcutaneously, the expression and activity of PEPT1 were rescued comparably to wild-type mice (Hindlet *et al.*, 2007).

Epidermal growth factor (EGF) also has agonist effect on PEPT1 activity. The stimulation was fairly fast since a significant increase could be measured after 5 mins treatment in Caco-2 cell. However, the agonist effect only took place when the EGF was present in the basolateral membrane side, which explained by the predominant expression of EGFR at basolateral membrane of Caco-2 cell (Bishop *et al.*, 1994). The increase of uptake only affected the capacity (V_{\max}) without influencing the affinity (K_m). However, the mechanism of the regulation was not conclusive (Nielsen *et al.*, 2003).

Most of hormones exhibited their effect upon binding to the corresponding receptor on the cell membrane (e.g. EGF – EGFR). Triiodothyronine (T_3), however, initiated the action inside the cell, within the nucleus. Ashida showed that pretreated Caco-2 cell with T_3 for 3 days significantly decrease the uptake of Gly-Sar. The kinetic analysis showed no change in affinity (K_m) and decrease nearly two fold in capacity (V_{\max}), suggesting

that a decrease of the population of PEPT1 on membrane. The mechanism was suggested to be transcriptional, either by inhibition of transcription and/or decrease in the stability of mRNA. The actual bind site within nucleus has not been identified since there was no thyroid hormone-responsive element found upstream promoter region of PEPT1 gene (Ashida *et al.*, 2002).

Interestingly, PEPT1 also has been shown to regulate along the day (diurnal rhythm) and development stages. Although there was no solid conclusion being made, the general trend was that PEPT1 peaked at 3 pm in mRNA, protein, uptake, and capacity in duodenum and jejunum, where the majority of absorption occurred (Qandeel *et al.*, 2009). As for the development stages, the mRNA and protein expression of PEPT1 peaked on day 3 to 5 after birth and transiently rose on day 24, when was about the time of weaning (Shen *et al.*, 2001).

Pharmacological factors:

5-fluorouracil was an anticancer agent, which has deleterious effect on the intestinal mucosa layer and intestinal villus. After 3 days orally administered of 5-fluorouracil in rat, the villus height was markedly decrease and atrophy of mucosa layer was noticed. Under this circumstance, the uptake activities of D-glucose and amino acid glycine were significantly impaired except for PEPT1 and the mRNA expression of all the detected enzymes and transporters were decreased except for PEPT1 (increase > 2 fold). Therefore, it was believed the preservation of PEPT1 activity was due to the increase of synthesis of PEPT1, which resulted in a normal protein expression as compared to control (Tanaka *et al.*, 1998).

Clonidine is an agonist for α_2 -adrenergic receptors, which has been shown to increase the cephalexin plasma concentration after i.v. bolus (Berlitz *et al.*, 1999). A subsequent study was found that the increase of cephalexin uptake was involved in the increase of expression of PEPT1, the transporter for cephalexin. The change affected only on V_{\max} , not on K_m and the regulatory mechanism was confirmed by clochicine abolishment of the stimulation, suggesting an increase of the translocation of preformed cytoplasmic PEPT1 (Berlitz *et al.*, 2000).

The regulation of a selective σ -ligand pentazocine was also investigated in the Caco-2 cells. The results revealed that PEPT1 mRNA was increased along with the uptake activity of Gly-Sar in a dose dependent and time dependent manners. The kinetic analysis showed that the stimulation of PEPT1 activity changed only in V_{\max} , not in K_m (Fujita *et al.*, 1999).

Immunosuppressive drugs tacrolimus and cyclosporine were other examples. They both have been found to decrease the PEPT1 activity by changing the V_{\max} rather than K_m (Motohashi *et al.*, 2001).

Pathological factors:

PEPT1 as the major peptide transporter in the intestine has been shown to have obligatory role in protein assimilation (Ganapathy *et al.*, 2006). Therefore, it appears to be interesting to study the effect of malnutrition on the function and expression of intestinal PEPT1. The effect of brief and prolonged fasting on PEPT1 has been studied. Thamotharan showed that the Gly-Gln uptake significantly increased after 1 day fasting in rat by brush-border membrane vesicle. The expression of PEPT1 was also increased in

both mRNA and protein levels. The kinetic analysis suggested that the V_{\max} was increase by 2 fold, whereas the K_m was unaffected (Thamotharan *et al.*, 1999a). A prolonged fasting (starvation) study, which rats were starved for 4 days and semistarved (50% amount of control) for 10 days has been performed and demonstrated an increase of mRNA and protein in both groups (mRNA increase 179% and 164% for starvation and semistarvation, respectively). In contrast to the increase mRNA expression of PEPT1, the mRNA of sodium-dependent glucose transporter 1 (SLGT1) had no significant change (Ihara *et al.*, 2000). Additional study visualized the PEPT1 upregulation by immunofluorescence localization technique and suggested the increasing PEPT1 protein was mainly at the tip of villus as opposed to the crypt (Ogihara *et al.*, 1999). Therefore, it has been suggested the upregulation of PEPT1 under starvation condition was possibly an adaptive response to absorb every possible nutrient in the lumen (Ogihara *et al.*, 1999).

Diabetes is another interesting pathological condition to study its effect on PEPT1. Since it has been demonstrated that insulin could increase PEPT1 activity by promoting the translocation of the preformed PEPT1 from the intracellular pool (Thamotharan *et al.*, 1999b), diabetes has been expected to have down-regulated effect on PEPT1. Unexpectedly, in the streptozotocin-injected diabetic animals, the uptake of Gly-Gln was increased with a change in V_{\max} rather than K_m . The mechanism of increasing PEPT1 activity in this insulin deprived diabetic rat was found to be the increase of mRNA stability since the transcriptional rate showed no difference (Gangopadhyay *et al.*, 2002).

Proinflammatory cytokines could be induced under bacteria or parasite infection. Studies have suggested that PEPT1 was upregulated under infection condition. *Cryptosporidium Parvum* induced diarrhea was commonly seen in humans. Study has

shown that PEPT1 mRNA was increased on day 10, when was the peak of infection in the distal small intestine in the suckling rats model. After the spontaneous clearance of the parasite, PEPT1 mRNA returned to normal (Barbot *et al.*, 2003). Although atrophy was normally present in the infection condition, which was a factor (malnutrition) that stimulated PEPT1 expression (Thamotharan *et al.*, 1999a), the increase of cytokine IFN- γ was believed to be the actual factor responsible for the upregulation (Marquet *et al.*, 2007).

Involvement of PEPT1 in Inflammatory Bowel Disease

It has been shown that PEPT1 normally expressed in small intestine, not in colon (Ogihara *et al.*, 1996). However, in an extreme condition, humans with short-bowel syndrome (SBS), PEPT1 has been shown to upregulate in the colon epithelium (Ziegler *et al.*, 2002). Merlin first hypothesized the possibility that aberrant colonic PEPT1 might interact with the bacterial peptides in colon. Caco-2 cell served as a best model for this purpose because Caco-2, a colon cancer cell, did express PEPT1 transporter. The bacterial peptide, N-formyl-Met-Leu-Phe (fMet-Leu-Phe) has been shown to be actively transported into Caco-2 cell via PEPT1. Most interestingly, fMet-Leu-Phe could promote the neutrophil transmembrane migration and the migration could be reduced by PEPT1 substrate Gly-Pro and Gly-Leu, but not glycine, suggesting that PEPT1 transporter was involved in the neutrophil transmembrane migration (Merlin *et al.*, 1998). In a subsequent study, the aberrant colonic PEPT1 expression in the colon epithelium of inflammatory bowel disease (IBD) patient (both CD and UC) has been demonstrated. By transfecting HT29-Cl.19A, a cell line does not express PEPT1 with a hPEPT1 construct,

the uptake of Gly-Sar increased and the uptake of fMet-Leu-Phe resulted in an increase the MHC class I expression, suggesting the functional consequence of the aberrant colonic expression of PEPT1 in the patient with IBD (Merlin *et al.*, 2001). In addition to *in vitro* system, an *in situ* perfusion system has demonstrated an increase of myeloperoxidase (MPO) activity after perfusion of fMet-Leu-Phe in jejunum, but not in colon, suggesting that the uptake of fMet-Leu-Phe (kinetic) could translate into the increase of MPO activity (dynamic) because by adding Gly-Gly, the increase of MPO activity would reversed to control level (Buyse *et al.*, 2002). After the hypothesis of the involvement of PEPT1 in intestinal inflammation and/or IBD, more studies focusing on the impact of proinflammatory cytokine on PEPT1 activity. Interferon- γ has been demonstrated to increase Gly-Sar uptake in a dose and time dependent manners in Caco-2 BBE cell. The uptake fMet-Leu-Phe, a bacterial peptide also has been shown to increase in the presence of interferon- γ . The stimulation of Gly-Sar uptake by interferon- γ was specific to PEPT1 since in another cell line HT29-Cl.19A, the stimulation was not observed. The mechanism of the stimulation of PEPT1 activity by interferon- γ was found to be the increase of intracellular pH upon application of interferon- γ . The protein and mRNA expression of PEPT1 did not change in the presence of interferon- γ (Buyse *et al.*, 2003). Similar effect of interferon- γ on Gly-Sar uptake was also observed in another study. However, in this study, after application of interferon- γ , an increase of mRNA and protein level of PEPT1 has been demonstrated (Foster *et al.*, 2009).

Muramyl dipeptide (MDP), a ligand of NOD2 receptor has been shown to be the substrate of PEPT1 as well (Ogura *et al.*, 2001). MDP has been demonstrated to exhibit an inhibitory effect on Gly-Sar uptake in a stereospecificity manner and could be

transported directly with Km around 4.3 mM in Caco-2 BBE cells. More importantly, the transport of MDP caused an increase release of IL-8 and MCP-1 and activation of NF- κ B. Application of siRNA of PEPT1 and NOD2 reduced the increasing release of IL-8 in the presence of MDP in the Caco-2 BBE cells (Vavricka *et al.*, 2004). Another bacterial peptide L-Ala- γ -D-Glu-meso-DAP (Tri-DAP) has also been suggested to be the substrate of PEPT1 recently (Dalmaso *et al.*, 2010).

The regulation of PEPT1 by proinflammatory cytokines has also been shown *in vivo*. Mice intraperitoneally injected TNF- α and IFN- γ have been demonstrated to upregulate the protein expression and the transport activity of PEPT1 (Gly-Sar uptake) in the proximal and distal colon, but no change of mRNA of PEPT1 has been observed, which provided supportive data for the hypothesis that PEPT1 was involved in the intestinal inflammation and/or IBD (Vavricka *et al.*, 2006). Therefore, a hypothesized model for the involvement of the aberrant colonic hPEPT1 in IBD has been proposed (Figure 2.3) (Charrier *et al.*, 2006b).

Soon after the model has been proposed, more studies using experimental colitis animal models to elucidate the role of colonic PEPT1 have been performed. Dextran sodium sulfate (DSS) and trinitrobenzene sulfonic acid (TNBS) induced colitis animal models were used to investigate the role of colonic PEPT1. Dalmaso showed that a bioactive tripeptide Lys-Pro-Val (KPV) could ameliorate the colitis in two animal models. Because Lys-Pro-Val (KPV) has been also shown to be the substrate of PEPT1 in the study and previously study demonstrated the upregulation of PEPT1 in colon under inflammation condition in rat after DSS treatment by immunohistochemistry (IHC) (Radeva *et al.*, 2007), Dalmaso suggested that the effect of Lys-Pro-Val (KPV) was

partly due to the increase of activity of PEPT1 in colon (Dalmaso *et al.*, 2008). Another intriguing colitis model has been used to investigate the role of PEPT1 in colon. In the study, an upregulation of PEPT1 has been demonstrated in the presence of pathogenic bacteria enteropathogenic *Escherichia coli* (EPEC) in HT29-Cl.19A cells *in vitro* and in the presence of *Citrobacter rodentium* *in vivo* (Nguyen *et al.*, 2009). Unexpectedly, the severity of infection by *Citrobacter rodentium* for hPEPT1 transgenic mice was lesser than that of wild-type mice regarding to the expression of pro-inflammatory cytokines, chemokines, and anti-inflammatory cytokines (i.e. IL-1 β , IL-6, IL-12p35, IL-12p40, TNF- α , IFN- γ , IL-10, and TGF- β). One explanation was that PEPT1 could attenuate the bacteria adherence to the lipid raft, which has been shown in the EPEC adherence study in hPEPT1 transfected HT29-Cl.19A cell. Although it seemed to conflict the hypothesis being proposed earlier, an interesting finding from a genetic polymorphism associated with inflammatory bowel disease study supported the contradiction (Zucchelli *et al.*, 2009). The common variant of PEPT1 (Ser117Asn) was found to associate with inflammatory bowel disease in two populations (Sweden and Finland) with opposite genetic effect (risk and protection, respectively), indicating the complexity of the role of PEPT1 in inflammatory bowel disease.

The results from the study investigating the role of colonic PEPT1 seemed to be disease model dependent. Unlike previous results in *Citrobacter rodentium* infection model, the colitis severity was higher in two types of hPEPT1 transgenic mice models than that of wild-type mice. However, not only the colitis induction method, but also the type of transgenic mice used affected the overall outcome. In the study, TNBS induced

colitis model failed to exhibit difference between villin-directed hPEPT1 transgenic mice and wild-type mice (Dalmasso *et al.*, 2011a).

Several other colitis induction models have suggested the important role of aberrant expression of colonic PEPT1. Intestine resection rat model has been shown to upregulate PEPT1 in the colon at week 2 (Shi *et al.*, 2006a; Shi *et al.*, 2006b). The functional consequence of the upregulation of colonic PEPT1 has been shown by perfusing the bacterial tripeptide fMet-Leu-Phe. The MPO activity was increased after perfusion of fMet-Leu-Phe in the resection rats but not in the transection rats. IL-10 knockout mice model has been shown to upregulate PEPT1 in colon as well (Chen *et al.*, 2010). The mRNA and protein expression level of PEPT1 were increased in the IL-10 knockout mice as compared to wild-type mice. Also, the uptake of cephalixin, a PEPT1 substrate from colonic perfusion was increase in the IL-10 knockout mice as compared to wild-type mice. One of the therapeutic alternatives, *Lactobacillus plantarum* (LP) was also investigated in this study. It demonstrated a reduction of pro-inflammatory cytokines TNF- α and IFN- γ along with the decrease expression of colonic PEPT1 in mRNA and protein and decrease of the uptake of cephalixin from colon. The results suggested that the decrease of inflammatory response by LP treatment might associate with the decrease of colonic PEPT1 since PEPT1 has been shown to transport many bacterial peptides (Merlin *et al.*, 1998; Vavricka *et al.*, 2004; Dalmasso *et al.*, 2010).

A novel post-transcriptional regulation of PEPT1 by MicroRNA-92b has been demonstrated in Caco-2 BBE cells (Dalmasso *et al.*, 2011b). The regulation might also be related to intestinal inflammation since the L-Ala- γ -D-Glu-meso-DAP (Tri-DAP)

induced proinflammatory responses could be ameliorated in the presence of MicroRNA-92b in Caco-2 BBE cells.

A table of studies focusing on PEPT1 related to intestinal inflammation was listed on Table 2.1.

INFLAMMATORY BOWEL DISEASE

Description

Inflammatory bowel disease (IBD) is characterized in two phenotypes, Crohn's disease (CD) and ulcerative colitis (UC). The distinction between two types of IBD is the clinical presentation (e.g. location of inflammation, type of inflammation). CD causes transmural inflammation and affects any part of the gastrointestinal tract, typified by the formation of granulomas, stricturing and fistulae histologically. In contrast, UC is limited to the colon and typified by mucosal inflammation (Abraham *et al.*, 2009).

Incidence and Prevalence

The prevalence of IBD (CD and UC) in the U.K. are 214 per 100,000 and 122 per 100,000, respectively. However, there are significant variations across the regions (Shivananda *et al.*, 1996). In the United States, it affects approximately 1.4 million Americans and its peak onset is at age 15 to 30 years (Loftus, 2004).

Aetiology

Although IBD has been known for over 50 years, the exact causes and mechanisms have remained unclear because of the different presentations of disease and the involvement of multifactorial background of disease patterns (Corfield *et al.*, 2011). Despite the uncertainties of the pathogenesis of IBD, there have been several factors

proposed to confer to the susceptibility of IBD, which were genetics (including immune response and epithelial barrier function), immune dysregulation, and environmental factors (e.g. microbial flora, smoking, diet, drug) (Kucharzik *et al.*, 2006; Xavier *et al.*, 2007).

Genetics:

There have > 100 susceptible genes for CD, > 50 genes for UC, and ~ 50 genes shared between them (Corfield *et al.*, 2011) been identified. They could generally be classified as:

- (1) Innate immune response linked: NOD2 (nucleotide-binding oligomerization domain 2), TLR4 (Toll-like receptor 4) and NALP3 [NLR (NOD-like receptor) family, pyrin domain-containing 3].
- (2) Autophagy linked: NOD2, ATG16L1 (autophagy-related 16-like 1), IRGM (immunity-related GTPase) and DAP (death-associated protein).
- (3) Epithelial barrier function linked: GNA12 (guanine-nucleotide-binding protein α 12), HNF4 (hepatocyte nuclear factor 4), CDH1 (cadherin 1), LAMB1 (laminin β 1), MDR1, and MUC2.
- (4) Adaptive immune response linked: HLA class 2, IL10 (IL is interleukin), IL12, IL17, IL23, and IL23R (IL-23 receptor) related to T-cell function.

NOD2 is an intracellular pattern-recognition receptor (PRR), which recognizes the common breakdown product of peptidoglycan cell wall, muramyl dipeptide (MDP), followed by activating innate immune system via NF- κ B and MAPK pathway (Kelsall, 2005). Genomic analysis of patients with CD revealed that people with NOD2 mutations were more susceptible to CD (Hugot *et al.*, 2001; Ogura *et al.*, 2001). In vitro data

showed that peripheral blood mononuclear cells (PBMCs) from CD patients with NOD2 frameshift mutation no longer respond to NOD2-activating agonists (Netea *et al.*, 2005). However, this loss of function phenomenon was conflicted with data from a mouse model with NOD2 frameshift mutation similar to human homologous, which showed an increase cytokine secretion when challenging with dextran sodium sulfate (DSS) (Maeda *et al.*, 2005). One explanation for the deficiency of *in vitro* and *in vivo* was proposed by using NOD2 knockout mice. The data have shown that the loss of NOD2 resulted in the decrease of cryptdins (α -defensin in human) expression produced in intestinal Paneth cells. Therefore, the control over the intestinal bacteria was impaired (Kobayashi *et al.*, 2005). Another explanation was that NOD2 was a negative regulator of TLR2 signaling pathway and the dysfunction of NOD2 enhanced the Th1-mediated inflammatory response (Watanabe *et al.*, 2004). It has been further supported from the data of NOD2 transgenic mice model, which resulted in the increase production of IL-12 and the susceptibility were decrease by challenging with peptidoglycan and trinitrobenzene sulfonic acid (TNBS) as compared to wild-type mice (Yang *et al.*, 2007).

Another gene related to the epithelial barrier of intestine MUC2, which encoded the mucin protein has been demonstrated to be a key gene for IBD as well. In a MUC2 knockout mice study, deletion of MUC2 resulted in the spontaneously development of colitis. When challenging with DSS, the MUC2 knockout mice exhibited earlier onset and higher disease activity index as compared to wild-type mice (Van der Sluis *et al.*, 2006).

Immune Dysregulation:

The mucosal homeostasis is a balancing act between effector cells and regulatory cells. Either excessive effector cells or shortage of regulatory cells would end up with a dysregulation of mucosal homeostasis (Kucharzik *et al.*, 2006). Both types of dysregulation have been demonstrated in the literature. IL-12 (Monteleone *et al.*, 1997), TNF- α (Breese *et al.*, 1994), and IFN- γ (Fuss *et al.*, 1996) have been shown to overproduce in CD patients. In addition, study has shown that the number of regulatory T cells decreased in the peripheral blood in active IBD patients (Maul *et al.*, 2005). The hypothesis of immune dysregulation has been further proven by the development of several colitis mice models. One example was TNF^{ARE} mutant mice, by increasing the mRNA stability of TNF- α resulting in the overproduction of TNF- α . These mice developed CD-like phenotype in the terminal ileum or proximal colon at age of 2 to 4 weeks. The other type of model was due to the impaired regulatory cell response, such as IL-10 deficient mouse (Kuhn *et al.*, 1993) and TGF- β deficient mice (Shull *et al.*, 1992). These mice developed colitis spontaneously at around age of 4 weeks. Taken together, from the clinical observation and experimental mice models, the importance of the balance of effector and regulatory cells to the IBD have been delineated.

Environmental Factors:

The clinical association between microbiome and IBD has been observed (Swidsinski *et al.*, 2002). However, the role of human gut microbiome in the IBD has been focused recently due to the better understanding and analytic methods of human microbial flora (Flanagan *et al.*, 2011). Both commensal organism and pathogenic organism have been shown to associate with IBD. *Faecalibacterium prauznitzii*, a member of the *C. leptum* group was found to be negatively associated with the ileal CD.

Individual with predominantly ileal CD had lower abundance of *Faecalibacterium prauznitzii*, but increasing abundance of *Escherichia coli* as compared to healthy subjects (Willing *et al.*, 2009). Interestingly, oral administration of either live or the supernatant of *Faecalibacterium prauznitzii* showed a reduction of the severity of TNBS induced colitis in mice (Sokol *et al.*, 2008). On the other hand, the pathogenic bacteria, such as *Mycobacterium avium* subsp. *Paratuberculosis* (MAP) has been postulated as a potential pathogenic agent in CD due to the finding of MAP's DNA within the granulomas of CD patients (Ryan *et al.*, 2002).

Conventional Medical Management of Inflammatory Bowel Disease

Since there is no known cure for IBD, the principles of therapy for IBD are first, to induce remission and to maintain remission over time. Second, to heal the inflamed mucosa, maintain the quality of life, improve nutritional status, and prevent complications (Katz, 2007). With the advancement of medicines and the experience and knowledge of IBD, the therapeutic strategy evolved over time in terms of the optimization of drug type, timing, and context (Burger *et al.*, 2011). Current options for IBD included 5-aminosalicylates (5-ASAs; sulphasalazine, mesalazine, olsalazine, balsalazide), corticosteroids (prednisolone, prednisone, 6-methylprednisolone, and budesonide), immunosuppressive agents (6-mercaptopurine (6-MP), azathioprine methotrexate), and anti-tumor necrosis factor agents (infliximab, adalimumab, certolizumab). In more severe situation, surgery will be another option.

Future Therapeutic Options for Inflammatory Bowel Diseases

With increasing knowledge in immunology and the mechanism of inflammatory bowel disease, development of new class of therapeutic alternatives has evolved dramatically. Some new class therapeutic agents were listed below (Plevy *et al.*, 2011):

- (1) Targets in mucosal immunity: anti-IL-12/23 mAb, anti-IL-23 mAb, anti-IL-17, IL-6 inhibitors, other TNF inhibitors, anti- α 4 β 7 mAb, anti- α 7 mAb, anti-MADCAM mAb, CCR9 antagonist.
- (2) Targeting therapies to sites of inflammation: delivery of KPV and siRNAs.
- (3) Cell-based therapeutics: Stem cell, autologous bone marrow transplant.

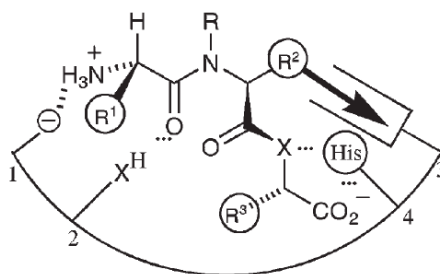


Figure 2.1. Structure template for PEPT1 (Adopted from Bailey et al., 2006).

#	Factor	description	score
1	An N-terminal -NH ₃ ⁺ group	1° amines 2° and/or aryl amines Others	+2 0 -2
2	Stereochemistry at C _α of R ¹	Template stereochemistry at α-C ¹ Planar Incorrect stereochemistry	+1 0 -1
3	Planar backbone from N-terminal C _α to R ²	Planar from α-C ¹ → side-chain of 2nd residue	+1
4	A hydrogen bond to the first peptide C=O	Any C=X (where X is heteroatom with lone pair) at the 1st peptide bond	+1
5	No alkylation of N ² -amide NH	Alkylation of N ² -amide nitrogen	-1
6	Stereochemistry at C _α of R ²	Template stereochemistry at α-C ¹ Planar Incorrect stereochemistry	+2 0 -2
7	Hydrophobic pocket for R ₂ , possessing a strong directional vector as indicated (+2 per aryl group)	Each aryl ring in pocket Each charge in pocket	+2 -1
8	A carboxylate binding site	Carboxylate within H-bonding distance of histidine in template	+2
9a	For larger substrates: space for side-chain R ³	Template stereochemistry at α-C ³ Planar Incorrect stereochemistry	0 -1 -2
9b	An alternative (tripeptide) carboxylate binding site	Carboxylate within H-bonding distance of histidine in template	+2
10	Size	M _r < 300 M _r > 300	-1 -2

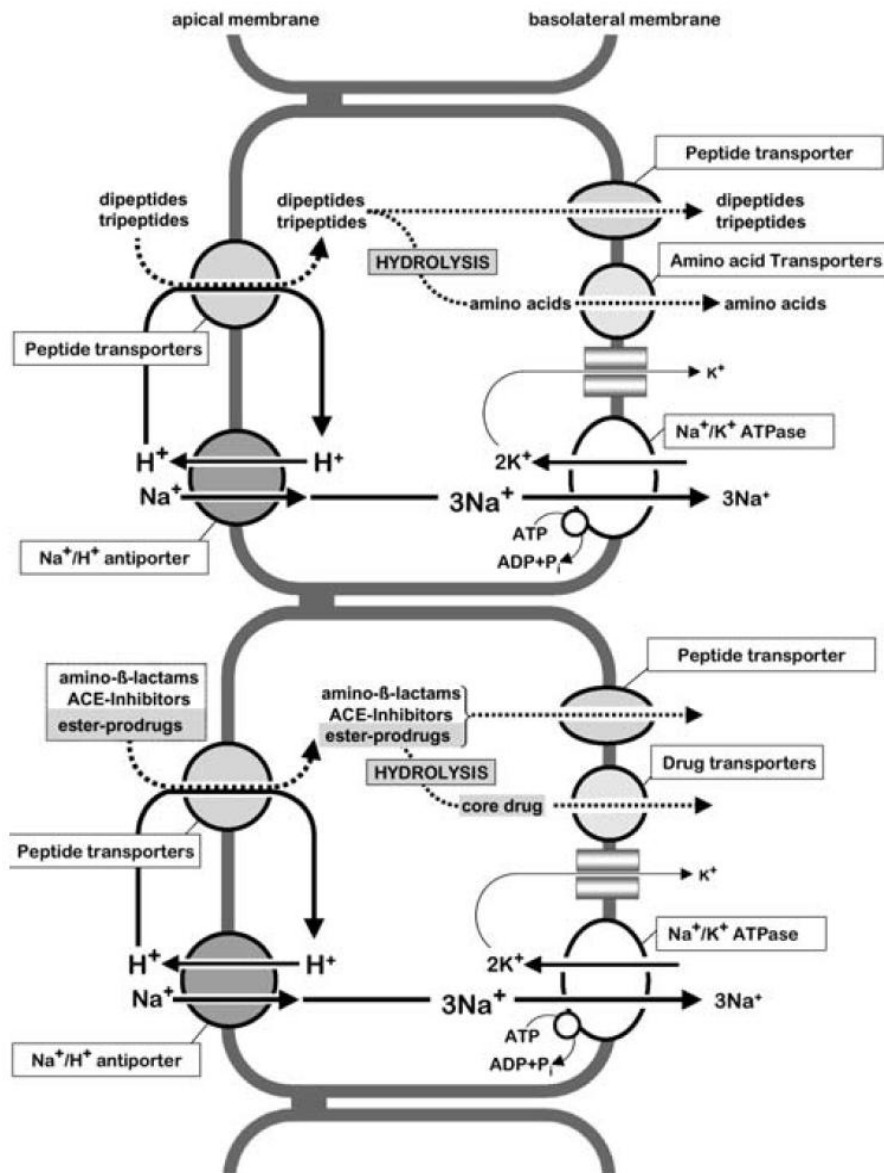


Figure 2.2. Pathway of peptide absorption (Adopted from Daniel et al., 2004).

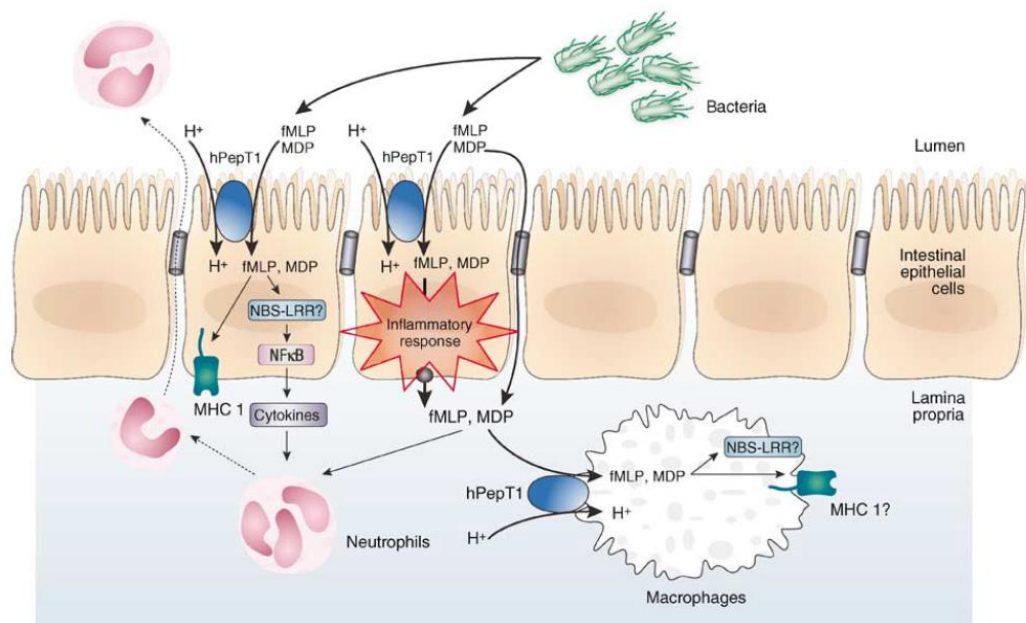


Figure 2.3. Model of the involvement of hPEPT1 in IBD (Adopted from Charrier et al., 2006).

Model	Result	Reference
Caco-2 BBE / neutrophil	* fMet-Leu-Phe was transported by PEPT1 * fMet-Leu-Phe induced neutrophil transmigration	(Merlin et al., 1998)
Oocyte	* fMet-Leu-Phe was transported by PEPT1 * Gly-Sar uptake was inhibited by fMet-Leu-Phe	(Merlin et al., 1998)
Colon of UC and CD patients	* Aberrant colonic PEPT1 expression in the colon of CD and UC patient	(Merlin et al., 2001)
HT29-Cl.19A / GFP-hPepT1	* Uptake of fMet-Leu-Phe increased MHC class I expression	(Merlin et al., 2001)
Rat perfusion	* fMLP perfusion increase the MPO activity in jejunum, but not in colon * Gly-Gly successfully inhibited the increased MPO activity in jejunum	(Buyse et al., 2002)
Caco-2 BBE	* fMet-Leu-Phe uptake stimulate NK- κ B and AP-1	(Buyse et al., 2002)
Caco-2 BBE	* IFN- γ increased Gly-Sar and fMet-Leu-Phe uptake * IFN- γ increased the intracellular pH rather than mRNA or protein expression level of PEPT1	(Buyse et al., 2003)
Caco-2	* IFN- γ increased Gly-Sar permeability	(Foster et al., 2009)
Caco-2 BBE	* IFN- γ increased the mRNA and protein expression level * MDP was transported by PEPT1 (Km = 4.3 mM)	(Vavricka et al., 2004)
Caco-2 BBE	* Stereoisomers of MDP (LL, DD) were not PEPT1 substrates * MDP induced IL-8, MCP-1, and NF- κ B	(Vavricka et al., 2006)
Caco-2 BBE	* TNF- α and IFN- γ increased the Gly-Sar uptake	(Vavricka et al., 2006)
Mouse	* TNF- α and IFN- γ increased the protein level of PEPT1 and Gly-Sar uptake * TNF- α and IFN- γ did not affect mRNA level of PEPT1	(Vavricka et al., 2006)
human	* PEPT1 upregulated in colon of IBD patient * Current model of PEPT1 involved in the IBD	(Charrier et al., 2006b)
Rat / DSS	* PEPT1 upregulation was observed by IHC in distal colon * mRNA decrease in most of intestinal segments except for distal colon * no protein level of PEPT1 changed was observed by western blot * Pharmacokinetic profiles of cephalexin and valacyclovir showed no difference	(Radeva et al., 2007)
Mouse / DSS and TNBS	* KPV ameliorate the inflammation induced by DSS and TNBS	(Dalmasso et al., 2008)
HT29-Cl.19A / EPEC	* Enteropathogenic Escherichia coli (EPEC) upregulated PEPT1 expression	(Nguyen et al., 2009)
Mouse / <i>Citrobacter rodentium</i>	* PEPT1 upregulation after <i>Citrobacter rodentium</i> infection in proximal and distal colon * Severity of <i>Citrobacter rodentium</i> infection in hPEPT1 transgenic mice was lesser than wild type mice regarding to cytokines mRNA expression	(Nguyen et al., 2009)
Human	* Genetic polymorphism study revealed an opposite genetic effect on PEPT1 associated with IBD	(Zucchelli et al., 2009)
Caco-2 BBE	* L-Ala-gamma-d-Glu-meso-DAP (Tri-DAP) decreased the Gly-Sar uptake	(Dalmasso et al., 2010)
Mouse	* L-Ala-gamma-d-Glu-meso-DAP (Tri-DAP) increased KC release in hPEPT1 transgenic mice	(Dalmasso et al., 2010)
Mouse / DSS and TNBS	* DSS treated mice showed higher severity in both β -actin and villin-directed transgenic mice * TNBS treated mice only showed higher severity in β -actin directed transgenic mice * hPEPT1 transgenic / NOD2 ^{-/-} suggested the inflammatory activity of hPepT1 is NOD2-dependent	(Dalmasso et al., 2011)
Caco-2 BBE	* MicroRNA-92b down-regulated PEPT1 and ameliorated the Tri-DAP induced inflammatory response	(Dalmasso et al., 2011b)
Mouse / <i>Lactobacillus plantarum</i> (LP)	* IL-10 knockout mice increased the mRNA and protein expression of PEPT1 in colon * Functional activity of PEPT1 also increased in IL-10 knockout mice in cephalexin colonic perfusion * LP ameliorated the inflammatory response (TNF- α , IFN- γ) and decreased the mRNA and protein expression of colonic PEPT1	(Chen et al., 2010)
Rabbit / <i>Eimeria magna</i> oocytes	* chronic inflammation induced by <i>Eimeria magna</i> oocytes decrease the Km of Gly-Sar rather than V _{max} * no change of PEPT1 mRNA was observed	(Sundaram U et al., 2005)
Rat / LPS	* no PEPT1 regulation was observed after 24 h LPS treatment	(Mori N et al., 2011)
Rat / DSS	* Decrease of PEPT1 mRNA was observed in jejunum and ileum	(Shu HJ et al., 2002)
Suckling rat / <i>Cryptosporidium parvum</i>	* PEPT1 mRNA increase was observed	(Barbot et al., 2003)
Suckling rat / <i>Cryptosporidium parvum</i>	* PEPT1 protein showed no change	(Marquet et al., 2007)
<i>Xenopus laevis</i> oocyte	* MDP and fMet-Leu-Phe were transported by hPEPT1 * NOD1 activating muramyl peptides were not hPEPT1 substrates	(Ismair MG et al., 2006)

Table 2.1. List of studies focusing on PEPT1 related to intestinal inflammation.

References

- Abraham C, Cho JH (2009). Inflammatory bowel disease. *N Engl J Med* **361**: 2066-2078.
- Adibi SA (2003). Regulation of expression of the intestinal oligopeptide transporter (Pept-1) in health and disease. *Am J Physiol Gastrointest Liver Physiol* **285**: G779-788.
- Adibi SA, Mercer DW (1973). Protein digestion in human intestine as reflected in luminal, mucosal, and plasma amino acid concentrations after meals. *J Clin Invest* **52**: 1586-1594.
- Agu R, Cowley E, Shao D, Macdonald C, Kirkpatrick D, Renton K, Massoud E (2011). Proton-coupled oligopeptide transporter (POT) family expression in human nasal epithelium and their drug transport potential. *Mol Pharm* **8**: 664-672.
- Anderle P, Nielsen CU, Pinsonneault J, Krog PL, Brodin B, Sadee W (2006). Genetic variants of the human dipeptide transporter PEPT1. *J Pharmacol Exp Ther* **316**: 636-646.
- Asatoor AM, Cheng B, Edwards KD, Lant AF, Matthews DM, Milne MD, Navab F, Richards AJ (1970). Intestinal absorption of two dipeptides in Hartnup disease. *Gut* **11**: 380-387.
- Ashida K, Katsura T, Motohashi H, Saito H, Inui K (2002). Thyroid hormone regulates the activity and expression of the peptide transporter PEPT1 in Caco-2 cells. *Am J Physiol Gastrointest Liver Physiol* **282**: G617-623.
- Bailey PD, Boyd CA, Bronk JR, Collier ID, Meredith D, Morgan KM, Temple CS (2000). How to Make Drugs Orally Active: A Substrate Template for Peptide Transporter PepT1. *Angew Chem Int Ed Engl* **39**: 505-508.
- Bailey PD, Boyd CA, Collier ID, George JP, Kellett GL, Meredith D, Morgan KM, Pettecrew R, Price RA (2006). Affinity prediction for substrates of the peptide transporter PepT1. *Chem Commun (Camb)*: 323-325.
- Barbot L, Windsor E, Rome S, Tricottet V, Reynes M, Topouchian A, Huneau JF, Gobert JG, Tome D, Kapel N (2003). Intestinal peptide transporter PepT1 is over-expressed during acute cryptosporidiosis in suckling rats as a result of both malnutrition and experimental parasite infection. *Parasitol Res* **89**: 364-370.
- Beauchamp LM, Orr GF, de Miranda P, Doucette M, Burnette T, Krenitsky TA (1992). Amino acid ester prodrugs of acyclovir. *Antiviral Chem Chemother* **3**: 157-164.

Berlitz F, Julien S, Tsocas A, Chariot J, Carbon C, Farinotti R, Roze C (1999). Neural modulation of cephalixin intestinal absorption through the di- and tripeptide brush border transporter of rat jejunum in vivo. *J Pharmacol Exp Ther* **288**: 1037-1044.

Berlitz F, Maoret JJ, Paris H, Laburthe M, Farinotti R, Roze C (2000). $\alpha(2)$ -adrenergic receptors stimulate oligopeptide transport in a human intestinal cell line. *J Pharmacol Exp Ther* **294**: 466-472.

Biegel A, Gebauer S, Hartrodt B, Brandsch M, Neubert K, Thondorf I (2005). Three-dimensional quantitative structure-activity relationship analyses of beta-lactam antibiotics and tripeptides as substrates of the mammalian H⁺/peptide cotransporter PEPT1. *J Med Chem* **48**: 4410-4419.

Bishop WP, Wen JT (1994). Regulation of Caco-2 cell proliferation by basolateral membrane epidermal growth factor receptors. *Am J Physiol* **267**: G892-900.

Bockman DE, Ganapathy V, Oblak TG, Leibach FH (1997). Localization of peptide transporter in nuclei and lysosomes of the pancreas. *Int J Pancreatol* **22**: 221-225.

Bolger MB, Haworth IS, Yeung AK, Ann D, von Grafenstein H, Hamm-Alvarez S, Okamoto CT, Kim KJ, Basu SK, Wu S, Lee VH (1998). Structure, function, and molecular modeling approaches to the study of the intestinal dipeptide transporter PepT1. *J Pharm Sci* **87**: 1286-1291.

Borner V, Fei YJ, Hartrodt B, Ganapathy V, Leibach FH, Neubert K, Brandsch M (1998). Transport of amino acid aryl amides by the intestinal H⁺/peptide cotransport system, PEPT1. *Eur J Biochem* **255**: 698-702.

Bossi E, Renna MD, Sangaletti R, D'Antoni F, Cherubino F, Kottra G, Peres A (2011). Residues R282 and D341 act as electrostatic gates in the proton-dependent oligopeptide transporter PepT1. *J Physiol* **589**: 495-510.

Boullin DJ, Crampton RF, Heading CE, Pelling D (1973). Intestinal absorption of dipeptides containing glycine, phenylalanine, proline, beta-alanine or histidine in the rat. *Clin Sci Mol Med* **45**: 49-58.

Brandsch M, Knutter I, Leibach FH (2004). The intestinal H⁺/peptide symporter PEPT1: structure-affinity relationships. *Eur J Pharm Sci* **21**: 53-60.

Brandsch M, Knutter I, Thuncke F, Hartrodt B, Born I, Borner V, Hirche F, Fischer G, Neubert K (1999). Decisive structural determinants for the interaction of proline derivatives with the intestinal H⁺/peptide symporter. *Eur J Biochem* **266**: 502-508.

Brandsch M, Miyamoto Y, Ganapathy V, Leibach FH (1994). Expression and protein kinase C-dependent regulation of peptide/H⁺ co-transport system in the Caco-2 human colon carcinoma cell line. *Biochem J* **299** (Pt 1): 253-260.

Brandsch M, Thunecke F, Kullertz G, Schutkowski M, Fischer G, Neubert K (1998). Evidence for the absolute conformational specificity of the intestinal H⁺/peptide symporter, PEPT1. *J Biol Chem* **273**: 3861-3864.

Breese EJ, Michie CA, Nicholls SW, Murch SH, Williams CB, Domizio P, Walker-Smith JA, MacDonald TT (1994). Tumor necrosis factor alpha-producing cells in the intestinal mucosa of children with inflammatory bowel disease. *Gastroenterology* **106**: 1455-1466.

Brodin B, Nielsen CU, Steffansen B, Frokjaer S (2002). Transport of peptidomimetic drugs by the intestinal Di/tri-peptide transporter, PepT1. *Pharmacol Toxicol* **90**: 285-296.

Burger D, Travis S (2011). Conventional medical management of inflammatory bowel disease. *Gastroenterology* **140**: 1827-1837 e1822.

Buyse M, Berlioz F, Guilmeau S, Tsocas A, Voisin T, Peranzi G, Merlin D, Laburthe M, Lewin MJ, Roze C, Bado A (2001). PepT1-mediated epithelial transport of dipeptides and cephalixin is enhanced by luminal leptin in the small intestine. *J Clin Invest* **108**: 1483-1494.

Buyse M, Charrier L, Sitaraman S, Gewirtz A, Merlin D (2003). Interferon-gamma increases hPepT1-mediated uptake of di-tripeptides including the bacterial tripeptide fMLP in polarized intestinal epithelia. *Am J Pathol* **163**: 1969-1977.

Buyse M, Tsocas A, Walker F, Merlin D, Bado A (2002). PepT1-mediated fMLP transport induces intestinal inflammation in vivo. *Am J Physiol Cell Physiol* **283**: C1795-1800.

Charrier L, Driss A, Yan Y, Nduati V, Klapproth JM, Sitaraman SV, Merlin D (2006a). hPepT1 mediates bacterial tripeptide fMLP uptake in human monocytes. *Lab Invest* **86**: 490-503.

Charrier L, Merlin D (2006b). The oligopeptide transporter hPepT1: gateway to the innate immune response. *Lab Invest* **86**: 538-546.

Chen HQ, Yang J, Zhang M, Zhou YK, Shen TY, Chu ZX, Hang XM, Jiang YQ, Qin HL (2010). *Lactobacillus plantarum* ameliorates colonic epithelial barrier dysfunction by modulating the apical junctional complex and PepT1 in IL-10 knockout mice. *Am J Physiol Gastrointest Liver Physiol* **299**: G1287-1297.

Chen XZ, Steel A, Hediger MA (2000). Functional roles of histidine and tyrosine residues in the H(+)-peptide transporter PepT1. *Biochem Biophys Res Commun* **272**: 726-730.

Corfield AP, Wallace HM, Probert CS (2011). The molecular biology of inflammatory bowel diseases. *Biochem Soc Trans* **39**: 1057-1060.

Covitz KM, Amidon GL, Sadee W (1998). Membrane topology of the human dipeptide transporter, hPEPT1, determined by epitope insertions. *Biochemistry* **37**: 15214-15221.

Crampton RF, Lis MT, Matthews DM (1973). Sites of maximal absorption and hydrolysis of two dipeptides by rat small intestine in vivo. *Clin Sci* **44**: 583-594.

Dalmaso G, Charrier-Hisamuddin L, Nguyen HT, Yan Y, Sitaraman S, Merlin D (2008). PepT1-mediated tripeptide KPV uptake reduces intestinal inflammation. *Gastroenterology* **134**: 166-178.

Dalmaso G, Nguyen HT, Charrier-Hisamuddin L, Yan Y, Laroui H, Demoulin B, Sitaraman SV, Merlin D (2010). PepT1 mediates transport of the proinflammatory bacterial tripeptide L-Ala- $\{\gamma\}$ -D-Glu-meso-DAP in intestinal epithelial cells. *Am J Physiol Gastrointest Liver Physiol* **299**: G687-696.

Dalmaso G, Nguyen HT, Ingersoll SA, Ayyadurai S, Laroui H, Charania MA, Yan Y, Sitaraman SV, Merlin D (2011a). The PepT1-NOD2 Signaling Pathway Aggravates Induced Colitis in Mice. *Gastroenterology*.

Dalmaso G, Nguyen HT, Yan Y, Laroui H, Charania MA, Obertone TS, Sitaraman SV, Merlin D (2011b). MicroRNA-92b regulates expression of the oligopeptide transporter PepT1 in intestinal epithelial cells. *Am J Physiol Gastrointest Liver Physiol* **300**: G52-59.

Daniel H, Fett C, Kratz A (1989). Demonstration and modification of intervillous pH profiles in rat small intestine in vitro. *Am J Physiol* **257**: G489-495.

Daniel H, Spanier B, Kottra G, Weitz D (2006). From bacteria to man: archaic proton-dependent peptide transporters at work. *Physiology (Bethesda)* **21**: 93-102.

Doring F, Dorn D, Bachfischer U, Amasheh S, Herget M, Daniel H (1996). Functional analysis of a chimeric mammalian peptide transporter derived from the intestinal and renal isoforms. *J Physiol* **497 (Pt 3)**: 773-779.

Doring F, Walter J, Will J, Focking M, Boll M, Amasheh S, Clauss W, Daniel H (1998a). Delta-aminolevulinic acid transport by intestinal and renal peptide transporters and its physiological and clinical implications. *J Clin Invest* **101**: 2761-2767.

Doring F, Will J, Amasheh S, Clauss W, Ahlbrecht H, Daniel H (1998b). Minimal molecular determinants of substrates for recognition by the intestinal peptide transporter. *J Biol Chem* **273**: 23211-23218.

Enjoh M, Hashimoto K, Arai S, Shimizu M (1996). Inhibitory effect of arphamenine A on intestinal dipeptide transport. *Biosci Biotechnol Biochem* **60**: 1893-1895.

Ezra A, Hoffman A, Breuer E, Alferiev IS, Monkkonen J, El Hanany-Rozen N, Weiss G, Stepensky D, Gati I, Cohen H, Tormalehto S, Amidon GL, Golomb G (2000). A peptide prodrug approach for improving bisphosphonate oral absorption. *J Med Chem* **43**: 3641-3652.

Faria TN, Timoszyk JK, Stouch TR, Vig BS, Landowski CP, Amidon GL, Weaver CD, Wall DA, Smith RL (2004). A novel high-throughput pepT1 transporter assay differentiates between substrates and antagonists. *Mol Pharm* **1**: 67-76.

Fei YJ, Kanai Y, Nussberger S, Ganapathy V, Leibach FH, Romero MF, Singh SK, Boron WF, Hediger MA (1994). Expression cloning of a mammalian proton-coupled oligopeptide transporter. *Nature* **368**: 563-566.

Fei YJ, Liu JC, Fujita T, Liang R, Ganapathy V, Leibach FH (1998). Identification of a potential substrate binding domain in the mammalian peptide transporters PEPT1 and PEPT2 using PEPT1-PEPT2 and PEPT2-PEPT1 chimeras. *Biochem Biophys Res Commun* **246**: 39-44.

Fei YJ, Liu W, Prasad PD, Kekuda R, Oblak TG, Ganapathy V, Leibach FH (1997). Identification of the histidyl residue obligatory for the catalytic activity of the human H⁺/peptide cotransporters PEPT1 and PEPT2. *Biochemistry* **36**: 452-460.

Fei YJ, Sugawara M, Liu JC, Li HW, Ganapathy V, Ganapathy ME, Leibach FH (2000). cDNA structure, genomic organization, and promoter analysis of the mouse intestinal peptide transporter PEPT1. *Biochim Biophys Acta* **1492**: 145-154.

Flanagan P, Campbell BJ, Rhodes JM (2011). Bacteria in the pathogenesis of inflammatory bowel disease. *Biochem Soc Trans* **39**: 1067-1072.

Foley DW, Rajamanickam J, Bailey PD, Meredith D (2010). Bioavailability through PepT1: the role of computer modelling in intelligent drug design. *Curr Comput Aided Drug Des* **6**: 68-78.

Foster DR, Landowski CP, Zheng X, Amidon GL, Welage LS (2009). Interferon-gamma increases expression of the di/tri-peptide transporter, h-PEPT1, and dipeptide transport in cultured human intestinal monolayers. *Pharmacol Res* **59**: 215-220.

Fujita T, Majikawa Y, Umehisa S, Okada N, Yamamoto A, Ganapathy V, Leibach FH (1999). sigma Receptor ligand-induced up-regulation of the H(+)/peptide transporter PEPT1 in the human intestinal cell line Caco-2. *Biochem Biophys Res Commun* **261**: 242-246.

Fujita T, Morishita Y, Ito H, Kuribayashi D, Yamamoto A, Muranishi S (1997). Enhancement of the small intestinal uptake of phenylalanylglycine via a H+/oligopeptide transport system by chemical modification with fatty acids. *Life Sci* **61**: 2455-2465.

Fuss IJ, Neurath M, Boirivant M, Klein JS, de la Motte C, Strong SA, Fiocchi C, Strober W (1996). Disparate CD4+ lamina propria (LP) lymphokine secretion profiles in inflammatory bowel disease. Crohn's disease LP cells manifest increased secretion of IFN-gamma, whereas ulcerative colitis LP cells manifest increased secretion of IL-5. *J Immunol* **157**: 1261-1270.

Ganapathy ME, Huang W, Wang H, Ganapathy V, Leibach FH (1998). Valacyclovir: a substrate for the intestinal and renal peptide transporters PEPT1 and PEPT2. *Biochem Biophys Res Commun* **246**: 470-475.

Ganapathy V, Gupta N, Martindale RG (2006). Protein digestion and absorption. In: *Physiology of the Gastrointestinal Tract* (Johnson LR ed), 4th Edition, pp. 1667-1692. Raven Press, New York.

Gangopadhyay A, Thamotharan M, Adibi SA (2002). Regulation of oligopeptide transporter (Pept-1) in experimental diabetes. *Am J Physiol Gastrointest Liver Physiol* **283**: G133-138.

Gebauer S, Knutter I, Hartrodt B, Brandsch M, Neubert K, Thondorf I (2003). Three-dimensional quantitative structure-activity relationship analyses of peptide substrates of the mammalian H+/peptide cotransporter PEPT1. *J Med Chem* **46**: 5725-5734.

Gilchrist SE, Alcorn J (2010). Lactation stage-dependent expression of transporters in rat whole mammary gland and primary mammary epithelial organoids. *Fundam Clin Pharmacol* **24**: 205-214.

Groneberg DA, Doring F, Eynott PR, Fischer A, Daniel H (2001). Intestinal peptide transport: ex vivo uptake studies and localization of peptide carrier PEPT1. *Am J Physiol Gastrointest Liver Physiol* **281**: G697-704.

Han JW, Zheng HF, Cui Y, Sun LD, Ye DQ, Hu Z, Xu JH, Cai ZM, Huang W, Zhao GP, Xie HF, Fang H, Lu QJ, Li XP, Pan YF, Deng DQ, Zeng FQ, Ye ZZ, Zhang XY, Wang QW, Hao F, Ma L, Zuo XB, Zhou FS, Du WH, Cheng YL, Yang JQ, Shen SK, Li J, Sheng YJ, Zuo XX, Zhu WF, Gao F, Zhang PL, Guo Q, Li B, Gao M, Xiao FL, Quan C, Zhang C, Zhang Z, Zhu KJ, Li Y, Hu DY, Lu WS, Huang JL, Liu SX, Li H, Ren YQ, Wang ZX, Yang CJ, Wang PG, Zhou WM, Lv YM, Zhang AP, Zhang SQ, Lin D, Low HQ, Shen M, Zhai ZF, Wang Y, Zhang FY, Yang S, Liu JJ, Zhang XJ (2009). Genome-wide association study in a Chinese Han population identifies nine new susceptibility loci for systemic lupus erythematosus. *Nat Genet* **41**: 1234-1237.

Hellier MD, Perrett D, Holdsworth CD (1970). Dipeptide absorption in cystinuria. *Br Med J* **4**: 782-783.

Herrera-Ruiz D, Wang Q, Gudmundsson OS, Cook TJ, Smith RL, Faria TN, Knipp GT (2001). Spatial expression patterns of peptide transporters in the human and rat gastrointestinal tracts, Caco-2 in vitro cell culture model, and multiple human tissues. *AAPS PharmSci* **3**: E9.

Hilgendorf C, Ahlin G, Seithel A, Artursson P, Ungell AL, Karlsson J (2007). Expression of thirty-six drug transporter genes in human intestine, liver, kidney, and organotypic cell lines. *Drug Metab Dispos* **35**: 1333-1340.

Hindlet P, Bado A, Farinotti R, Buyse M (2007). Long-term effect of leptin on H⁺-coupled peptide cotransporter 1 activity and expression in vivo: evidence in leptin-deficient mice. *J Pharmacol Exp Ther* **323**: 192-201.

Hoogerwerf WA, Tsao SC, Devuyst O, Levine SA, Yun CH, Yip JW, Cohen ME, Wilson PD, Lazenby AJ, Tse CM, Donowitz M (1996). NHE2 and NHE3 are human and rabbit intestinal brush-border proteins. *Am J Physiol* **270**: G29-41.

Hugot JP, Chamaillard M, Zouali H, Lesage S, Cezard JP, Belaiche J, Almer S, Tysk C, O'Morain CA, Gassull M, Binder V, Finkel Y, Cortot A, Modigliani R, Laurent-Puig P, Gower-Rousseau C, Macry J, Colombel JF, Sahbatou M, Thomas G (2001). Association of NOD2 leucine-rich repeat variants with susceptibility to Crohn's disease. *Nature* **411**: 599-603.

Ihara T, Tsujikawa T, Fujiyama Y, Bamba T (2000). Regulation of PepT1 peptide transporter expression in the rat small intestine under malnourished conditions. *Digestion* **61**: 59-67.

Jappard D, Wu SP, Hu Y, Smith DE (2010). Significance and regional dependency of peptide transporter (PEPT) 1 in the intestinal permeability of glycylsarcosine: in situ single-pass perfusion studies in wild-type and Pept1 knockout mice. *Drug Metab Dispos* **38**: 1740-1746.

Jung D, Dorr A (1999). Single-dose pharmacokinetics of valganciclovir in HIV- and CMV-seropositive subjects. *J Clin Pharmacol* **39**: 800-804.

Katz JA (2007). Management of inflammatory bowel disease in adults. *J Dig Dis* **8**: 65-71.

Kelsall B (2005). Getting to the guts of NOD2. *Nat Med* **11**: 383-384.

Kennedy DJ, Leibach FH, Ganapathy V, Thwaites DT (2002). Optimal absorptive transport of the dipeptide glycylsarcosine is dependent on functional Na⁺/H⁺ exchange activity. *Pflugers Arch* **445**: 139-146.

Klang JE, Burnworth LA, Pan YX, Webb KE, Jr., Wong EA (2005). Functional characterization of a cloned pig intestinal peptide transporter (pPepT1). *J Anim Sci* **83**: 172-181.

Kleta R, Romeo E, Ristic Z, Ohura T, Stuart C, Arcos-Burgos M, Dave MH, Wagner CA, Camargo SR, Inoue S, Matsuura N, Helip-Wooley A, Bockenhauer D, Warth R, Bernardini I, Visser G, Eggermann T, Lee P, Chairoungdua A, Jutabha P, Babu E, Nilwarangkoon S, Anzai N, Kanai Y, Verrey F, Gahl WA, Koizumi A (2004). Mutations in SLC6A19, encoding B0AT1, cause Hartnup disorder. *Nat Genet* **36**: 999-1002.

Knutter I, Rubio-Aliaga I, Boll M, Hause G, Daniel H, Neubert K, Brandsch M (2002). H⁺-peptide cotransport in the human bile duct epithelium cell line SK-ChA-1. *Am J Physiol Gastrointest Liver Physiol* **283**: G222-229.

Kobayashi KS, Chamaillard M, Ogura Y, Henegariu O, Inohara N, Nunez G, Flavell RA (2005). Nod2-dependent regulation of innate and adaptive immunity in the intestinal tract. *Science* **307**: 731-734.

Kottra G, Daniel H (2001). Bidirectional electrogenic transport of peptides by the proton-coupled carrier PEPT1 in *Xenopus laevis* oocytes: its asymmetry and symmetry. *J Physiol* **536**: 495-503.

Kottra G, Stamford A, Daniel H (2002). PEPT1 as a paradigm for membrane carriers that mediate electrogenic bidirectional transport of anionic, cationic, and neutral substrates. *J Biol Chem* **277**: 32683-32691.

Kramer W, Girbig F, Gutjahr U, Kleemann HW, Leipe I, Urbach H, Wagner A (1990). Interaction of renin inhibitors with the intestinal uptake system for oligopeptides and beta-lactam antibiotics. *Biochim Biophys Acta* **1027**: 25-30.

Kucharzik T, Maaser C, Luger A, Kagnoff M, Mayer L, Targan S, Domschke W (2006). Recent understanding of IBD pathogenesis: implications for future therapies. *Inflamm Bowel Dis* **12**: 1068-1083.

Kuhn R, Lohler J, Rennick D, Rajewsky K, Muller W (1993). Interleukin-10-deficient mice develop chronic enterocolitis. *Cell* **75**: 263-274.

Kulkarni AA, Davies DL, Links JS, Patel LN, Lee VH, Haworth IS (2007). A charge pair interaction between Arg282 in transmembrane segment 7 and Asp341 in transmembrane segment 8 of hPepT1. *Pharm Res* **24**: 66-72.

Kulkarni AA, Haworth IS, Lee VH (2003a). Transmembrane segment 5 of the dipeptide transporter hPepT1 forms a part of the substrate translocation pathway. *Biochem Biophys Res Commun* **306**: 177-185.

Kulkarni AA, Haworth IS, Uchiyama T, Lee VH (2003b). Analysis of transmembrane segment 7 of the dipeptide transporter hPepT1 by cysteine-scanning mutagenesis. *J Biol Chem* **278**: 51833-51840.

Leny H (2001). Hartnup disorder. In: *The metabolic & molecular bases of inherited disease* (Scriver CR, Beaudet AL, Sly WS, Valle D eds), pp. 4957-4969. McGraw-Hill, New York.

Li J, Hidalgo IJ (1996). Molecular modeling study of structural requirements for the oligopeptide transporter. *J Drug Target* **4**: 9-17.

Li J, Tamura K, Lee CP, Smith PL, Borchardt RT, Hidalgo IJ (1998). Structure-affinity relationships of Val-Val and Val-Val-Val stereoisomers with the apical oligopeptide transporter in human intestinal Caco-2 cells. *J Drug Target* **5**: 317-327.

Liang R, Fei YJ, Prasad PD, Ramamoorthy S, Han H, Yang-Feng TL, Hediger MA, Ganapathy V, Leibach FH (1995). Human intestinal H⁺/peptide cotransporter. Cloning, functional expression, and chromosomal localization. *J Biol Chem* **270**: 6456-6463.

Liapakis G, Simpson MM, Javitch JA (2001). The substituted-cysteine accessibility method (SCAM) to elucidate membrane protein structure. *Curr Protoc Neurosci* **Chapter 4**: Unit 4 15.

Links JL, Kulkarni AA, Davies DL, Lee VH, Haworth IS (2007). Cysteine scanning of transmembrane domain three of the human dipeptide transporter: implications for substrate transport. *J Drug Target* **15**: 218-225.

Liu W, Liang R, Ramamoorthy S, Fei YJ, Ganapathy ME, Hediger MA, Ganapathy V, Leibach FH (1995). Molecular cloning of PEPT 2, a new member of the H⁺/peptide cotransporter family, from human kidney. *Biochim Biophys Acta* **1235**: 461-466.

Loftus EV, Jr. (2004). Clinical epidemiology of inflammatory bowel disease: Incidence, prevalence, and environmental influences. *Gastroenterology* **126**: 1504-1517.

Lu H, Klaassen C (2006). Tissue distribution and thyroid hormone regulation of Pept1 and Pept2 mRNA in rodents. *Peptides* **27**: 850-857.

Mackenzie B, Loo DD, Fei Y, Liu WJ, Ganapathy V, Leibach FH, Wright EM (1996). Mechanisms of the human intestinal H⁺-coupled oligopeptide transporter hPEPT1. *J Biol Chem* **271**: 5430-5437.

Maeda S, Hsu LC, Liu H, Bankston LA, Iimura M, Kagnoff MF, Eckmann L, Karin M (2005). Nod2 mutation in Crohn's disease potentiates NF-kappaB activity and IL-1beta processing. *Science* **307**: 734-738.

Marquet P, Barbot L, Plante A, Huneau JF, Gobert JG, Kapel N (2007). Cryptosporidiosis induces a transient upregulation of the oligopeptides transporter (PepT1) activity in neonatal rats. *Exp Biol Med (Maywood)* **232**: 454-460.

Matthews DM (1975). Intestinal absorption of peptides. *Physiol Rev* **55**: 537-608.

Matthews DM, Craft IL, Geddes DM, Wise IJ, Hyde CW (1968). Absorption of glycine and glycine peptides from the small intestine of the rat. *Clin Sci* **35**: 415-424.

Maul J, Loddenkemper C, Mundt P, Berg E, Giese T, Stallmach A, Zeitz M, Duchmann R (2005). Peripheral and intestinal regulatory CD4⁺ CD25(high) T cells in inflammatory bowel disease. *Gastroenterology* **128**: 1868-1878.

Meredith D (2004). Site-directed mutation of arginine 282 to glutamate uncouples the movement of peptides and protons by the rabbit proton-peptide cotransporter PepT1. *J Biol Chem* **279**: 15795-15798.

Meredith D, Temple CS, Guha N, Sword CJ, Boyd CA, Collier ID, Morgan KM, Bailey PD (2000). Modified amino acids and peptides as substrates for the intestinal peptide transporter PepT1. *Eur J Biochem* **267**: 3723-3728.

Merlin D, Si-Tahar M, Sitaraman SV, Eastburn K, Williams I, Liu X, Hediger MA, Madara JL (2001). Colonic epithelial hPepT1 expression occurs in inflammatory bowel disease: transport of bacterial peptides influences expression of MHC class 1 molecules. *Gastroenterology* **120**: 1666-1679.

Merlin D, Steel A, Gewirtz AT, Si-Tahar M, Hediger MA, Madara JL (1998). hPepT1-mediated epithelial transport of bacteria-derived chemotactic peptides enhances neutrophil-epithelial interactions. *J Clin Invest* **102**: 2011-2018.

Miyamoto K, Shiraga T, Morita K, Yamamoto H, Haga H, Taketani Y, Tamai I, Sai Y, Tsuji A, Takeda E (1996). Sequence, tissue distribution and developmental changes in rat intestinal oligopeptide transporter. *Biochim Biophys Acta* **1305**: 34-38.

Monteleone G, Biancone L, Marasco R, Morrone G, Marasco O, Lizza F, Pallone F (1997). Interleukin 12 is expressed and actively released by Crohn's disease intestinal lamina propria mononuclear cells. *Gastroenterology* **112**: 1169-1178.

Motohashi H, Katsura T, Saito H, Inui K (2001). Effects of tacrolimus and cyclosporin A on peptide transporter PEPT1 in Caco-2 cells. *Pharm Res* **18**: 713-717.

Nduati V, Yan Y, Dalmasso G, Driss A, Sitaraman S, Merlin D (2007). Leptin transcriptionally enhances peptide transporter (hPepT1) expression and activity via the cAMP-response element-binding protein and Cdx2 transcription factors. *J Biol Chem* **282**: 1359-1373.

Netea MG, Ferwerda G, de Jong DJ, Werts C, Boneca IG, Jehanno M, Van Der Meer JW, Mengin-Lecreulx D, Sansonetti PJ, Philpott DJ, Dharancy S, Girardin SE (2005). The frameshift mutation in Nod2 results in unresponsiveness not only to Nod2- but also Nod1-activating peptidoglycan agonists. *J Biol Chem* **280**: 35859-35867.

Newstead S, Drew D, Cameron AD, Postis VL, Xia X, Fowler PW, Ingram JC, Carpenter EP, Sansom MS, McPherson MJ, Baldwin SA, Iwata S (2011). Crystal structure of a prokaryotic homologue of the mammalian oligopeptide-proton symporters, PepT1 and PepT2. *EMBO J* **30**: 417-426.

Nguyen HT, Dalmasso G, Powell KR, Yan Y, Bhatt S, Kalman D, Sitaraman SV, Merlin D (2009). Pathogenic bacteria induce colonic PepT1 expression: an implication in host defense response. *Gastroenterology* **137**: 1435-1447 e1431-1432.

Nielsen CU, Amstrup J, Nielsen R, Steffansen B, Frokjaer S, Brodin B (2003). Epidermal growth factor and insulin short-term increase hPepT1-mediated glycylsarcosine uptake in Caco-2 cells. *Acta Physiol Scand* **178**: 139-148.

Nixon SE, Mawer GE (1970). The digestion and absorption of protein in man. 2. The form in which digested protein is absorbed. *Br J Nutr* **24**: 241-258.

Nussberger S, Steel A, Trotti D, Romero MF, Boron WF, Hediger MA (1997). Symmetry of H⁺ binding to the intra- and extracellular side of the H⁺-coupled oligopeptide cotransporter PepT1. *J Biol Chem* **272**: 7777-7785.

Ocheltree SM, Shen H, Hu Y, Keep RF, Smith DE (2005). Role and relevance of peptide transporter 2 (PEPT2) in the kidney and choroid plexus: in vivo studies with glycylsarcosine in wild-type and PEPT2 knockout mice. *J Pharmacol Exp Ther* **315**: 240-247.

Ogihara H, Saito H, Shin BC, Terado T, Takenoshita S, Nagamachi Y, Inui K, Takata K (1996). Immuno-localization of H⁺/peptide cotransporter in rat digestive tract. *Biochem Biophys Res Commun* **220**: 848-852.

Ogihara H, Suzuki T, Nagamachi Y, Inui K, Takata K (1999). Peptide transporter in the rat small intestine: ultrastructural localization and the effect of starvation and administration of amino acids. *Histochem J* **31**: 169-174.

Ogura Y, Bonen DK, Inohara N, Nicolae DL, Chen FF, Ramos R, Britton H, Moran T, Karaliuskas R, Duerr RH, Achkar JP, Brant SR, Bayless TM, Kirschner BS, Hanauer SB, Nunez G, Cho JH (2001). A frameshift mutation in NOD2 associated with susceptibility to Crohn's disease. *Nature* **411**: 603-606.

Okano T, Inui K, Takano M, Hori R (1986). H⁺ gradient-dependent transport of aminocephalosporins in rat intestinal brush-border membrane vesicles. Role of dipeptide transport system. *Biochem Pharmacol* **35**: 1781-1786.

Palacin M, Borsani G, Sebastio G (2001a). The molecular bases of cystinuria and lysinuric protein intolerance. *Curr Opin Genet Dev* **11**: 328-335.

Palacin M, Goodyer P, Nunes V, Gasparini P (2001b). Cystinuria. In: *The metabolic & molecular bases of inherited disease* (Scriver CR, Beaudet AL, Sly WS, Valle D eds), pp. 4909-4932. McGraw-Hill, New York.

Pan Y, Wong EA, Bloomquist JR, Webb KE, Jr. (2001). Expression of a cloned ovine gastrointestinal peptide transporter (oPepT1) in *Xenopus* oocytes induces uptake of oligopeptides in vitro. *J Nutr* **131**: 1264-1270.

Phan DD, Chin-Hong P, Lin ET, Anderle P, Sadee W, Guglielmo BJ (2003). Intra- and interindividual variabilities of valacyclovir oral bioavailability and effect of coadministration of an hPEPT1 inhibitor. *Antimicrob Agents Chemother* **47**: 2351-2353.

Pieri M, Hall D, Price R, Bailey P, Meredith D (2008). Site-directed mutagenesis of Arginine282 suggests how protons and peptides are co-transported by rabbit PepT1. *Int J Biochem Cell Biol* **40**: 721-730.

Plevy SE, Targan SR (2011). Future therapeutic approaches for inflammatory bowel diseases. *Gastroenterology* **140**: 1838-1846.

Qandeel HG, Duenes JA, Zheng Y, Sarr MG (2009). Diurnal expression and function of peptide transporter 1 (PEPT1). *J Surg Res* **156**: 123-128.

Radeva G, Buyse M, Hindlet P, Beaufils B, Walker F, Bado A, Farinotti R (2007). Regulation of the oligopeptide transporter, PEPT-1, in DSS-induced rat colitis. *Dig Dis Sci* **52**: 1653-1661.

Rubio-Aliaga I, Daniel H (2002). Mammalian peptide transporters as targets for drug delivery. *Trends Pharmacol Sci* **23**: 434-440.

Ryan P, Bennett MW, Aarons S, Lee G, Collins JK, O'Sullivan GC, O'Connell J, Shanahan F (2002). PCR detection of Mycobacterium paratuberculosis in Crohn's disease granulomas isolated by laser capture microdissection. *Gut* **51**: 665-670.

Saito H, Okuda M, Terada T, Sasaki S, Inui K (1995). Cloning and characterization of a rat H⁺/peptide cotransporter mediating absorption of beta-lactam antibiotics in the intestine and kidney. *J Pharmacol Exp Ther* **275**: 1631-1637.

Sakata K, Yamashita T, Maeda M, Moriyama Y, Shimada S, Tohyama M (2001). Cloning of a lymphatic peptide/histidine transporter. *Biochem J* **356**: 53-60.

Sala-Rabanal M, Loo DD, Hirayama BA, Turk E, Wright EM (2006). Molecular interactions between dipeptides, drugs and the human intestinal H⁺-oligopeptide cotransporter hPEPT1. *J Physiol* **574**: 149-166.

Sasawatari S, Okamura T, Kasumi E, Tanaka-Furuyama K, Yanobu-Takanashi R, Shirasawa S, Kato N, Toyama-Sorimachi N (2011). The solute carrier family 15A4 regulates TLR9 and NOD1 functions in the innate immune system and promotes colitis in mice. *Gastroenterology* **140**: 1513-1525.

Seow HF, Broer S, Broer A, Bailey CG, Potter SJ, Cavanaugh JA, Rasko JE (2004). Hartnup disorder is caused by mutations in the gene encoding the neutral amino acid transporter SLC6A19. *Nat Genet* **36**: 1003-1007.

Shen H, Ocheltree SM, Hu Y, Keep RF, Smith DE (2007). Impact of genetic knockout of PEPT2 on cefadroxil pharmacokinetics, renal tubular reabsorption, and brain penetration in mice. *Drug Metab Dispos* **35**: 1209-1216.

Shen H, Smith DE, Brosius FC, 3rd (2001). Developmental expression of PEPT1 and PEPT2 in rat small intestine, colon, and kidney. *Pediatr Res* **49**: 789-795.

Shen H, Smith DE, Yang T, Huang YG, Schnermann JB, Brosius FC, 3rd (1999). Localization of PEPT1 and PEPT2 proton-coupled oligopeptide transporter mRNA and protein in rat kidney. *Am J Physiol* **276**: F658-665.

Shi B, Song D, Xue H, Li J, Li N (2006a). Abnormal expression of the peptide transporter PepT1 in the colon of massive bowel resection rat: a potential route for colonic mucosa damage by transport of fMLP. *Dig Dis Sci* **51**: 2087-2093.

Shi B, Song D, Xue H, Li N, Li J (2006b). PepT1 mediates colon damage by transporting fMLP in rats with bowel resection. *J Surg Res* **136**: 38-44.

Shivananda S, Lennard-Jones J, Logan R, Fear N, Price A, Carpenter L, van Blankenstein M (1996). Incidence of inflammatory bowel disease across Europe: is there a difference between north and south? Results of the European Collaborative Study on Inflammatory Bowel Disease (EC-IBD). *Gut* **39**: 690-697.

Shull MM, Ormsby I, Kier AB, Pawlowski S, Diebold RJ, Yin M, Allen R, Sidman C, Proetzel G, Calvin D, et al. (1992). Targeted disruption of the mouse transforming growth factor-beta 1 gene results in multifocal inflammatory disease. *Nature* **359**: 693-699.

Sokol H, Pigneur B, Watterlot L, Lakhdari O, Bermudez-Humaran LG, Gratadoux JJ, Blugeon S, Bridonneau C, Furet JP, Corthier G, Grangette C, Vasquez N, Pochart P, Trugnan G, Thomas G, Blottiere HM, Dore J, Marteau P, Seksik P, Langella P (2008). Faecalibacterium prausnitzii is an anti-inflammatory commensal bacterium identified by gut microbiota analysis of Crohn disease patients. *Proc Natl Acad Sci U S A* **105**: 16731-16736.

Steel A, Nussberger S, Romero MF, Boron WF, Boyd CA, Hediger MA (1997). Stoichiometry and pH dependence of the rabbit proton-dependent oligopeptide transporter PepT1. *J Physiol* **498** (Pt 3): 563-569.

Swidsinski A, Ladhoff A, Pernthaler A, Swidsinski S, Loening-Baucke V, Ortner M, Weber J, Hoffmann U, Schreiber S, Dietel M, Lochs H (2002). Mucosal flora in inflammatory bowel disease. *Gastroenterology* **122**: 44-54.

Tanaka H, Miyamoto KI, Morita K, Haga H, Segawa H, Shiraga T, Fujioka A, Kouda T, Taketani Y, Hisano S, Fukui Y, Kitagawa K, Takeda E (1998). Regulation of the PepT1 peptide transporter in the rat small intestine in response to 5-fluorouracil-induced injury. *Gastroenterology* **114**: 714-723.

Taub M, Moss BA, Steffansen B, Frokjaer S (1997). Influence of oligopeptide transporter binding affinity upon uptake and transport of d-Asp(OBzl)-Ala and Asp(OBzl)-Sar in filter-grown Caco-2 monolayers. *Int. J. Pharm.* **156**: 219-228.

Terada T, Inui K (2004). Peptide transporters: structure, function, regulation and application for drug delivery. *Curr Drug Metab* **5**: 85-94.

Terada T, Saito H, Mukai M, Inui KI (1996). Identification of the histidine residues involved in substrate recognition by a rat H⁺/peptide cotransporter, PEPT1. *FEBS Lett* **394**: 196-200.

Terada T, Saito H, Sawada K, Hashimoto Y, Inui K (2000a). N-terminal halves of rat H⁺/peptide transporters are responsible for their substrate recognition. *Pharm Res* **17**: 15-20.

Terada T, Sawada K, Irie M, Saito H, Hashimoto Y, Inui K (2000b). Structural requirements for determining the substrate affinity of peptide transporters PEPT1 and PEPT2. *Pflugers Arch* **440**: 679-684.

Thamotharan M, Bawani SZ, Zhou X, Adibi SA (1999a). Functional and molecular expression of intestinal oligopeptide transporter (Pept-1) after a brief fast. *Metabolism* **48**: 681-684.

Thamotharan M, Bawani SZ, Zhou X, Adibi SA (1999b). Hormonal regulation of oligopeptide transporter pept-1 in a human intestinal cell line. *Am J Physiol* **276**: C821-826.

Thamotharan M, Bawani SZ, Zhou X, Adibi SA (1998). Mechanism of dipeptide stimulation of its own transport in a human intestinal cell line. *Proc Assoc Am Physicians* **110**: 361-368.

Thwaites DT, Cavet M, Hirst BH, Simmons NL (1995). Angiotensin-converting enzyme (ACE) inhibitor transport in human intestinal epithelial (Caco-2) cells. *Br J Pharmacol* **114**: 981-986.

Thwaites DT, Ford D, Glanville M, Simmons NL (1999). H(+)/solute-induced intracellular acidification leads to selective activation of apical Na(+)/H(+) exchange in human intestinal epithelial cells. *J Clin Invest* **104**: 629-635.

Thwaites DT, Kennedy DJ, Raldua D, Anderson CM, Mendoza ME, Bladen CL, Simmons NL (2002). H/dipeptide absorption across the human intestinal epithelium is controlled indirectly via a functional Na/H exchanger. *Gastroenterology* **122**: 1322-1333.

Tomita Y, Katsura T, Okano T, Inui K, Hori R (1990). Transport mechanisms of bestatin in rabbit intestinal brush-border membranes: role of H+/dipeptide cotransport system. *J Pharmacol Exp Ther* **252**: 859-862.

Uchiyama T, Kulkarni AA, Davies DL, Lee VH (2003). Biophysical evidence for His57 as a proton-binding site in the mammalian intestinal transporter hPepT1. *Pharm Res* **20**: 1911-1916.

Urtti A, Johns SJ, Sadee W (2001). Genomic structure of proton-coupled oligopeptide transporter hPEPT1 and pH-sensing regulatory splice variant. *AAPS PharmSci* **3**: E6.

Van der Sluis M, De Koning BA, De Bruijn AC, Velcich A, Meijerink JP, Van Goudoever JB, Buller HA, Dekker J, Van Seuningen I, Renes IB, Einerhand AW (2006). Muc2-deficient mice spontaneously develop colitis, indicating that MUC2 is critical for colonic protection. *Gastroenterology* **131**: 117-129.

Vavricka SR, Musch MW, Chang JE, Nakagawa Y, Phanvijhitsiri K, Waypa TS, Merlin D, Schneewind O, Chang EB (2004). hPepT1 transports muramyl dipeptide, activating NF-kappaB and stimulating IL-8 secretion in human colonic Caco2/bbe cells. *Gastroenterology* **127**: 1401-1409.

Vavricka SR, Musch MW, Fujiya M, Kles K, Chang L, Eloranta JJ, Kullak-Ublick GA, Drabik K, Merlin D, Chang EB (2006). Tumor necrosis factor-alpha and interferon-gamma increase PepT1 expression and activity in the human colon carcinoma cell line Caco-2/bbe and in mouse intestine. *Pflugers Arch* **452**: 71-80.

Vig BS, Stouch TR, Timoszyk JK, Quan Y, Wall DA, Smith RL, Faria TN (2006). Human PEPT1 pharmacophore distinguishes between dipeptide transport and binding. *J Med Chem* **49**: 3636-3644.

Walker D, Thwaites DT, Simmons NL, Gilbert HJ, Hirst BH (1998). Substrate upregulation of the human small intestinal peptide transporter, hPepT1. *J Physiol* **507 (Pt 3)**: 697-706.

Watanabe C, Kato Y, Ito S, Kubo Y, Sai Y, Tsuji A (2005). Na⁺/H⁺ exchanger 3 affects transport property of H⁺/oligopeptide transporter 1. *Drug Metab Pharmacokinet* **20**: 443-451.

Watanabe T, Kitani A, Murray PJ, Strober W (2004). NOD2 is a negative regulator of Toll-like receptor 2-mediated T helper type 1 responses. *Nat Immunol* **5**: 800-808.

Wenzel U, Gebert I, Weintraut H, Weber WM, Clauss W, Daniel H (1996). Transport characteristics of differently charged cephalosporin antibiotics in oocytes expressing the cloned intestinal peptide transporter PepT1 and in human intestinal Caco-2 cells. *J Pharmacol Exp Ther* **277**: 831-839.

Willing B, Halfvarson J, Dicksved J, Rosenquist M, Jarnerot G, Engstrand L, Tysk C, Jansson JK (2009). Twin studies reveal specific imbalances in the mucosa-associated microbiota of patients with ileal Crohn's disease. *Inflamm Bowel Dis* **15**: 653-660.

Xavier RJ, Podolsky DK (2007). Unravelling the pathogenesis of inflammatory bowel disease. *Nature* **448**: 427-434.

Yamashita T, Shimada S, Guo W, Sato K, Kohmura E, Hayakawa T, Takagi T, Tohyama M (1997). Cloning and functional expression of a brain peptide/histidine transporter. *J Biol Chem* **272**: 10205-10211.

Yang Z, Fuss IJ, Watanabe T, Asano N, Davey MP, Rosenbaum JT, Strober W, Kitani A (2007). NOD2 transgenic mice exhibit enhanced MDP-mediated down-regulation of TLR2 responses and resistance to colitis induction. *Gastroenterology* **133**: 1510-1521.

Zhang EY, Emerick RM, Pak YA, Wrighton SA, Hillgren KM (2004a). Comparison of human and monkey peptide transporters: PEPT1 and PEPT2. *Mol Pharm* **1**: 201-210.

Zhang EY, Fu DJ, Pak YA, Stewart T, Mukhopadhyay N, Wrighton SA, Hillgren KM (2004b). Genetic polymorphisms in human proton-dependent dipeptide transporter PEPT1: implications for the functional role of Pro586. *J Pharmacol Exp Ther* **310**: 437-445.

Zhou X, Thamotharan M, Gangopadhyay A, Serdikoff C, Adibi SA (2000). Characterization of an oligopeptide transporter in renal lysosomes. *Biochim Biophys Acta* **1466**: 372-378.

Ziegler TR, Fernandez-Estivariz C, Gu LH, Bazargan N, Umeakunne K, Wallace TM, Diaz EE, Rosado KE, Pascal RR, Galloway JR, Wilcox JN, Leader LM (2002). Distribution of the H⁺/peptide transporter PepT1 in human intestine: up-regulated expression in the colonic mucosa of patients with short-bowel syndrome. *Am J Clin Nutr* **75**: 922-930.

Zucchelli M, Torkvist L, Bresso F, Halfvarson J, Hellquist A, Anedda F, Assadi G, Lindgren GB, Svanfeldt M, Janson M, Noble CL, Pettersson S, Lappalainen M, Paavola-Sakki P, Halme L, Farkkila M, Turunen U, Satsangi J, Kontula K, Lofberg R, Kere J, D'Amato M (2009). PepT1 oligopeptide transporter (SLC15A1) gene polymorphism in inflammatory bowel disease. *Inflamm Bowel Dis* **15**: 1562-1569.

Chapter 3

IMPACT OF INTESTINAL PEPT1 ON THE KINETICS AND DYNAMICS OF N-FORMYL-METHIONYL-LEUCYL-PHENYLALANINE (FMET-LEU-PHE), A BACTERIALLY-PRODUCED CHEMOTACTIC PEPTIDE

ABSTRACT

PEPT1 has been suggested recently to transport bacterially-produced small peptides, which raised the possibility that PEPT1 has a pathological role in intestinal inflammation. The purpose of this study was to evaluate the impact of PEPT1 on the kinetics and dynamics of a bacterially-produced chemotactic tripeptide N-formyl-methionyl-leucyl-phenylalanine (fMet-Leu-Phe). Using an *in situ* single-pass intestinal perfusion technique in wild-type and *Pept1* knockout mice, the intestinal transport of fMet-Leu-Phe was saturable and primarily due to PEPT1 ($K_m = 1.6$ mM). The peptide-histidine transporters, PHT1 and PHT2, were not involved in the intestinal transport of fMet-Leu-Phe due to a lack of inhibition by L-histidine. The permeability of fMet-Leu-Phe was substantial and comparable in the duodenum and jejunum of wild-type mice, about one-half that in ileum, and very low in colon. In contrast, the permeability of fMet-Leu-Phe was very low in all intestinal segments of *Pept1* knockout mice and showed no difference between these segments or that of colon in wild-type mice.

Myeloperoxidase activity (a measure of neutrophil migration) was significantly increased when perfusing fMet-Leu-Phe in the jejunum of wild-type mice and was abolished by adding glycylglycine, an inhibitor of PEPT1 transport; no change was observed in the jejunum of *Pept1* knockout mice. Likewise, no increase of MPO activity was observed in the colon of both wild-type and *Pept1* knockout mice. Difference in enzymatic activity between genotypes was ruled out since fMet-Leu-Phe hydrolysis in jejunal homogenates was not different between wild-type and *Pept1* knockout mice. In conclusion, our data suggested that intestinal PEPT1 was responsible for the transport and the dynamic activity of the bacterially-produced compound fMet-Leu-Phe.

INTRODUCTION

Since PEPT1, a proton-coupled oligopeptide transporter, has been cloned from the rabbit intestine (Fei *et al.*, 1994), several studies have suggested that the end products of the digested protein were predominantly absorbed by PEPT1 in the form of di/tripeptides rather than free single amino acids (Ganapathy *et al.*, 2006). PEPT1 expressed throughout the small intestine (duodenum, jejunum, and ileum), but with little or none expression in the colon (Ogihara *et al.*, 1996). The immunofluorescent staining showed that PEPT1 expressed mainly at the apical side of the enterocyte with decreasing expression from the tip to the crypt of the villus (Ogihara *et al.*, 1996). Theoretically, PEPT1 transports 400 dipeptides and 8,000 tripeptides, but it has been suggested that not all the di/tripeptides are transported by PEPT1 (Vig *et al.*, 2006). In addition to endogenous oligopeptides, PEPT1 can transport several peptidomimetics such as β -lactam antibiotics (Okano *et al.*, 1986), angiotensin-converting enzyme inhibitor (Thwaites *et al.*, 1995), the anticancer drug bestatin (Tomita *et al.*, 1990), and the antiviral drug valacyclovir (Ganapathy *et al.*, 1998). Due to the broad spectrum of substrate specificity, PEPT1 has been targeted as a delivery route to increase the bioavailability of poorly absorbed compounds recently. A successful example, valacyclovir has been shown to exhibit 3-5 fold increase in bioavailability as compared to its parent compound acyclovir (Soul-Lawton *et al.*, 1995).

PEPT1 regulation in various conditions have been reported recently (Adibi, 2003). Substrates, pharmacological agents, hormones, and diseases have been shown to modify the expression of PEPT1 in the mRNA or protein levels. Most interestingly, PEPT1 can also be regulated in the colon, where normally no PEPT1 expressed, under some intestinal disease conditions. For example, PEPT1 was detected at the apical membrane

of colon in patients with Crohn's disease and ulcerative colitis by immunohistochemical staining (Merlin *et al.*, 2001). This upregulation of PEPT1 was also observed in the colon of patients with short bowel syndrome (SBS) (Ziegler *et al.*, 2002). Therefore, a pathological role of PEPT1 in colon related to the upregulation has recently been proposed (Charrier *et al.*, 2006b), based on the ability of transporting bacterially-produced peptides and the aberrant expression in colon. One category of bacterial peptide is N-formyl peptide. Study has shown that the major one produced by *E. Coli.* was a tripeptide, N-formyl-methionyl-leucyl-phenylalanine (fMet-Leu-Phe) (Marasco *et al.*, 1984). The endogenous concentration of fMet-Leu-Phe was around 100 nM in human colon (Marasco *et al.*, 1984). PEPT1 transporter as well as its homolog, PEPT2 transporter have been shown to transport some bacterially-derived compounds, such as fMet-Leu-Phe, muramyl-dipeptide (MDP), and γ -D-glutamyl-meso-diaminopimelic acid (γ -iE-DAP) (Merlin *et al.*, 1998; Vavricka *et al.*, 2004; Swaan *et al.*, 2008). The functional consequence of uptaking bacterially-derived compounds has also been demonstrated in the cell culture systems and perfusion study (Merlin *et al.*, 1998; Merlin *et al.*, 2001; Buyse *et al.*, 2002). The MHC class I expression and the neutrophil transmigration increased in CaCo-2 and cell line that expressing PEPT1 transporter and the increase can be moderated by specific substrate inhibition indicating a PEPT1-mediated fMet-Leu-Phe transport was involved. In addition to the *in vitro* studies, one study performing *in situ* intestinal perfusion of fMet-Leu-Phe in rat jejunum also demonstrated an increasing myeloperoxidase (MPO) activity in the presence of PEPT1. The other animal model of SBS, 80% small intestine resection also showed increasing MPO activity when perfusing fMet-Leu-Phe in colon, which provided the possible

consequence of the upregulation of PEPT1 in the colon (Buyse *et al.*, 2002; Shi *et al.*, 2006). Therefore, a hypothesis was proposed that colonic PEPT1 is involved in the intestinal inflammation in disease condition rather than just being as a nutritional transporter (Charrier *et al.*, 2006b).

Nonetheless, most of the kinetic studies were performed in the cell culture models, and only functional consequences were examined in those *in situ* studies. Direct measurement of the kinetic of bacterially-produced peptides transport *in situ* has not been demonstrated so far. Also, the possibility that other oligopeptide transporter involved in the transport of those bacterially-produced peptides still cannot be ruled out. In our previous studies, by using single-pass intestinal perfusion technique, a significant reduction of effective permeability of glycylsarcosine (Gly-Sar) has been shown in the *Pept1* knockout mice as compared to wild-type mice, which provided a useful technique to examine the substrate specificity and kinetics of PEPT1 in the intestine (Jappan *et al.*, 2010). Therefore, in the present study the PEPT1-mediated transport of fMet-Leu-Phe (a bacterially-produced peptide) was evaluated using a single-pass intestinal perfusion technique in mice. In particular, the regional permeability, concentration dependency, substrate specificity, and dynamic activity of fMet-Leu-Phe were studied in wild-type and *Pept1* knockout mice.

MATERIALS AND METHODS

Materials

[³H-Phe] fMet-Leu-Phe (15 Ci/mmol) was purchased from AmBios Labs (Newington, CT). [¹⁴C] Inulin (2.38 mCi/g) was purchased from Moravek Biochemicals and Radiochemicals (Brea, CA). Glycyl-Proline (Gly-Pro) was obtained from Bachem (Torrance, CA). All other chemicals were acquired from Sigma-Aldrich (St. Louis, MO).

Animals

Mouse experiments were conducted in accordance with the Guide for the Care and Use of Laboratory Animals as adopted by the U.S. National Institutes of Health. Gender-matched wild-type and *Pept1* knockout mice (8-10 week old) were used in all the experiments. The mice were kept under a 12-hr light and 12-hr dark cycle, and fed *ad libitum* with standard diet and water (Unit for Laboratory Animal Medicine, University of Michigan, Ann Arbor, MI).

Intestinal fMet-Leu-Phe Metabolism and Exposure in Portal Vein

1 cm of each intestinal segment (duodenum, jejunum, ileum, colon) of wild-type mice was taken and exposed the luminal surface longitudinally. Each intestinal segment was incubated with 0.5 ml PBS (pH 7.4) containing 0.8 mM fMet-Leu-Phe at 37°C for 5 mins. After incubation, solution was placed on ice and added 10 µl 10% TFA. Analysis was done by HPLC with 250 x 4.6 mm C18 column (Symmetric®, Waters, Milford, MA). The mobile phase consisted of 100% acetonitrile plus 0.1% TFA (buffer A) and 100% H₂O plus 0.1% TFA (buffer B). A gradient flow was used, starting from 15% buffer A to

30% buffer A over 30 min. The UV absorbance of fMet-Leu-Phe and metabolites were measured at 210 nm. For the portal vein blood collection, 2 μ Ci/ml (0.1 μ M) [3 H-Phe] fMet-Leu-Phe was perfused in the jejunum of wild-type mice for 90 min. The portal vein blood was collected during the period of 80-90 min. The whole blood was centrifuged at 3,300 g for 3 mins. 100 μ l plasma was then extracted by adding 200 μ l of acetonitrile. The supernatant was further condensed by SpeedVac concentrator SVC-200H and reconstituted into 20 μ l water following by HPLC analysis with 250 x 4.6 mm C18 column (Discovery®, Supelco, Bellefonte, PA) and Packard 500TR radiochemical detector (PerkinElmer Life and Analytical Sciences, Boston, MA). 30% acetonitrile plus 0.1% TFA was used as the mobile phase.

***In situ* Single-pass Intestinal Perfusion**

Intestinal perfusion were performed in wild-type and *Pept1* knockout mice (8-10 week old) according to previous described (Jappan *et al.*, 2010) In brief, animals were fasted overnight and anesthetized with sodium pentobarbital (40-60 mg/kg ip). An 8 cm segment was isolated (i.e., ~2 cm distal to the ligament of Treitz). A glass cannula (2.0 mm outer diameter), attached to Tygon® Laboratory tubing, were inserted at both ends of intestinal segment and secured in place with silk sutures. Following cannulation, the isolated intestinal segment was rinsed with isotonic saline solution, and covered with saline-wetted gauze and parafilm to prevent dehydration. After the surgical procedure, the mice were transferred to a temperature-controlled chamber (31°C) to maintain the body temperature of mice during the experiment. The inlet cannula was connected to a 30-ml syringe placed on a perfusion pump (Harvard Apparatus, Syringe Infusion Pump 22, South Natick, MA).

The perfusate contained 135 mM NaCl, 5 mM KCl, 10 mM MES (pH 6.5), 0.01% [^{14}C]inulin, and 0.1 μM [^3H -Phe] fMet-Leu-Phe in the presence of 0 mM, 25 mM, 50 mM, 100 mM, 150 mM phenylalanine was perfused through the jejunum at a rate of 0.1 ml/min for the inhibitory curve study and 100 mM was used in the rest of experiments (concentration dependency, specificity study and the regional dependency). The exiting perfusate was collected every 10 mins for 90 mins. A 100 μl aliquot of each time point was added to a vial containing scintillation fluid (CytoScint[®], MP Biomedicals, Solon, OH) and measured by a dual-channel liquid scintillation counter (Beckman LS 6000 SC, Beckman Coulter, Inc, Fullerton, CA). The water flux was corrected by the non-permeable [^{14}C]inulin. For the specificity study, the potential inhibitors were used at 50 mM.

Regional Intestinal Permeability

Four intestinal segments were perfused separately as described above for jejunum. For duodenal perfusion, a 2 cm segment was isolated (i.e. ~0.25 cm distal to the pyloric sphincter). For jejunal perfusion, an 8 cm segment was isolated (i.e. ~2 cm distal to the ligament of Treitz). For ileal perfusion, a 6 cm segment was isolated (i.e. ~1 cm proximal to the cecum). For colonic perfusion, a 3 cm segment was isolated (i.e. ~0.5 cm distal to the cecum).

Effect of *in situ* Perfusion of fMet-Leu-Phe on the Myeloperoxidase (MPO) Activity

Gender-matched wild-type and *Pept1* knockout mice (8-10 week old) were perfused as described above in jejunum and colon with modification. The Krebs-Ringer buffer was perfused through the intestinal segment at rate of 0.067 ml/min for jejunum

and 0.1 ml/min for colon for 30 min and shifted to Krebs-Ringer buffer containing 0 or 10 μ M fMet-Leu-Phe for 4 hours. For inhibition study, 50 mM glycylglycine (Gly-Gly) was used. After 4 hour perfusion, the MPO activity was determined by spectrophotometric method based on the oxidation of o-dianisidine as previously described (Buyse *et al.*, 2002). Briefly, intestinal segment (50-100 mg) was homogenized by homogenizer (PowerGen Model 125 Homogenizer, Fisher Scientific, Pittsburgh, PA) on ice for 30 seconds in 50 mM potassium phosphate buffer (pH = 6.0) containing 0.5% hexadecyltrimethyl ammonium bromide (1 ml / 50-100 mg). After homogenization, homogenates were introduced to the freeze-thawed procedure for three times (-80°C / 37°C). Then, the homogenates were centrifuged at 12,800 g for 15 mins at 4°C. The supernatant (0.1 ml) was added to 2.9 ml 50 mM phosphate buffer (pH = 6.0) containing 0.167 mg/ml (0.53 mM) o-dianisidine dihydrochloride and 0.0005% (0.15 mM) hydrogen peroxide. The change of absorbance at 460 nm was measured for 2 mins at 15 s intervals. The slope of the change of absorbance was calculated by the kinetics mode of UV/Vis spectrophotometer (BU-530[®] Beckman Coulter[™], Fullerton, CA). The myeloperoxidase (MPO) activity was reported as IU/g wet tissue. One IU of MPO activity was defined as the quantity of enzyme able to convert 1 μ mol of hydrogen peroxide to water in 1 min at room temperature.

fMet-Leu-Phe Hydrolysis Kinetics by Jejunal Homogenates

Intestinal homogenates were prepared by scraping off the mucus layers from the jejunum by glass slide and homogenated in 0.5 ml ice-cold PBS by homogenator (PowerGen Model 125 Homogenizer, Fisher Scientific, Pittsburgh, PA) at speed 2 for 2 mins on ice. The homogenates were then centrifuged at 12,000 x g for 15 mins. The

supernatant was taken and the total protein concentration was measured by the Pierce protein assay kit (Thermo Scientific, Rockford, IL). 25 µl of 0.5 mg/ml protein were taken and incubated with different concentrations of [³H-Phe] fMet-Leu-Phe (0.4 µM – 100 µM) for 1 min at 37°C. 50 µl 10% TFA was then added following by 15,000 x g centrifugation for 15 mins. 20 µl of the supernatant will be analyzed by HPLC with 250 x 4.6 mm C18 column (Discovery®, Supelco, Bellefonte, PA) and Packard 500TR radiochemical detector (PerkinElmer Life and Analytical Sciences, Boston, MA) using 30% acetonitrile plus 0.1% TFA as the mobile phase. The rate of hydrolysis was calculated by measuring the loss of fMet-Leu-Phe in the supernatant.

Histological Examination

Samples after 4 hour perfusion with and without 10 µM fMet-Leu-Phe were fixed in buffered formalin in a Swiss-roll shape for overnight and embedded in paraffin (3 wild-type mice ± fMet-Leu-Phe, 3 *Pept1* knockout mice ± fMet-Leu-Phe, and 2 wild-type mice + fMet-Leu-Phe + Gly-Gly, totally 11 slides). 5 µm sections were taken and stained with hematoxylin-eosin (H&E) to reveal structural features and examined with light microscopy in a blinded manner by a pathologist.

Data Analysis

The effective permeability (P_{eff}) was determined by the loss of drug from the perfusate at steady-state according to a complete radial mixing (parallel tube) model. (Komiya *et al.*, 1980; Kou *et al.*, 1991)

$$P_{eff} = \frac{-Q \times \ln(C_{out}/C_{in})}{2\pi RL}$$

In the equation, Q is the flow rate (ml/min), R is the intestinal radius (cm), L is the length of intestine (cm), C_{out} is the outlet drug concentration (corrected for water flux by [^{14}C]inulin), and C_{in} is the inlet drug concentration. In current study, the steady-state was reached after 30 min perfusion. The steady-state flux (J) was referenced to the intestinal wall concentration (C_w) to estimate the intrinsic kinetic parameters (V_{max} , K_m) after factoring out the resistance of the unstirred water layer.

$$J = \frac{V_{max} \times C_w}{K_m + C_w}$$

The transformation of the inlet concentration to the intestinal wall concentration was based on the equation, where the P_{aq} is the estimated unstirred aqueous permeability (Johnson *et al.*, 1988).

$$C_w = C_{in} \times (1 - \frac{P_{eff}}{P_{aq}})$$

The aqueous permeability was determined by following equations.

$$P_{aq} = (A \frac{R}{D} Gz^{1/3})^{-1}$$

$$Gz = \frac{\pi DL}{2Q}$$

The aqueous diffusion coefficient ($D = 3.18 \times 10^{-4} \text{ cm}^2/\text{min}$) was calculated by Hayduk-Laudie expression (Reid *et al.*, 1977). Gz is the Graetz number (0.0399), and A is a unitless constant (1.225) estimated by $A = 2.5 Gz + 1.125$.

For the fMet-Leu-Phe hydrolysis study, the hydrolysis kinetic parameters (V_{\max} , K_m) were estimated by Michaelis-Menten equation.

$$V = \frac{V_{\max} \times C}{K_m + C}$$

In this equation, the V is the hydrolysis rate of fMet-Leu-Phe (nmole/mg/min) and C is the concentration of fMet-Leu-Phe (μM).

Statistical Analysis

Data were expressed as mean \pm SE. Two-tailed student's t-test was used to compare difference between two groups. For multiple comparisons, one-way ANOVA followed by Dunnett's or Tukey's post hoc comparison was used (GraphPad Prism, v5.0; GraphPad Software, Inc., La Jolla, CA). A probability of $p \leq 0.05$ was considered significant. Nonlinear regression analyses were performed using GraphPad Prism software, where the goodness of fit was determined by the coefficient of determination (r^2), the standard error of parameter estimates, and visual inspection of the residuals.

RESULTS

Intestinal Metabolism of fMet-Leu-Phe and Exposure in Portal Vein

The metabolic pattern was determined by directly incubating fMet-Leu-Phe in different intestinal segments. As shown in Fig. 3.1A-D, the hydrolysis of fMet-Leu-Phe was highest in the duodenum, followed by jejunum, ileum and colon, with the major metabolite being phenylalanine. During perfusion with [^3H -Phe]fMet-Leu-Phe for 90 min, only phenylalanine was detectable in the blood of portal vein (Fig. 3.1E). These results are consistent with a previous paper, where they suggested fMet-Leu-Phe would be completely metabolized after passing through the intestinal membrane (Woodhouse *et al.*, 1987). The results also demonstrate that while f-Met-Leu is formed as a metabolite, the dipeptide Leu-Phe is not. This is important as it allows an accurate assessment of fMet-Leu-Phe permeability when studied in the presence of unlabelled Phe (as shown later).

Regional Intestinal Permeability

To determine whether fMet-Leu-Phe was a substrate of PEPT1 and if differences existed in its permeability between intestinal segments, fMet-Leu-Phe was perfused in the duodenum, jejunum, ileum, and colon of both wild-type and *Pept1* knockout mice. Since fMet-Leu-Phe was metabolized in the intestine as shown in Fig. 3.1A-D, the forming metabolite, [^3H]Phe would confound the results by being taken up through other transporter systems. By adding excess non-radiolabeled Phe, the confounding effect can be eliminated. As shown in Fig. 3.2, the effective permeability decreased when increasing the concentration of non-radiolabeled Phe, and showed completely inhibition around 100 mM. Therefore, perfusing fMet-Leu-Phe in the presence of 100 mM non-

radiolabeled Phe was used as a standard condition for the remaining experiments. In the presence of 100 mM non-radiolabeled Phe, the effective permeability was measured in both small and large intestines of wild-type and *Pept1* knockout mice. As shown in Fig. 3.3, the effective permeability of fMet-Leu-Phe was considerably lower in duodenum, jejunum, and ileum of *Pept1* knockout mice as compared to that of wild-type mice. However, the permeability of fMet-Leu-Phe was very low and similar in the colon of both genotypes. When comparing the results among intestinal segments, there was no difference between all four segments of *Pept1* knockout mice. By contrast, the permeability of fMet-Leu-Phe in wild-type mice was higher in duodenum and jejunum following by ileum (40% lower) and colon (98% lower). These findings were similar to our previous results with Gly-Sar, a model dipeptide substrate for PEPT1 (Jappan *et al.*, 2010).

Specificity Studies

The specificity of fMet-Leu-Phe uptake was examined in jejunum of both wild-type and *Pept1* knockout mice by adding the known PEPT1 substrate glycylproline (Gly-Pro) and the known PHT1/PHT2 substrate L-histidine. By co-perfusing the PEPT1 substrate Gly-Pro in the jejunum of both genotypes, the effective permeability of fMet-Leu-Phe was reduced in wild-type mice but not in *Pept1* knockout mice (Fig. 3.4). In contrast, L-histidine showed no effect on the effective permeability of fMet-Leu-Phe in both genotypes (Fig. 3.4), which suggested PHT1/PHT2 have no contribution on the transport of fMet-Leu-Phe in jejunum.

Concentration Dependency Study

To examine whether the uptake of fMet-Leu-Phe was saturable, the permeability of fMet-Leu-Phe was measured over the concentration range 0.1 μ M – 7.5 mM. As shown in Fig. 3.5, fMet-Leu-Phe exhibited a nonlinear uptake and the intrinsic V_{\max} and K_m values (i.e., after correcting for the unstirred water layer) were estimated by nonlinear regression. After fitting the data to a single-term Michaelis-Menten equation, a V_{\max} of 0.73 ± 0.07 nmole/cm²/s and K_m of 1.6 ± 0.37 mM were obtained. This K_m value was comparable to a previous study, where a K_m value of 2.9 mM was reported in the KG-1 cell line (Charrier *et al.*, 2006a).

Effect of *in situ* Perfusion of fMet-Leu-Phe on Myeloperoxidase (MPO) activity

It has been shown previously in rats that MPO activity increased when perfusing 10 μ M fMet-Leu-Phe in the intestine (Buyse *et al.*, 2002). The results of MPO activity after fMet-Leu-Phe perfusion in jejunum of wild-type mice were shown as Fig. 3.6A, which showed a comparable result to previous studies in rat. Perfusing 10 μ M fMet-Leu-Phe for 4 hours in the jejunum of wild-type mice increased the MPO activity around 2-fold. The increase of MPO activity could be abolished by adding the dipeptide glycylglycine (50 mM), thereby inhibiting the PEPT1-mediated uptake of fMet-Leu-Phe. In contrast, this phenomenon was not observed when perfusing 10 μ M fMet-Leu-Phe in the jejunum of *Pept1* knockout mice for 4 hours, suggesting that fMet-Leu-Phe was not being transported into enterocytes in the absence of PEPT1 (Fig. 3.6B). Likewise, there was no MPO activity increase when perfusing 10 μ M fMet-Leu-Phe in the colon of both genotypes for 4 hours (Fig. 3.6C). Interestingly, the baseline MPO activity between wild-type mice and *Pept1* knockout mice in colon showed no difference. The MPO activity of

wild-type mice was 3-fold higher than that of *Pept1* knockout mice, although all values in colon were much lower than that in jejunum.

fMet-Leu-Phe Hydrolysis Kinetics in Jejunal Homogenates

The hydrolysis of fMet-Leu-Phe in both wild-type and *Pept1* knockout mice were examined using jejunal homogenates. The hydrolysis rate exhibited nonlinear kinetics with increasing fMet-Leu-Phe concentrations. As shown in Fig. 3.7, the hydrolysis curves of wild-type and *Pept1* knockout mice were virtually superimposable. The estimated intrinsic kinetic parameters, obtained from nonlinear regression analyses, showed no difference between wild-type and *Pept1* knockout mice. V_{\max} values of 3.2 ± 0.23 and 3.3 ± 0.12 nmole/mg/min ($p = 0.66$), and K_m values of 7.0 ± 2.4 and 6.9 ± 1.2 μ M ($p = 0.968$) were obtained for wild-type and *Pept1* knockout mice, respectively.

Histological Examination

The H & E staining showed no significantly difference across samples with different treatments. All of the slides showed neutrophils within the submucosa and infiltrating the muscularis externa to varying degrees. Inflammation was qualitatively similar across groups and there were only minor differences in intensity between samples (Table 3.1). No significant differences in villus shape and no true villus blunting were observed (Figure 3.9).

DISCUSSION

The importance and the specificity of PEPT1-mediated transport of di/tripeptides in intestinal segments were previously shown by single-pass intestinal perfusions in *Pept1* knockout mice (Jappar *et al.*, 2010). The effective permeability of a hydrolysis-resistant dipeptide, Gly-Sar, was significantly reduced in the intestine of mice lacking PEPT1 expression. In the current study, PEPT1-mediated transport of a bacterially-produced peptide, fMet-Leu-Phe, was demonstrated directly by measuring its effective permeability in mouse intestine. The effective permeability of fMet-Leu-Phe in wild-type mice was significant higher than that of *Pept1* knockout mice in all segments of small intestine (i.e. duodenum, jejunum, and ileum), except for colon. The residual permeability of fMet-Leu-Phe in mice lacking PEPT1 expression was only 5-17% of values in mice with PEPT1 expression, suggesting that PEPT1 was the main transporter responsible for fMet-Leu-Phe transport in small intestine. In addition, the difference of effective permeability of fMet-Leu-Phe along the entire intestine was consistent with the protein expression of PEPT1 in the intestine, with higher and comparable values in duodenum and jejunum, followed by the ileum, and little to none permeability in colon, which was consistent with Gly-Sar uptake in our previous results (Jappar *et al.*, 2010).

The potential contribution of PHT1/PHT2 in the transport of fMet-Leu-Phe in intestine was examined in the jejunum of both genotypes. In the presence of L-histidine, a known substrate of PHT1/PHT2, the effective permeability of fMet-Leu-Phe in jejunum was not changed in both wild-type and *Pept1* knockout mice. Although the expression of PHT1 in the apical membrane in jejunum has been suggested (Bhardwaj *et al.*, 2006), its contribution to the transport of fMet-Leu-Phe was not significant as compared to PEPT1.

The concentration dependency of fMet-Leu-Phe transport was evaluated in the jejunum of wild-type mice. Although the curve did not fully reach a plateau due to solubility limitations of fMet-Leu-Phe in our buffer, the nonlinear transport of fMet-Leu-Phe was clear with estimates of $K_m = 1.6 \pm 0.37$ mM and $V_{max} = 0.73 \pm 0.07$ nmole/cm²/s. Our K_m value was comparable to a previous report in cell culture (Charrier *et al.*, 2006a) and to K_m values for PEPT1 in the literature for various compounds such as cefadroxil and cephalexin (Sinko *et al.*, 1988), which suggested that PEPT1 was a low-affinity transporter.

Our findings have shown that perfusion of fMet-Leu-Phe in the jejunum induced the activity of myeloperoxidase, which implied that fMet-Leu-Phe can be transported into the enterocytes through PEPT1 transporter. This finding was in contradiction to another report (Woodhouse *et al.*, 1987) in which the authors claimed that fMet-Leu-Phe would be non-permeable to intestinal membranes due to the combination of hydrolysis enzymes and intrinsic membrane barrier. Our results clearly showed that fMet-Leu-Phe can be transported into enterocytes along the entire small intestine, but not in colon, and that PEPT1 was the main transporter contributing to this transport (Fig. 3.3). Interestingly, when using carboxypeptidase inhibitors, 25 mM benzylsuccinic acid (BzS) or 10 mM EDTA, as in the previous paper (Woodhouse *et al.*, 1987), the permeability of Gly-Sar in jejunum was significantly reduced (1.7×10^{-4} cm/s for control, 0.21×10^{-4} cm/s for BzS, 0.69×10^{-4} cm/s for EDTA, $n=3$, Fig. 3.8). Our results suggested that carboxypeptidase inhibitors such as BzS and EDTA would compromise the transport activity of PEPT1 leading to the false conclusion that fMet-Leu-Phe was non-permeable to intestinal membranes. .

The perfusion of 10 μ M fMet-Leu-Phe in jejunum and colon in both wild-type and *Pept1* knockout mice demonstrated that PEPT1 was involved in the dynamic consequence of increasing MPO activity. In Fig. 5A, the increased MPO activity was reduced after co-perfusing fMet-Leu-Phe with the PEPT1 substrate Gly-Gly, which showed no effect on MPO activity when being perfused alone. In *Pept1* knockout mice (Fig. 3.5B), perfusion of fMet-Leu-Phe failed to result in a similar increase of MPO activity. Both results suggested that without PEPT1 transporter, fMet-Leu-Phe would not be transported into the enterocytes to increase MPO activity. However, when perfusing fMet-Leu-Phe in the colon of both genotypes, no increase of MPO activity was observed, which was consistent the fact that little or no PEPT1 was expressed in colon. Interestingly, the baseline activity of MPO between wild-type and *Pept1* knockout mice showed a small but significant difference in colon. However, the difference may be due to experimental variation since the measured activity was very low as compared to jejunum. Alternatively, it may be due to the contribution of very low but undetectable PEPT1 expression in the colon. More experiments will be needed to clarify this unexpected result.

It was important to rule out any possible differences of hydrolysis enzymes between wild-type and *Pept1* knockout mice, especially if a reduced permeability and unchanged MPO activity after fMet-Leu-Phe perfusion in *Pept1* knockout mice were due to an increased hydrolysis activity after genetic knockout of PEPT1. For this reason, fMet-Leu-Phe hydrolysis kinetics was examined in both wild-type and *Pept1* knockout mice. In this study, we found no difference between wild-type and *Pept1* knockout mice in the intrinsic kinetic parameters, V_{\max} and K_m . In the current study, specific enzymes

contributing to the hydrolysis of fMet-Leu-Phe were not evaluated only the nonspecific process. . Although the responsible enzymes for the hydrolysis of fMet-Leu-Phe were uncertain, one category of enzymes was reported to be responsible for the hydrolysis of fMet-Leu-Phe, that being carboxypeptidase (Chadwick *et al.*, 1990). According to the literature (depending on the specific isoform, compound, and experimental system), the K_m of carboxypeptidases can range from 6 to 1573 μM (Deiteren *et al.*, 2007). The low K_m value of 7 μM in our study is consistent with these literature values. Moreover, the metabolite pattern of fMet-Leu-Phe intestinal degradation agrees with carboxypeptidases being responsible for the hydrolysis of fMet-Leu-Phe. In this regard, the major metabolite of fMet-Leu-Phe was Phe, suggesting that the direction of hydrolysis was from the carboxyl terminus (Fig. 3.1A-D).

Colonic PEPT1 has been suggested to be involved in intestinal inflammation based on the results of direct and indirect data such as: 1) the upregulation of PEPT1 in the apical membrane of patients with inflammatory bowel disease; 2) increasing amounts of bacteria in the colons of patients with inflammatory bowel disease (Swidsinski *et al.*, 2002); this was confirmed by some animal colitis models (Hernandez *et al.*, 2003); 3) the ability of PEPT1 to transport bacterial compounds; 4) immune cells, such as macrophages, have been shown to express PEPT1 on their surface; and 5) a genetic polymorphism study demonstrating the possibility of PEPT1 being involved in inflammatory bowel disease (Zucchelli *et al.*, 2009); still, the results showed the influence of PEPT1 in two opposite directions (risk and protection). Interestingly, an alternate hypothesis was proposed by the same group in which the possible role of PEPT1 in intestinal inflammation was investigated by studies in wild-type and hPEPT1

transgenic mice after *citrobacter rodentium* infection (Nguyen *et al.*, 2009). Surprisingly, PEPT1 transgenic mice showed less inflammatory responses due to the presence of fewer bacteria adhesion on colonic membranes. These studies demonstrate the very complex nature of inflammation and IBD in which the environment, genetics, immunology, microbiome, and diet may all play an important role. More thoughtful/creative studies will be needed in order to elucidate the role of colonic PEPT1 in intestinal inflammation.

In conclusion, the present studies provide several new findings: 1) PEPT1 can transport bacterially-produced peptide fMet-Leu-Phe with comparable permeability in the duodenum and jejunum of mice, followed by ileum; there is little to no transport in colon ; 2) the transport of fMet-Leu-Phe in mouse small intestine was specific for PEPT1; 3) the estimated intrinsic K_m of fMet-Leu-Phe was 1.6 mM; 4) PEPT1 was responsible for the increased MPO activity in jejunum after perfusion of fMet-Leu-Phe; and 5) the hydrolysis of fMet-Leu-Phe was unchanged after genetic knockout of PEPT1 in mice.

FIGURES

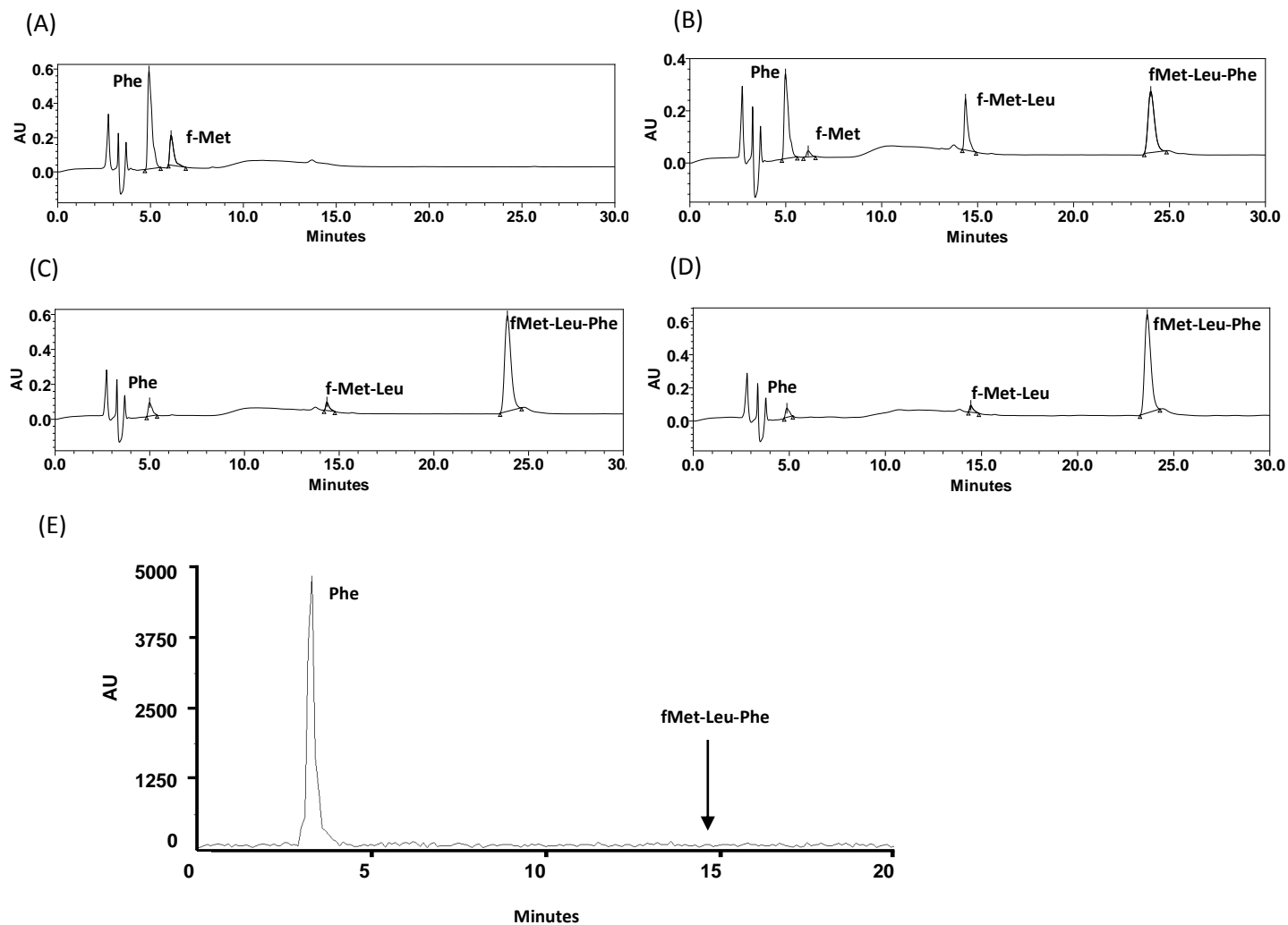


Figure 3.1. Chromatogram of metabolites of fMet-Leu-Phe after incubation with 1 cm intestinal segments of wild-type mice for 5 min at 37°C and metabolites in the portal vein plasma after *in situ* perfusion for 90 mins. (A) duodenum (B) jejunum (C) ileum (D) colon (E) portal vein plasma. Phe: phenylalanine, f-Met: formyl-methionine, f-Met-Leu: formyl-methionyl-leucine, fMet-Leu-Phe: N-formyl-methionyl-leucyl-phenylalanine.

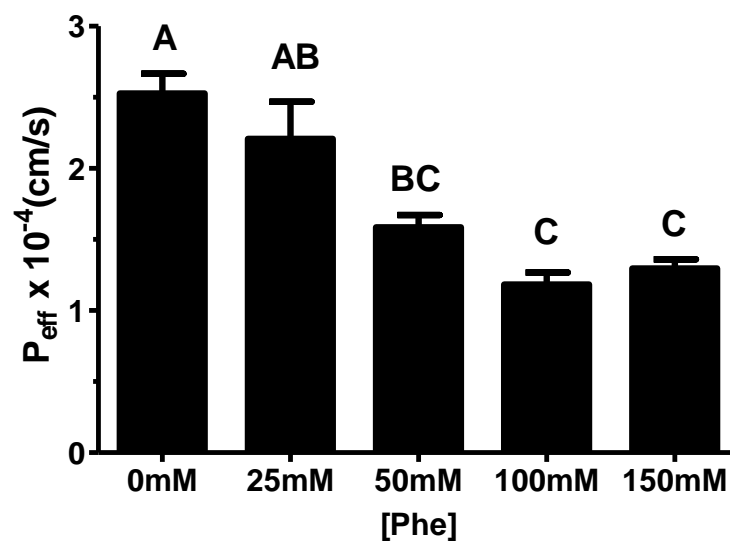


Figure 3.2. Effective permeability of fMet-Leu-Phe in jejunum of wild-type mice in the presence of phenylalanine at different concentrations (Mean \pm SE, $n=3$). Groups with different letters represented statistical difference which performed by one-way ANOVA with Tukey's comparison.

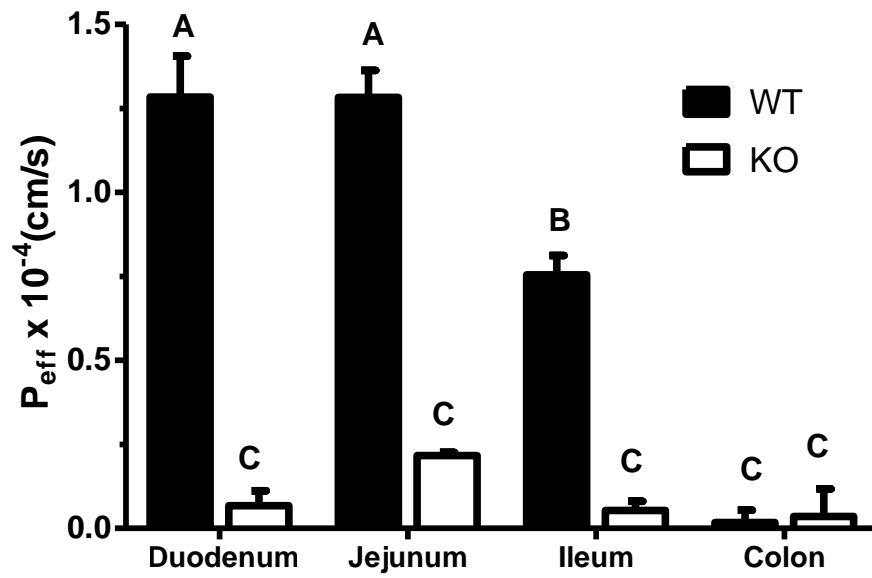


Figure 3.3. Effective permeability of fMet-Leu-Phe in different intestinal segments of wild-type mice and *Pept1* knockout mice in the presence of 100 mM phenylalanine (Mean \pm SE, n=6). Groups with different letters represented statistical difference which performed by one-way ANOVA with Tukey's comparison for the same genotype and by t-test between different genotypes for each intestinal segment.

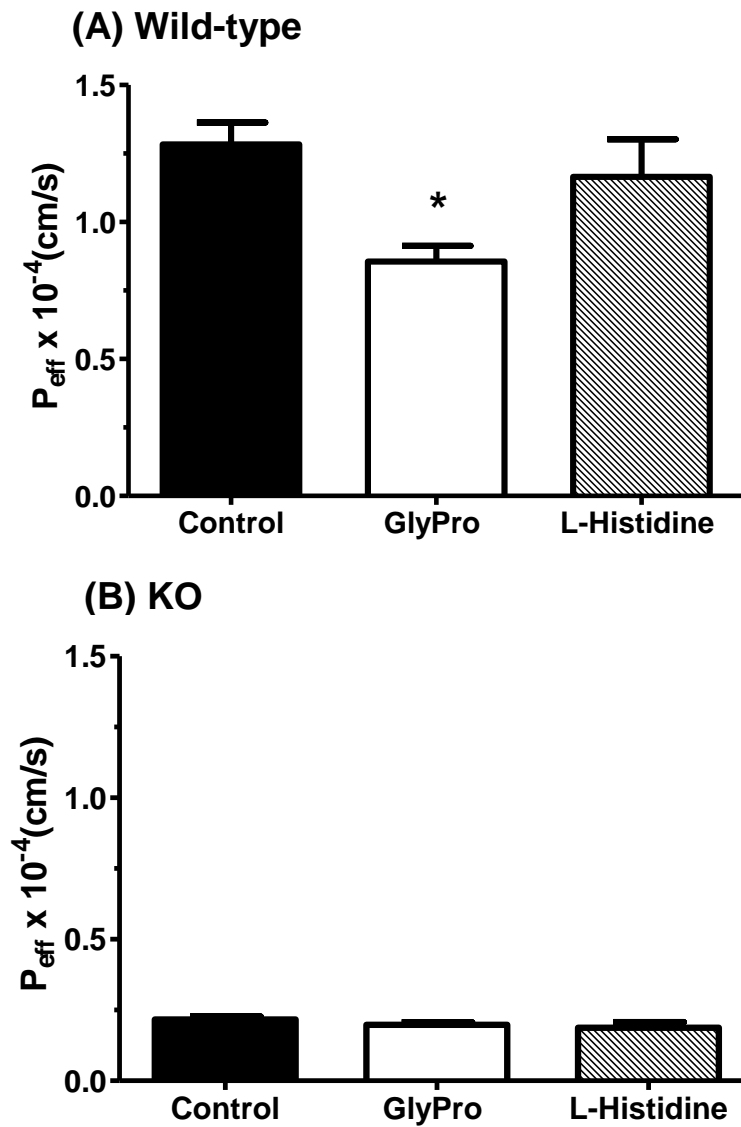


Figure 3.4. Gly-Pro (50 mM) inhibited the effective permeability of fMet-Leu-Phe in the jejunum of wild-type mice (A) but not in that of *Pept1* knockout mice (B) (Mean \pm SE, n=4). L-histidine (50 mM) showed no inhibitory effects in the jejunum of both wild-type and *Pept1* knockout mice (Mean \pm SE, n=4). Statistical analysis was performed by one-way ANOVA with Dunnett's analysis as compared to control. * $p < 0.05$.

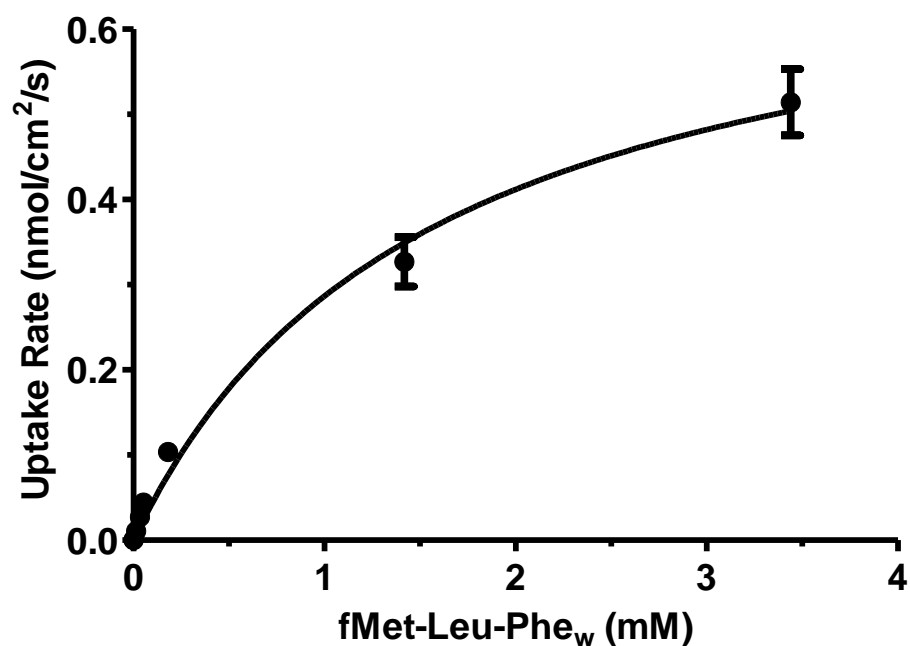


Figure 3.5. Concentration dependency of fMet-Leu-Phe uptake in the jejunum of wild-type mice (Mean \pm SE, n=4). fMet-Leu-Phe_w was referenced to the estimated concentration at intestinal wall.

Michaelis-Menten	
Best-fit values	
Vmax	0.7314
Km	1.551
Std. Error	
Vmax	0.07031
Km	0.3666
95% Confidence Intervals	
Vmax	0.5879 to 0.8750
Km	0.8028 to 2.300
Goodness of Fit	
Degrees of Freedom	30
R ²	0.9645
Absolute Sum of Squares	0.03697
Sy.x	0.03511
Constraints	
Km	Km > 0.0
Number of points	
Analyzed	32

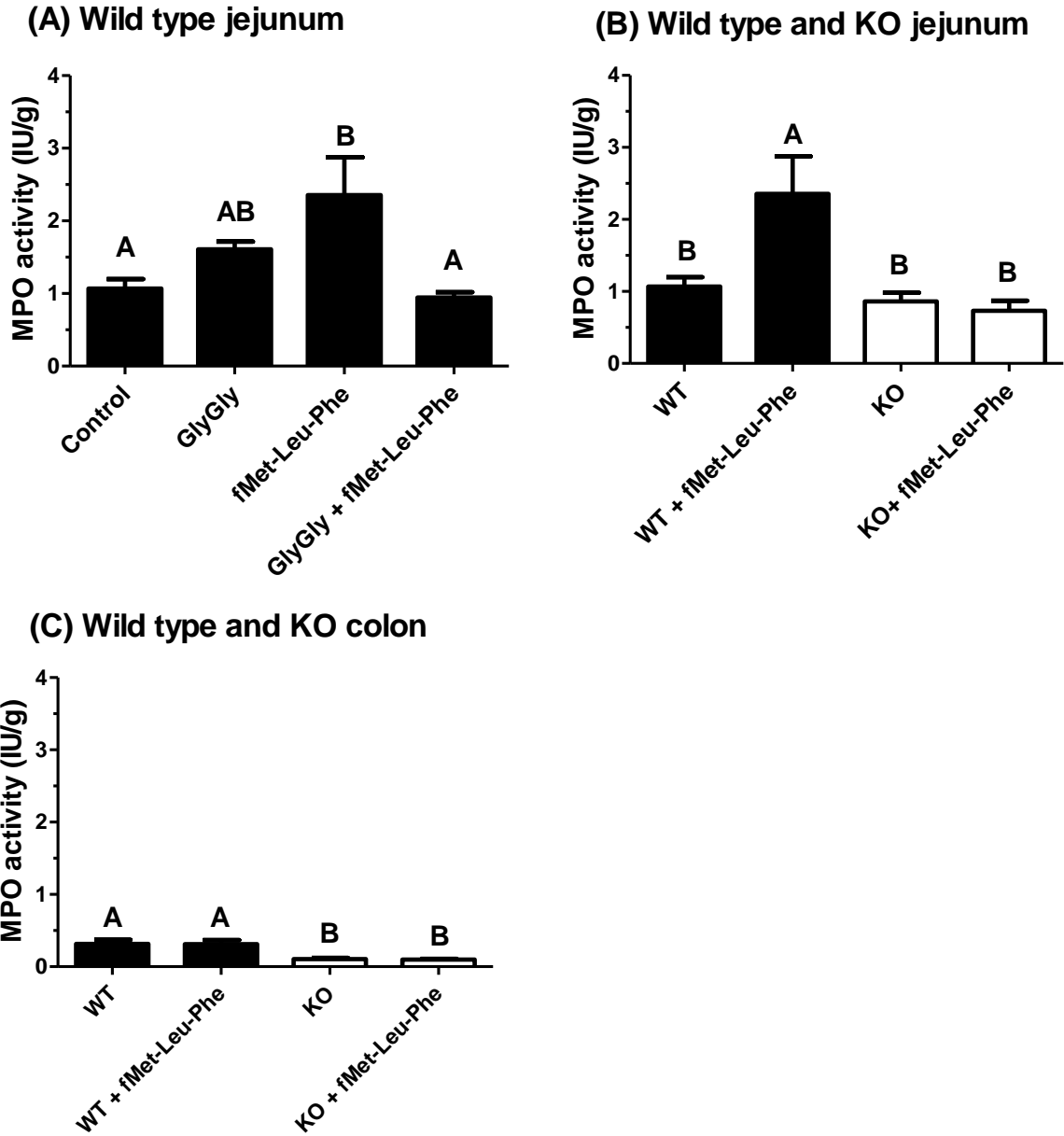


Figure 3.6. (A) fMet-Leu-Phe induced MPO activity and Gly-Gly (50 mM) reversed the fMet-Leu-Phe-induced MPO activity in the jejunum of wild-type mice (Mean \pm SE, n=5). (B) fMet-Leu-Phe-induced MPO activity was not observed in the jejunum of *Pept1* knockout mice (Mean \pm SE, n=5). (C) fMet-Leu-Phe showed no effects in the colon of both wild-type and *Pept1* knockout mice (Mean \pm SE, n=5). Groups with different letters represented statistical difference which performed by one-way ANOVA with Tukey's comparison.

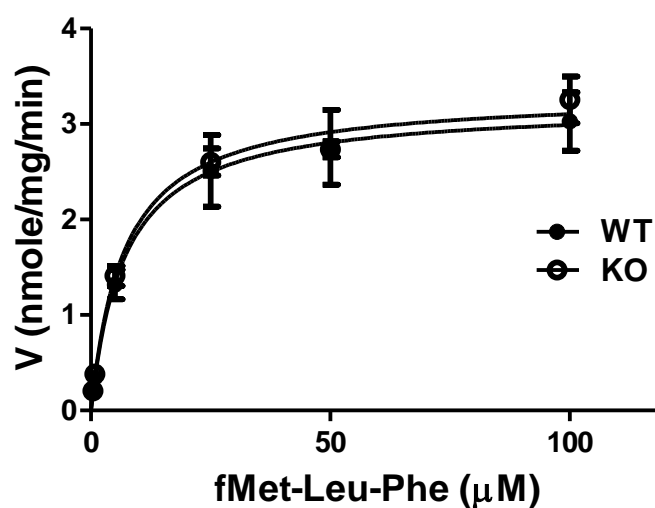


Figure 3.7. fMet-Leu-Phe hydrolysis kinetics by jejunal homogenates of wild-type and *Pept1* knockout mice (Mean \pm SE, n=4). The data were fitted to Michaelis-Menten equation.

Michaelis-Menten	WT	KO
Best-fit values		
Vmax	3.200	3.318
Km	7.027	6.918
Std. Error		
Vmax	0.2327	0.1223
Km	2.355	1.179
95% Confidence Intervals		
Vmax	2.718 to 3.683	3.065 to 3.572
Km	2.143 to 11.91	4.472 to 9.364
Goodness of Fit		
Degrees of Freedom	22	22
R ²	0.8602	0.9593
Absolute Sum of Squares	5.012	1.403
Sy.x	0.4773	0.2526
Constraints		
Km	Km > 0.0	Km > 0.0
Number of points		
Analyzed	24	24

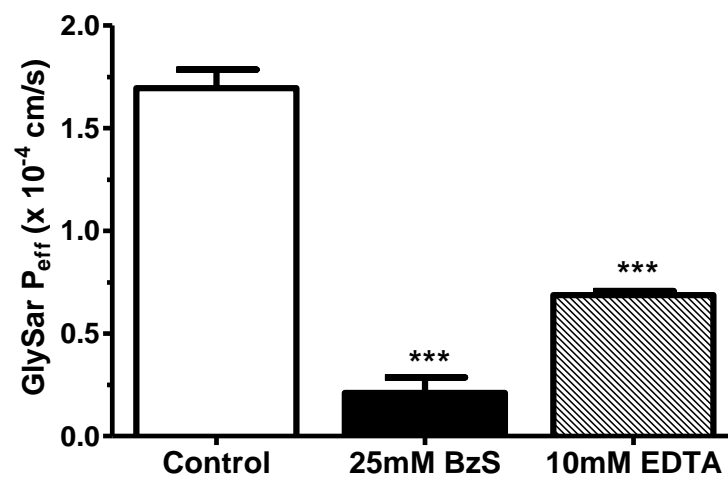


Figure 3.8. Effective permeability of Gly-Sar were affected in the presence of the inhibitor of carboxypeptidase BzS and EDTA (Mean \pm SE, n=3).

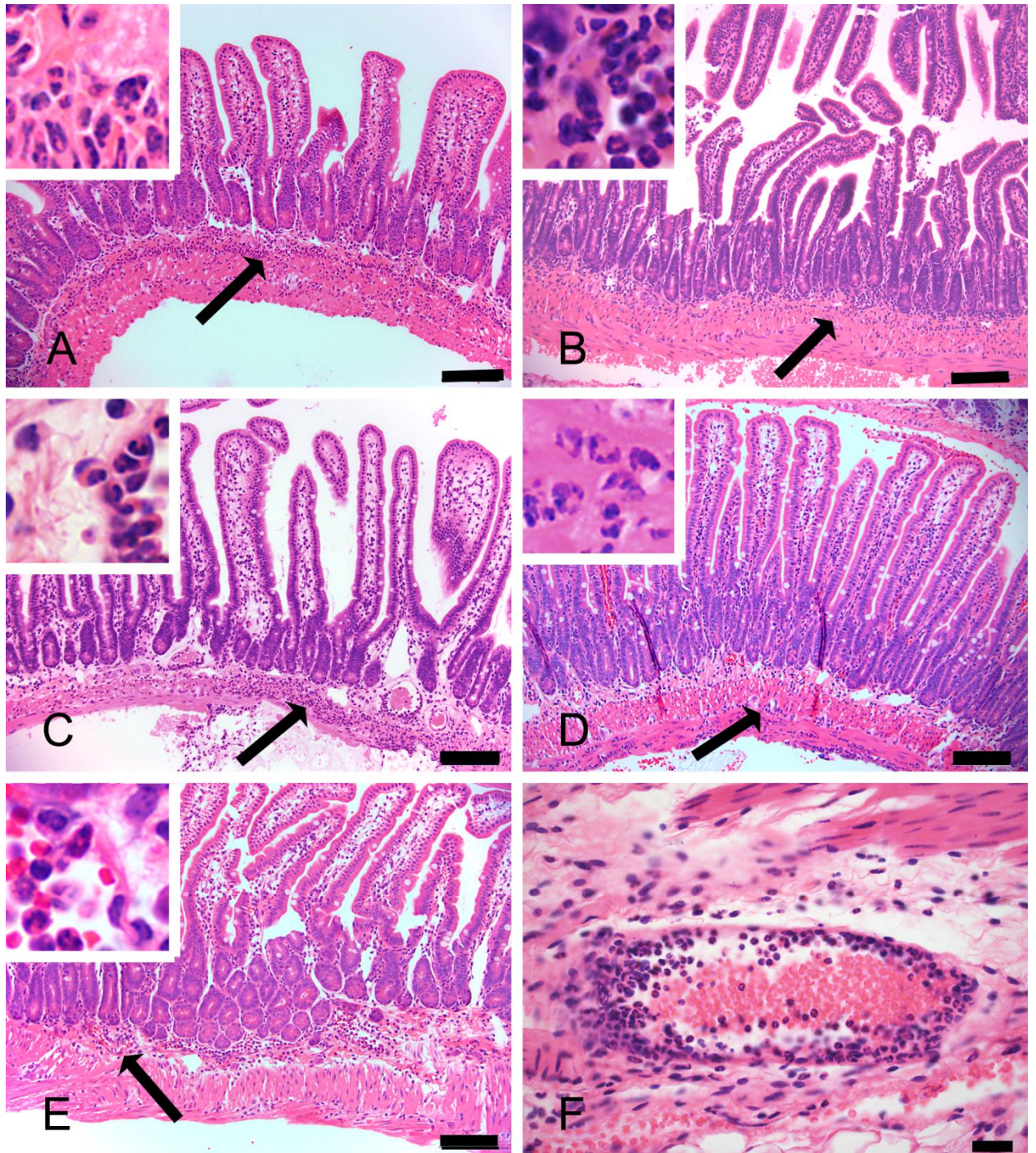


Figure 3.9. Representative photomicrographs of jejunum of experimental groups. A. wild-type control. B, F. *Pept1* knockout control. C. wild-type + fMet-Leu-Phe. D. *Pept1* knockout + fMet-Leu-Phe. E. wild-type + fMet-Leu-Phe + Gly-Gly. A-E: original magnification (x200), bars = 100 μ m. Insets (x1800). F. original magnification (x600), bar = 20 μ m.

Rank ordering	Group ID (lab has info)	Scoring			comment	photos
		edema	inflammation	Total score		
1-1	WT1	1	2	3	less edema, more neutrophils	
1-2	WT2	2	1	3	lamina propria and submucosal edema	x
1-3	WT3	2	1	3	lamina propria and submucosal edema	
2-1	WT+Met-Leu-Phe1	2	1	3	lamina propria and submucosal edema	
2-2	WT+Met-Leu-Phe2	1	3	4	neutrophils full thickness through the gut wall(focal)	x
2-3	WT+Met-Leu-Phe3	2	1	3	lamina propria and submucosal edema	
3-1	KO1	2	1	3	lamina propria and submucosal edema	
3-2	KO2	1	3	4	vasculitis (neutrophils in submucosal vascular wall)	x
3-3	KO3	2	1	3	lamina propria and submucosal edema	
4-1	KO+Met-Leu-Phe1	1	2	3	less edema, more neutrophils	
4-2	KO+Met-Leu-Phe2	1	2	3	less edema, more neutrophils	x
4-3	KO+Met-Leu-Phe3	2	1	3	lamina propria and submucosal edema	
5-1	WT+Met-Leu-Phe+GlyGly1	1	1	2	lamina propria and submucosal edema	
5-2	WT+Met-Leu-Phe+GlyGly2	1	1	2	lamina propria and submucosal edema	x

Scoring key
0: absent
1: mild
2: moderate
3: severe
4: marked

Table 3.1. Scores of edema and inflammation of each sample.

REFERENCES

- Adibi SA (2003). Regulation of expression of the intestinal oligopeptide transporter (Pept-1) in health and disease. *Am J Physiol Gastrointest Liver Physiol* **285**: G779-788.
- Bhardwaj RK, Herrera-Ruiz D, Eltoukhy N, Saad M, Knipp GT (2006). The functional evaluation of human peptide/histidine transporter 1 (hPHT1) in transiently transfected COS-7 cells. *Eur J Pharm Sci* **27**: 533-542.
- Buyse M, Tsocas A, Walker F, Merlin D, Bado A (2002). PepT1-mediated fMLP transport induces intestinal inflammation in vivo. *Am J Physiol Cell Physiol* **283**: C1795-1800.
- Chadwick VS, Schlup MMT, Cooper BT, Broom MF (1990). Enzymes degrading bacterial chemotactic F-met peptides in human ileal and colonic mucosa. *Journal of Gastroenterology and Hepatology* **5**: 375-381.
- Charrier L, Driss A, Yan Y, Nduati V, Klapproth JM, Sitaraman SV, Merlin D (2006a). hPepT1 mediates bacterial tripeptide fMLP uptake in human monocytes. *Lab Invest* **86**: 490-503.
- Charrier L, Merlin D (2006b). The oligopeptide transporter hPepT1: gateway to the innate immune response. *Lab Invest* **86**: 538-546.
- Deiteren K, Surpateanu G, Gilany K, Willemse JL, Hendriks DF, Augustyns K, Laroche Y, Scharpe S, Lambeir AM (2007). The role of the S1 binding site of carboxypeptidase M in substrate specificity and turn-over. *Biochim Biophys Acta* **1774**: 267-277.
- Fei YJ, Kanai Y, Nussberger S, Ganapathy V, Leibach FH, Romero MF, Singh SK, Boron WF, Hediger MA (1994). Expression cloning of a mammalian proton-coupled oligopeptide transporter. *Nature* **368**: 563-566.
- Ganapathy ME, Huang W, Wang H, Ganapathy V, Leibach FH (1998). Valacyclovir: a substrate for the intestinal and renal peptide transporters PEPT1 and PEPT2. *Biochem Biophys Res Commun* **246**: 470-475.
- Ganapathy V, Gupta N, Martindale RG (2006). Protein Digestion and Absorption. In: *Physiology of the Gastrointestinal Tract (Fourth Edition)*, pp. 1667-1692. Academic Press, Burlington.
- Hernandez GA, Appleyard CB (2003). Bacterial load in animal models of acute and chronic 'reactivated' colitis. *Digestion* **67**: 161-169.

Jappara D, Wu SP, Hu Y, Smith DE (2010). Significance and regional dependency of peptide transporter (PEPT) 1 in the intestinal permeability of glycylsarcosine: in situ single-pass perfusion studies in wild-type and Pept1 knockout mice. *Drug Metab Dispos* **38**: 1740-1746.

Johnson DA, Amidon GL (1988). Determination of intrinsic membrane transport parameters from perfused intestine experiments: a boundary layer approach to estimating the aqueous and unbiased membrane permeabilities. *J Theor Biol* **131**: 93-106.

Komiya I, Park JY, Kamani A, Ho NFH, Higuchi WI (1980). Quantitative mechanistic studies in simultaneous fluid flow and intestinal absorption using steroids as model solutes. *International Journal of Pharmaceutics* **4**: 249-262.

Kou JH, Fleisher D, Amidon GL (1991). Calculation of the aqueous diffusion layer resistance for absorption in a tube: application to intestinal membrane permeability determination. *Pharm Res* **8**: 298-305.

Marasco WA, Phan SH, Krutzsch H, Showell HJ, Feltner DE, Nairn R, Becker EL, Ward PA (1984). Purification and identification of formyl-methionyl-leucyl-phenylalanine as the major peptide neutrophil chemotactic factor produced by *Escherichia coli*. *J Biol Chem* **259**: 5430-5439.

Merlin D, Si-Tahar M, Sitaraman SV, Eastburn K, Williams I, Liu X, Hediger MA, Madara JL (2001). Colonic epithelial hPepT1 expression occurs in inflammatory bowel disease: transport of bacterial peptides influences expression of MHC class 1 molecules. *Gastroenterology* **120**: 1666-1679.

Merlin D, Steel A, Gewirtz AT, Si-Tahar M, Hediger MA, Madara JL (1998). hPepT1-mediated epithelial transport of bacteria-derived chemotactic peptides enhances neutrophil-epithelial interactions. *J Clin Invest* **102**: 2011-2018.

Nguyen HT, Dalmaso G, Powell KR, Yan Y, Bhatt S, Kalman D, Sitaraman SV, Merlin D (2009). Pathogenic bacteria induce colonic PepT1 expression: an implication in host defense response. *Gastroenterology* **137**: 1435-1447 e1431-1432.

Ogihara H, Saito H, Shin BC, Terado T, Takenoshita S, Nagamachi Y, Inui K, Takata K (1996). Immuno-localization of H⁺/peptide cotransporter in rat digestive tract. *Biochem Biophys Res Commun* **220**: 848-852.

Okano T, Inui K, Takano M, Hori R (1986). H⁺ gradient-dependent transport of aminocephalosporins in rat intestinal brush-border membrane vesicles. Role of dipeptide transport system. *Biochem Pharmacol* **35**: 1781-1786.

Reid RC, Prausnitz JM, Sherwood TK (1977). In: *The Properties of Gases and Liquids, 3rd*, 3rd, pp. 573. McGraw-Hill Book Company, New York.

Shi B, Song D, Xue H, Li N, Li J (2006). PepT1 mediates colon damage by transporting fMLP in rats with bowel resection. *J Surg Res* **136**: 38-44.

Sinko PJ, Amidon GL (1988). Characterization of the oral absorption of beta-lactam antibiotics. I. Cephalosporins: determination of intrinsic membrane absorption parameters in the rat intestine in situ. *Pharm Res* **5**: 645-650.

Soul-Lawton J, Seaber E, On N, Wootton R, Rolan P, Posner J (1995). Absolute bioavailability and metabolic disposition of valaciclovir, the L-valyl ester of acyclovir, following oral administration to humans. *Antimicrob Agents Chemother* **39**: 2759-2764.

Swaan PW, Bensman T, Bahadduri PM, Hall MW, Sarkar A, Bao S, Khantwal CM, Ekins S, Knoell DL (2008). Bacterial peptide recognition and immune activation facilitated by human peptide transporter PEPT2. *Am J Respir Cell Mol Biol* **39**: 536-542.

Swidsinski A, Ladhoff A, Pernthaler A, Swidsinski S, Loening-Baucke V, Ortner M, Weber J, Hoffmann U, Schreiber S, Dietel M, Lochs H (2002). Mucosal flora in inflammatory bowel disease. *Gastroenterology* **122**: 44-54.

Thwaites DT, Cavet M, Hirst BH, Simmons NL (1995). Angiotensin-converting enzyme (ACE) inhibitor transport in human intestinal epithelial (Caco-2) cells. *Br J Pharmacol* **114**: 981-986.

Tomita Y, Katsura T, Okano T, Inui K, Hori R (1990). Transport mechanisms of bestatin in rabbit intestinal brush-border membranes: role of H⁺/dipeptide cotransport system. *J Pharmacol Exp Ther* **252**: 859-862.

Vavricka SR, Musch MW, Chang JE, Nakagawa Y, Phanvijhitsiri K, Waypa TS, Merlin D, Schneewind O, Chang EB (2004). hPepT1 transports muramyl dipeptide, activating NF-kappaB and stimulating IL-8 secretion in human colonic Caco2/bbe cells. *Gastroenterology* **127**: 1401-1409.

Vig BS, Stouch TR, Timoszyk JK, Quan Y, Wall DA, Smith RL, Faria TN (2006). Human PEPT1 pharmacophore distinguishes between dipeptide transport and binding. *J Med Chem* **49**: 3636-3644.

Woodhouse AF, Anderson RP, Myers DB, Broom MF, Hobson CH, Chadwick VS (1987). Intestinal absorption, metabolism and effects of bacterial chemotactic peptides in rat intestine. *Journal of Gastroenterology and Hepatology* **2**: 35-43.

Ziegler TR, Fernandez-Estivariz C, Gu LH, Bazargan N, Umeakunne K, Wallace TM, Diaz EE, Rosado KE, Pascal RR, Galloway JR, Wilcox JN, Leader LM (2002). Distribution of the H⁺/peptide transporter PepT1 in human intestine: up-regulated expression in the colonic mucosa of patients with short-bowel syndrome. *Am J Clin Nutr* **75**: 922-930.

Zucchelli M, Torkvist L, Bresso F, Halfvarson J, Hellquist A, Anedda F, Assadi G, Lindgren GB, Svanfeldt M, Janson M, Noble CL, Pettersson S, Lappalainen M, Paavola-Sakki P, Halme L, Farkkila M, Turunen U, Satsangi J, Kontula K, Lofberg R, Kere J, D'Amato M (2009). PepT1 oligopeptide transporter (SLC15A1) gene polymorphism in inflammatory bowel disease. *Inflamm Bowel Dis* **15**: 1562-1569.

Chapter 4

IMPACT OF INTESTINAL PEPT1 ON THE REGIONAL PERMEABILITY OF LYS-PRO-VAL, AN ANTI-INFLAMMATORY TRIPEPTIDE DERIVED FROM α -MELANOCYTE-STIMULATING HORMONE

ABSTRACT

Lys-Pro-Val, which is derived from α -melanocyte-stimulating hormone (α -MSH), has been shown to possess anti-inflammatory activity and suggested to be a novel therapeutic agent for inflammatory diseases. Although studies suggested that Lys-Pro-Val is transported by the PEPT1 transporter, no direct measurement of intestinal permeability has been performed. In addition, the intestinal stability of Lys-Pro-Val has not been addressed. In the present study, intestinal homogenates were used to study the stability of Lys-Pro-Val in different intestinal regions of wild-type mice. The effective permeability of [3 H-Pro]Lys-Pro-Val in duodenum, jejunum, ileum, and colon was determined by single-pass intestinal perfusions in wild-type and *Pept1* knockout mice. Based on stability studies, the intrinsic clearances (CL_{int}) of Lys-Pro-Val were associated with the mRNA expression of two intestinal peptidases, namely dipeptidyl peptidase IV (DPPIV) and aminopeptidase P (APP). Therefore, two peptidase inhibitors (Phe-Pyrrolidide and o-phenathroline) were incorporated in the perfusion experiments.

Compared with wild-type mice, *Pept1* knockout mice exhibited greater than 90% reduction in Lys-Pro-Val uptake in all small intestinal segments, but showed no difference in colon. Lys-Pro-Val uptake was significantly inhibited by dipeptide and cefadroxil in duodenum, jejunum and ileum, but not colon. Lys-Pro-Val exhibited nonlinear uptake kinetics with an estimated K_m of 0.11 mM (based on C_{wall}) and a nonsaturable component in the jejunum of wild-type mice. The findings demonstrated that PEPT1 played a critical role in the uptake of Lys-Pro-Val in small intestines and suggested that the stability of Lys-Pro-Val was a significant concern when using Lys-Pro-Val as a therapeutic agent, especially after oral administration.

INTRODUCTION

α -Melanocyte-stimulating hormone (α -MSH) has been known to exert different biological activity in addition to its pigmentary activity for decades. The anti-inflammatory effect of α -MSH was one of the bioactivities that received the most interest. Many studies have been performed to elucidate the required pharmacophore of α -MSH to interact with melanocortin receptors, which indicated that the core peptide histidine-phenylalanine-arginine-tryptophane (HFRW, α -MSH₆₋₉) was responsible for binding. Upon binding to melanocortin receptors, α -MSH exerts its anti-inflammatory effect mainly by inhibiting the activation of NF- κ B through an increase of intracellular cAMP (Manna *et al.*, 1998). Although α -MSH demonstrated promising anti-inflammatory effect, the major concern for practical use was its melanotropic effect. Therefore, more attention focused on the C-terminal tripeptide of α -MSH and its related derivatives, such as KPV, KdPV and KPT, which have been shown to retain the anti-inflammatory activity of α -MSH with no significant melanotropic effect. The anti-inflammatory activity of tripeptide KPV and its derivatives have been demonstrated by both *in vitro* and *in vivo* models. For example, KPV demonstrated a similarly effective suppression of LPS/IFN- γ -induced NF- κ B activation and NO production as full-length α -MSH in the RAW 264.7 murine macrophage cell line (Mandrika *et al.*, 2001). After an intracerebroventricular (i.c.v.) injection of lipopolysaccharide (LPS), mice, pretreated with 200 mg i.p. KPV showed a reduction of NF- κ B activation (Ichiyama *et al.*, 1999). In another study, dextran sodium sulfate (DSS) or trinitrobenzene sulfonic acid (TNBS) was used to induce colitis after which 100 μ M KPV was added to the drinking water and mice allowed to drink the water

ad libitum. Most interesting, the results showed that KPV was able to reduce the mRNA of IL-6 and IL-12 in the DSS model and to effectively decrease the mRNA of IL-1 β , IL-6, TNF- α , and IFN- γ in the TNBS model, all proinflammatory cytokines (Dalmasso *et al.*, 2008).

PEPT1 transporter belongs to the solute carrier 15 family (SLC15), which consists of four mammalian members, including the high-capacity, low-affinity peptide transporter 1 (PEPT1; SLC15A1), the low-capacity, high-affinity transporter PEPT2 (SLC15A2), and the peptide/histidine transporters PHT1 (SLC15A4) and PHT2 (SLC15A3). PEPT1 is expressed throughout the small intestine (duodenum, jejunum, and ileum), but with little or no expression in the colon. Immunofluorescent staining also showed that PEPT1 was expressed mainly at the apical side of the enterocyte with decreasing expression from the tip to the crypt of the villus (Ogihara *et al.*, 1996). Studies suggested that PEPT1 was very important for nutrition aspect because it facilitated the absorption of digested protein in the form of di/tripeptides (Ganapathy *et al.*, 2006). Besides having nutritive relevance, PEPT1 was also important for the uptake of some peptidomimetics, such as β -lactam antibiotics (Okano *et al.*, 1986), valacyclovir (Ganapathy *et al.*, 1998), ACE inhibitors (Thwaites *et al.*, 1995), and bestatin (Tomita *et al.*, 1990).

Although the bioactive tripeptide Lys-Pro-Val has been shown to be a substrate for PEPT1 in Caco-2 cells (Dalmasso *et al.*, 2008), no direct measurement of its intestinal permeability has been done before. As a potential therapeutic for inflammatory bowel disease, intestinal permeability is an important property to understand. The single-pass intestinal perfusion technique is a useful tool to determine the effective permeability of

drug in intestines. By using this perfusion method in wild-type and *Pept1* knockout mice, it has been successfully demonstrated that PEPT1 was responsible for the uptake of a hydrolysis-resistant dipeptide, Glycylsarcosine (Gly-Sar) in duodenum, jejunum, and ileum (Jappar *et al.*, 2010). Therefore, the objective for the current study was to determine the regional effective permeability of [³H-Pro]Lys-Pro-Val in small and large intestines by using *Pept1* knockout mice and in doing so, provide more rational results for evaluating whether or not intestinal PEPT1 might be a good target for KPV.

MATERIALS AND METHODS

Materials

[³H-Pro] Lys-Pro-Val (40 Ci/mmol) was purchased from AmBios Labs, Inc (Newington, CT). [¹⁴C] inulin (2.38 mCi/g) was purchased from MP Biomedicals (Solon, OH). GlycylProline (Gly-Pro), Lys-Pro-Val (KPV; α -MSH₁₁₋₁₃), and Phe-pyrrolidide were obtained from Bachem, Inc (Torrance, CA). All other chemicals were acquired from Sigma-Aldrich (St. Louis, MO).

Animals

Mouse experiments were conducted in accordance with the Guide for the Care and Use of Laboratory Animals as adopted by the U.S. National Institutes of Health. Gender-matched wild-type and *Pept1* knockout mice (8-10 week old) were used in all the experiments. The mice were kept under a 12-hr light and 12-hr dark cycle, and fed *ad libitum* with standard diet and water (Unit for Laboratory Animal Medicine, University of Michigan, Ann Arbor, MI).

Lys-Pro-Val Hydrolysis Kinetics by Intestinal Homogenates

Intestinal homogenates were prepared by scraping off the mucus layers from the segments of interest by glass slide and homogenated in 0.5 ml ice-cold PBS by tissue homogenator (PowerGen Model 125 Homogenizer, Fisher Scientific, Pittsburgh, PA) at speed 2 for 2 min on ice. The homogenates were then centrifuged at 12,000 x g for 15 min. The supernatant was taken and the total protein concentration was measured by the Pierce protein assay kit (Thermo Scientific, Rockford, IL). 50 μ l of 0.5 mg/ml protein

were taken and incubated with 50 µl of Lys-Pro-Val (final concentration = 1 mM) for different time points (5, 10, 20, 30, and 50 min) at 37°C. 10 µl 10% TFA was added to stop the enzymatic reaction and samples were filtered with 0.2 µm filter and centrifuged at 5,000 x g for 3 mins. 55 µl of the supernatant were analyzed by HPLC with C18 column (Symmetric®, Waters, Milford, MA). Mobile phase consists of A: 0.1 mM NaH₂PO₄/H₂O and B: 100% Acetonitrile. A gradient flow was used, starting from 100% buffer A for 3 mins and changed to 60% buffer A and 40% buffer B over 15 mins. The UV absorbance of KPV was measured at 214 nm. The amount of Lys-Pro-Val being hydrolyzed was calculated by measuring the loss of Lys-Pro-Val in the supernatant and expressed as the percentage of remaining (%) of original.

Regional Intestinal Permeability of [³H-Pro]Lys-Pro-Val

10 µM [³H-Pro]Lys-Pro-Val was perfused in intestinal segments of wild-type and *Pept1* knockout mice (8-10 week old). Animals were fasted overnight and anesthetized with sodium pentobarbital (40-60 mg/kg ip). Four intestinal segments were isolated and perfused simultaneously as follows: A 2 cm duodenum was isolated (i.e. ~0.25 cm distal to the pyloric sphincter), an 8 cm jejunum was isolated (i.e., ~2 cm distal to the ligament of Treitz), a 6 cm ileum was isolated (i.e. ~1 cm proximal to the cecum), and a 3 cm colon was isolated (i.e. ~0.5 cm distal to the cecum). Glass cannula (2.0 mm outer diameter), attached to Tygon® Laboratory tubing, were inserted at both ends of intestinal segments and secured in place with silk sutures. Following cannulation, the isolated intestinal segment was rinsed with isotonic saline solution, and covered with saline-wetted gauze and parafilm to prevent dehydration. After the surgical procedure, the mice

were transferred to a temperature-controlled chamber (31°C) to maintain the body temperature of mice during the experiment. The inlet cannula was connected to a 30-ml syringe placed on a perfusion pump (Harvard Apparatus, Syringe Infusion Pump 22, South Natick, MA). The perfusate contained 135 mM NaCl, 5 mM KCl, 10 mM MES/Tris (pH 6.5), 0.01% [¹⁴C]inulin, 10 μM [³H-Pro]Lys-Pro-Val, 5 mM Phe-pyrrolidide, and 0.25 mM o-phenanthroline was perfused through the intestinal segments at a rate of 0.1 ml/min, and in the inhibition studies, the perfusate contained 25 mM inhibitors (L-histidine, L-proline, Gly-Pro, Cefadroxil, TEA) in the solution above. For pH dependency studies, pH was adjusted by different ratio between 10 mM MES/Tris and 10 mM HEPES/Tris buffer. The effective permeability of Lys-Pro-Val was measured over a range of pH (5.0 - 7.5) in different intestinal segments. A Na⁺/H⁺ inhibitor, dimethyl amiloride (DMA) at 2 mM was also used to examine the pH dependency of Lys-Pro-Val transport in jejunum. For concentration dependency study, 0.01, 0.1, 0.5, 1, 2.5, 5, 7.5, 10, 20, 30 mM Lys-Pro-Val were perfused at pH 6.5.

mRNA Expression of Dipeptidyl Peptidase IV (DPPIV) and Aminopeptidase P (APP) in Wild-type and *Pept1* Knockout Mice.

Quantification of DPPIV and APP transcripts were carried out in different intestinal segments from wild-type mice and *Pept1* knockout mice using the 7300 Real-Time PCR System (Applied Biosystems, Foster City, CA). The total mRNA was isolated using an RNeasy Plus Mini Kit (QIAGEN, Valencia, CA) and then reverse-transcribed using Omniscript® reverse transcription kit (QIAGEN, Valencia, CA). Primers and probes were designed by Primer Express 3.0 software (Applied Biosystems, Foster City, CA), and all the primers, probes were synthesized by Integrated DNA Technologies, Inc.

(Coralville, IA). The forward and reverse primers for DPPIV and APP were 5'-CGGTCTGCCCCTCTACACTCT-3', 5'-TTCCAGGACTCGCAGCTCTT-3', and 5'-AGCTGCACAAGGAAGTTAGCATT-3', 5'-GCCCACGTTCTGTCCATCA-3', respectively. The forward and reverse primers for glyceraldehyde 3-phosphate dehydrogenase (GAPDH) were 5'-GAGACAGCCGCATCTTCTTGT-3', 5'-CACACCGACCTTCACCATTTT-3', respectively. Quantitative polymerase chain reaction (qPCR) was performed with SYBR green system (Applied Biosystems, Foster City, CA). The thermal profile was 1 cycle at 50°C for 2 mins, 1 cycle at 95°C for 10 mins, 40 cycles at 95°C for 15 s, and 60°C for 1 min.

Portal vein Exposure of Lys-Pro-Val during Perfusion

For the portal vein blood collection, 8.6 $\mu\text{Ci/ml}$ (10 μM) [$^3\text{H-Pro}$]Lys-Pro-Val was perfused in the jejunum of wild-type mice for 90 mins with/ without peptidase inhibitors at condition above. The portal vein blood was collected during the period of 80-90 min. The whole blood was centrifuged at 3,300 g for 3 mins. 500 μl of acetonitrile was added to 250 μl plasma and centrifuged at 15,000 x g for 5 mins for extraction. The supernatant was further condensed by SpeedVac concentrator SVC-200H and reconstituted into 20 μl water following by HPLC analysis with 250 x 4.6 mm C18 column (Discovery®, Supelco, Bellefonte, PA) and Packard 500TR radiochemical detector (PerkinElmer Life and Analytical Sciences, Boston, MA). 5% acetonitrile with 0.1% TFA was used as the mobile phase.

Data Analysis

The first order rate constant of hydrolysis, k , were estimated by fitting the data to the equation.

$$Y = 100 \cdot e^{-k \cdot t} \quad (1)$$

Y : percentage of remaining at time t (%), k : hydrolysis constant (1/minute), t : time (minute) and CL_{int} : apparent intrinsic clearance ($\mu\text{l}/\text{min}/\text{mg}$ protein) were calculated by the formula.

$$CL_{int} = \frac{\text{volume of incubation } (\mu\text{l})}{\text{protein in the incubation } (\text{mg})} \times k \quad (2)$$

The relative amount of DPPIV and APP transcripts to GAPDH transcripts were by following formula.

$$\text{Relative abundance} = 2^{-(Ct_{gene} - Ct_{GAPDH})} \times 10000 \quad (3)$$

The effective permeability (P_{eff}) was determined by the loss of drug from the perfusate at steady-state according to a complete radial mixing (parallel tube) model. (Komiya *et al.*, 1980; Kou *et al.*, 1991)

$$P_{eff} = \frac{-Q \times \ln(C_{out}/C_{in})}{2\pi RL} \quad (4)$$

In the equation, Q is the flow rate (ml/min), R is the intestinal radius (cm), L is the length of intestine (cm), C_{out} is the outlet drug concentration (corrected for water flux by [^{14}C]inulin), and C_{in} is the inlet drug concentration. In current study, the steady-state was reached after 30 min perfusion. The steady-state flux (J) was referenced to the inlet drug concentration (C_{in}) to estimate the kinetic parameters (V_{max} , K_m) as shown in eq.5.

$$J = \frac{V'_{max} \times C_{in}}{K'_m + C_{in}} \quad (5)$$

The intrinsic parameter (V_{max} and K_m) were also estimated after factoring out the resistance across the unstirred water layer, where the steady-state flux (J) was referenced to intestinal wall concentration (C_w) as shown in eq. 6.

$$J = \frac{V_{max} \times C_w}{K_m + C_w} + K_d \times C_w \quad (6)$$

The flux in eqs. 5 and 6 were modeled using a single saturable process (i.e., Michaelis-Menten), and a single saturable process plus a linear term respectively. All kinetic parameters were then estimated by nonlinear regression (GraphPad Prism, v5.0; GraphPad Software, Inc., La Jolla, CA).

The transformation of the inlet concentration to the intestinal wall concentration was based on the equation, where the P_{aq} is the estimated unstirred aqueous permeability (Johnson *et al.*, 1988).

$$C_w = C_{in} \times \left(1 - \frac{P_{eff}}{P_{aq}}\right)$$

The aqueous permeability was determined by following equations.

$$P_{aq} = \left(A \frac{R}{D} Gz^{1/3}\right)^{-1}$$

$$Gz = \frac{\pi DL}{2Q}$$

The aqueous diffusion coefficient ($D = 3.60 \times 10^{-4} \text{ cm}^2/\text{min}$) was calculated by Hayduk-Laudie expression (Reid *et al.*, 1977). Gz is the Graetz number (0.0452), and A is a unitless constant (1.238) estimated by $A = 2.5 \text{ Gz} + 1.125$.

Statistical Analysis

Data were expressed as mean \pm SE. Two-tailed student's t-test was used to compare difference between two groups. For multiple comparisons, one-way ANOVA followed by Dunnett's or Tukey's post hoc comparison was used (GraphPad Prism, v5.0; GraphPad Software, Inc., La Jolla, CA). A probability of $p \leq 0.05$ was considered significant. Nonlinear regression analyses were performed using GraphPad Prism software, where the goodness of fit was determined by the coefficient of determination (r^2), the standard error of parameter estimates, and visual inspection of the residuals.

RESULTS

Lys-Pro-Val Hydrolysis Kinetics by Intestinal Homogenates

Lys-Pro-Val (1 mM) was incubated with homogenates prepared from different intestinal segments at 37°C in PBS. The data showed that Lys-Pro-Val was least stable in the ileum following by jejunum, but relatively stable in duodenum and colon (Fig. 4.1). The half-life of Lys-Pro-Val was 20 and 29 min, respectively, for ileum and jejunum (duodenum and colon were less than 5% degraded over 50 min). The calculated intrinsic clearance for ileum and jejunum were 153 and 105 $\mu\text{l}/\text{min}/\text{mg}$, respectively.

Regional Intestinal Permeability of Lys-Pro-Val

Since radiolabel was on the proline position in the current study, metabolites such as Lys-Pro (KP), Pro-Val (PV), or Pro (P) would affect the accuracy of permeability results. For this reason, we elected to inhibit the formation of potential degradation metabolites of the tripeptide. Our results demonstrate that co-perfusing KPV with the peptidase inhibitors Phe-pyrrolidide (5 mM) and o-phenanthroline (0.25 mM) would successfully prevent the degradation of Lys-Pro-Val during the perfusion in *Pept1* knockout mice (Fig. 4.2A). Therefore, the regional intestinal perfusion studies were performed under the same conditions. As shown in the results (Fig. 4.2B), the effective permeability of Lys-Pro-Val in the small intestines (duodenum, jejunum, and ileum) of wild-type mice were significantly greater than that of *Pept1* knockout mice, which showed 13-fold, 21-fold, and 19-fold difference in duodenum, jejunum, and ileum, respectively. This finding suggested that PEPT1 contributed to greater than 90% of the uptake of Lys-Pro-Val in all segments of the small intestine, with negligible contribution

from either paracellular or passive routes. . In contrast, the colon showed no difference in the effective permeability of Lys-Pro-Val between genotypes. When comparing the effective permeability of Lys-Pro-Val between different small intestinal segments of wild-type mice, no significant differences were. However, the effective permeability of Lys-Pro-Val in duodenum, jejunum or ileum showed 18- to 22-fold greater values than that in colon.

Specificity Studies

The specificity of KPV transport was examined in four intestinal segments by co-perfusing glycylproline (Gly-Pro) and cefadroxil (known PEPT1 substrates), L-histidine (a known PHT1/PHT2 substrate), L-proline (a known PAT1 substrate), and TEA (a known OCT substrate). In the presence of Gly-Pro and cefadroxil, the effective permeability of Lys-Pro-Val decreased by about 50-90% in duodenum, jejunum, and ileum. No decrease was observed in the colon for both compounds. Moreover, no inhibitory effect was noted when co-perfusing KPV with L-histidine, L-proline, or TEA, suggesting that PHT1/2, PAT1, or OCT did not contribute to the uptake of Lys-Pro-Val. Thus, it appears that PEPT1 was the main transporter responsible for the uptake of Lys-Pro-Val in small intestine (Fig. 4.3).

Concentration Dependency Study

The uptake of Lys-Pro-Val was studied across a wide range of perfusate concentrations (0.01-30 mM). As shown in Fig. 4.4A, the uptake was nonlinear and, when fitted to a single Michaelis-Menten term, had kinetic parameters of $V_{\max}' = 2.4 \pm 0.2$ nmole/cm²/s and $K_m' = 14.7 \pm 1.9$ mM by ($r^2 = 0.974$). When referencing Lys-Pro-

Val to estimated intestinal wall concentrations, and fitting the data to a single Michaelis-Menten term and linear component, the intrinsic kinetic parameters were $V_{\max} = 0.83 \pm 0.08$ nmole/cm²/s, $K_m = 0.11 \pm 0.06$ mM, and $K_d = 0.0456 \pm 0.007$ cm/s ($r^2 = 0.891$) (Fig. 4.4B).

pH Dependency Studies and DMA Inhibition

Because PEPT1 has been known as a proton-coupled transporter, the proton gradient might influence the activity of PEPT1 transport. However, the results showed that there was no significant pH dependency among the four intestinal segments (Fig. 4.7 A-D). Furthermore, the Na⁺/H⁺ exchanger inhibitor DMA, at high concentration (2 mM), showed no significant effect on the effective permeability in the jejunum of wild-type mice (Fig. 4.7E).

Relative mRNA Expression of DPPIV and APP between Genotypes

Two intestinal peptidases were hypothesized to be responsible for the metabolism of Lys-Pro-Val in the intestinal lumen, namely DPPIV and APP since they are thought as proline-specific enzymes. In the presence of two inhibitors for DPPIV and APP, the Lys-Pro-Val degradation was completely inhibited as shown in Fig. 4.2A. However, since the experiment was performed in *Pept1* knockout mice, we were concerned that expression of these two peptidases might be different between wild-type and *Pept1* knockout mice. . We tested this possibility and as shown in Fig. 4.5, the mRNA expression of both DPPIV and APP were not significantly different between the two genotypes in all intestinal segments. Although the mRNA expression of both enzymes for *Pept1* knockout mice was

somewhat higher in ileum as compared to wild-type mice, the results were not statistically different (n=6 replicates).

Portal Vein Exposure of Lys-Pro-Val during Perfusion

Chromatograms of perfusate in wild-type mice, with and without peptidase inhibitors, supported our contention that hydrolysis activity was completely inhibited in the presence of peptidase inhibitors (Fig. 4.8). The presence of intact Lys-Pro-Val in the portal vein was also examined during the perfusion of 10 μ M Lys-Pro-Val. As shown, all the Lys-Pro-Val was completely degraded during the transepithelial transport in jejunum since no detectable intact [3 H-Pro]Lys-Pro-Val was found in plasma from the portal vein (Fig. 4.9).

DISCUSSION

In this study, the intestinal stability of Lys-Pro-Val was examined for the first time by using intestinal homogenates. The data demonstrated that Lys-Pro-Val was unstable in jejunum and ileum, but stable in duodenum and colon over 50 min. (Fig. 4.1). The peptidases for the hydrolysis were probably dipeptidyl peptidase IV (DPPIV) and aminopeptidase P (APP) because they are both proline-specific enzymes. The regional activity of these two peptidases has been reported in rat, where the activity is highest in ileum ~ jejunum > jejunoileal junction > duodenum > cecum for DPPIV and the activity is highest in jejunoileal junction ~ ileum > cecum ~ duodenum ~ jejunum for APP (Bai, 1994). Our hydrolysis data with Lys-Pro-Val were in agreement with that of Bai (1994), in which the ileum had the highest hydrolysis activity. Meanwhile, the mRNA expression of DPPIV and APP were examined in both wild-type and *Pept1* knockout mice. There was no difference between the two genotypes in all intestinal segments, which showed the highest expression in ileum, following by jejunum, duodenum, and colon. The mRNA expression results were also consistent with the hydrolysis results from our intestinal homogenate studies demonstrating that ileum and jejunum were the major segments for Lys-Pro-Val hydrolysis. In order to minimize the influence of peptidases when performing perfusion experiments, two peptidase inhibitors were used in our perfusate (Phe-pyrrolidide for DPPIV and o-phenanthroline for APP). At the concentration of 5 mM phe-pyrrolidide and 0.25 mM o-phenanthroline, the effective permeability of Gly-Sar was not compromised (Fig. 4.6) and showed completely inhibition of hydrolysis in the perfusion study of *Pept1* knockout mice and wild-type mice (Fig. 4.2A and Fig. 4.8). In a previous study using the single-pass intestinal perfusion technique, the effective

permeability of Gly-Sar was significantly decreased in the absence of PEPT1 in small intestine, thereby demonstrating the importance and specificity of PEPT1 in transporting the hydrolysis-resistant dipeptide, Gly-Sar (Jappan *et al.*, 2010). In the present study, the intestinal permeability of Lys-Pro-Val, an α -MSH related tripeptide, was directly measured using the single-pass intestinal perfusion technique. As shown in our results, the effective permeability of Lys-Pro-Val was dramatically reduced in *Pept1* knockout mice as compared to that of wild-type mice in the small intestines. PEPT1 contributed at least 90% of the total uptake of Lys-Pro-Val in the small intestine, demonstrating that PEPT1 was the main transporter responsible for transport of the tripeptide. In contrast, the effective permeability of Lys-Pro-Val showed no difference between wild-type and *Pept1* knockout mice in colon, which agrees with the fact that PEPT1 has little to no expression in the colon (Fig. 4.2B). The specificity of Lys-Pro-Val was examined by co-perfusing the PEPT1 substrates Gly-Pro and cefadroxil, and the effective permeability decreased in all three small intestinal segments, further supporting that PEPT1 was responsible for the uptake of Lys-Pro-Val in these segments (Fig. 4.3).

PEPT1 was characterized as a high-capacity and low-affinity transporter. The reported K_m for PEPT1 ranged from 0.1 – 15 mM depending on the substrate, tissue cell types, experimental systems, conditions and data analysis (Fei *et al.*, 1994; Brandsch *et al.*, 2004). The uptake of Lys-Pro-Val was studied with escalating concentrations in this study and the estimated intrinsic K_m value was 0.11 ± 0.058 mM after factoring out the influence of the unstirred aqueous layer. The K_m of KPV in our study was comparable to that previously reported in CaCo2-BBE cells (i.e., $K_m = 0.16$ mM) and the Jurkat cells (i.e., $K_m = 0.7$ mM) (Dalmasso *et al.*, 2008), suggesting that Lys-Pro-Val has a relatively

high affinity for PEPT1. The nonsaturable component (K_d) contributed only 0.6% to the total transport of KPV under linear conditions range, which also agrees with the data from *Pept1* knockout mice demonstrating that PEPT1 contributed at least 90% of the total uptake of Lys-Pro-Val in small intestine (Fig. 4.2B). Taken it as a whole, PEPT1 was the major transporter responsible for the uptake of Lys-Pro-Val in small intestines and has a relatively high affinity for ($K_m = 0.11$ mM) this POT protein.

The contribution of PHT1/PHT2 in the transport of Lys-Pro-Val in small and large intestines was examined in several segments of wild-type mice. In the presence of L-histidine, a known substrate of PHT1/PHT2, the effective permeability of Lys-Pro-Val was not changed in duodenum, jejunum, ileum or colon. . Although the expression of PHT1 in the apical membrane of jejunum has been suggested (Bhardwaj *et al.*, 2006), its contribution to the transport of Lys-Pro-Val was not apparent. . Contribution of other transporters was also examined, including that of PAT1 and OCT. In the presence of L-proline, a known substrate of PAT1, the effective permeability of Lys-Pro-Val showed no difference, suggesting that PAT1 was not responsible for the uptake of Lys-Pro-Val in small intestine. Since Lys-Pro-Val would bear a net positive charge in the pH of our condition (pH 6.5), the contribution of organic cation transport was also studied. We found that TEA had no effect on the permeability of KPV, suggesting that OCTs did not contribute to the uptake of Lys-Pro-Val in small intestine.

A lack of pH dependency was observed in our study (Fig. 7 A-D). This finding is most likely due to the fact that changes in bulk pH might not translate into changes in microclimate pH (Hogerle *et al.*, 1983). Surprisingly, when adding 2 mM DMA, an inhibitor of the Na^+/H^+ exchanger, the effective permeability still showed no difference.

This lack of change might be due to the concentration of DMA not being high enough since DMA is a more selective inhibitor of NHE1 and NHE2; only at very high concentration (3 mM), did DMA show an inhibitory effect on NHE3 (Furukawa *et al.*, 2004). A similar lack of effect on PEPT2 activity by inhibitors of Na^+/H^+ exchange has also been reported in the human nasal epithelium (Agu *et al.*, 2011). It suggested that the uptake of dipeptide was driven by proton pump rather than Na^+/H^+ exchanger in their system. In addition, membrane potential has been suggested to be more important than pH as for the driving force of PEPT1 (Weitz *et al.*, 2007).

Like Lys-Pro-Val, there are several other bioactive peptides that have been reported in the literature such as carnosine (β -alanyl-L-histidine), anserine (β -alanyl-1-N-methyl-L-histidine) (Tan *et al.*, 1998), Ile-Pro-Pro, and Val-Pro-Pro (Foltz *et al.*, 2007). Although they are all substrates for PEPT1 transport conceptually due to their di/tripeptide structure, a study demonstrated that the major absorptive mechanism of Val-Pro-Pro was paracellular transport (Satake *et al.*, 2002). Another study focusing on the pharmacophore of PEPT1 suggested that not all the di/tripeptides were substrates of PEPT1 (Vig *et al.*, 2006). Therefore, it is important to understand the transport mechanism of bioactive peptides, especially after their oral administration. Another concern for bioactive peptides is their *in vivo* stability. Our intestinal homogenate studies showed that Lys-Pro-Val was not very stable during its transepithelial transport across the epithelial membrane (Fig. 4.1). Depending on the target disease, some formulation techniques might be the way to overcome this hydrolysis issue. For example, a nanoparticle loaded with Lys-Pro-Val was designed to achieve local delivery to its site of action in the colon (Laroui *et al.*, 2010). The data showed that a 12,000-fold lower of

dose could achieve a similar effect. The reason for this nanoparticle formulation being effective might be due to the colonic PEPT1 expression under inflammatory conditions increasing the uptake of Lys-Pro-Val, but also protection of Lys-Pro-Val by the formulation against high peptidase activity along the intestine.

A final point is that the Lys-Pro-Val used in this study was in a free acid form with no acetylation at the N-terminal. However, in the literature, some of the α -MSH related peptides (e.g., KPV, KdPV, KdPT) were N-acetylated and C-amidated peptides (Hiltz *et al.*, 1991) while others were not (Getting *et al.*, 2003). Although no comparison has been made for the N-acetylated and C-amidated forms of the Lys-Pro-Val on anti-inflammatory effect, it has been known that N-acetylated and C-amidated substrates might affect their affinity to PEPT1 (Meredith *et al.*, 2000). Since PEPT1 has been shown to transport Lys-Pro-Val in both this and previous studies, its intracellular concentration in the target cell (e.g. epithelial cell or macrophage) could be affected by the form of actual compound that is used. Therefore, systematic experiments on the structure-activity relationship of the Lys-Pro-Val (and derivatives) and effects on pharmacokinetics are worth pursuing.

In conclusion, our findings provided valuable insight on the intestinal transport of a new α -MSH related tripeptide. First, Lys-Pro-Val was least stable in the ileum following by jejunum, and relatively stable in the duodenum, and colon. To become a promising therapeutic agent, strategies such as nanoparticle formulations might be needed to protect against potential hydrolysis in the intestine after oral dosing. Second, PEPT1 was the main transporter responsible for the uptake of Lys-Pro-Val in small intestine, but not colon. However, systematic pharmacokinetic/ pharmacodynamic study

of Lys-Pro-Val is worth conducting, particularly in the case of oral administration. Finally, the utilization of *Pept1* knockout mice successfully demonstrated the importance of PEPT1 in the absorption of Lys-Pro-Val. Future studies should look to evaluate the importance of PEPT1 in disease models of inflammatory bowel disease, and potential therapeutic interventions.

FIGURES

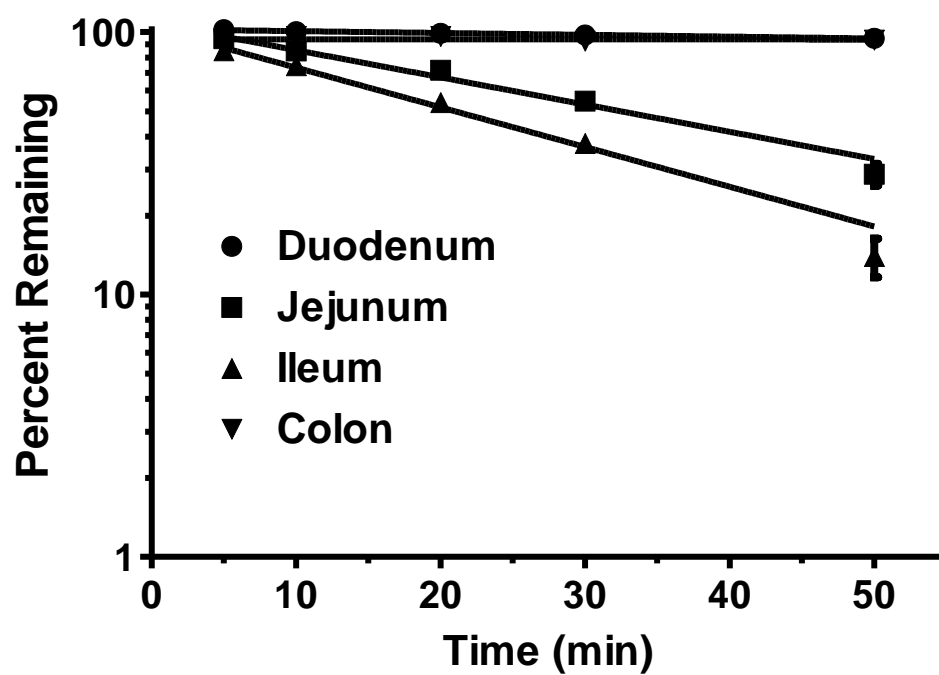


Figure 4.1. The hydrolysis of Lys-Pro-Val by intestinal homogenates (Mean \pm SE, n=3).

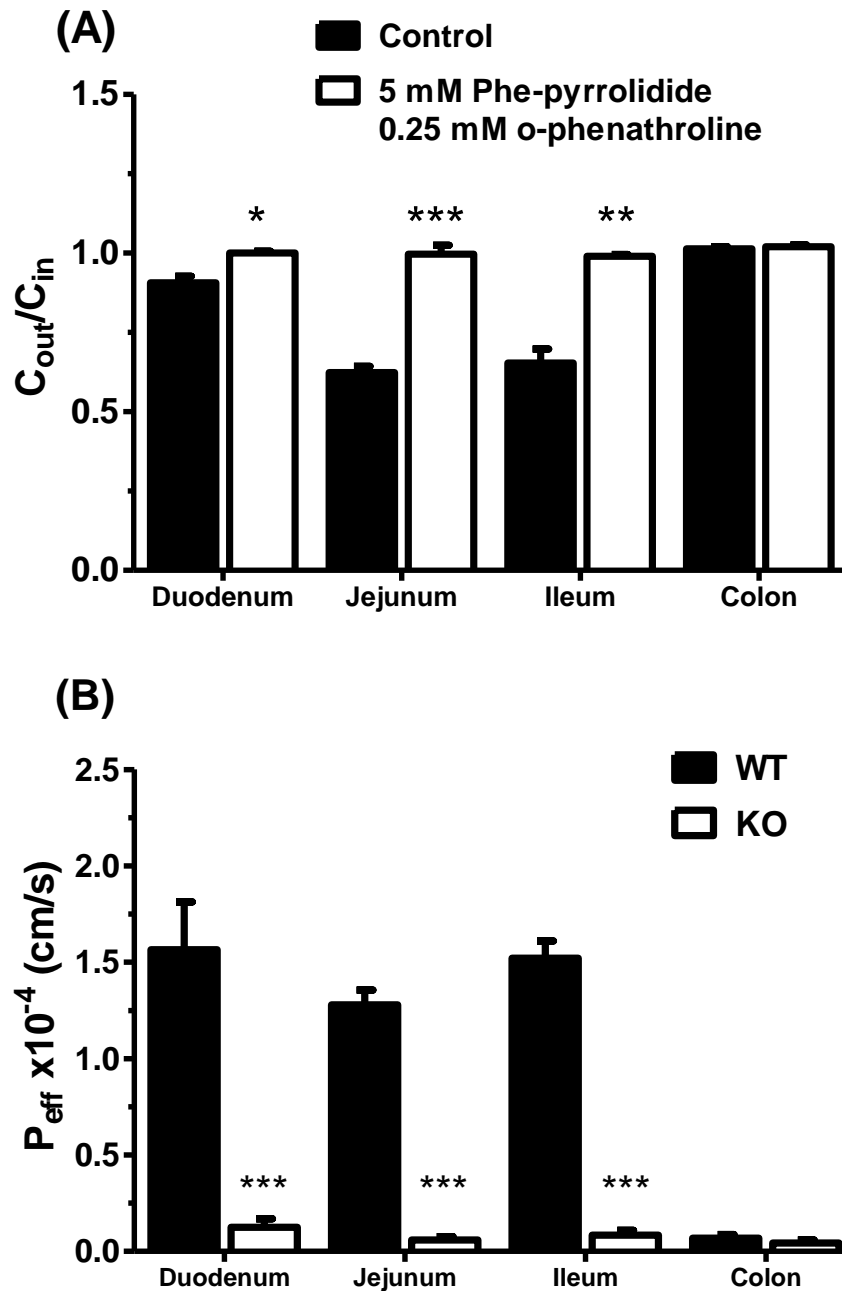


Figure 4.2. (A) Co-perfusion of peptidase inhibitors (5 mM Phe-pyrrolidide and 0.25 mM o-phenanthroline) demonstrated completely inhibition of hydrolysis of Lys-Pro-Val during perfusion in the *Pept1* knockout mice (Mean \pm SE, n=3). (B) Regional permeability of Lys-Pro-Val in wild-type mice and *Pept1* knockout mice (Mean \pm SE, n=6). * < 0.05, ** < 0.01, *** < 0.001 as compared to each wild-type segment by student's t-test.

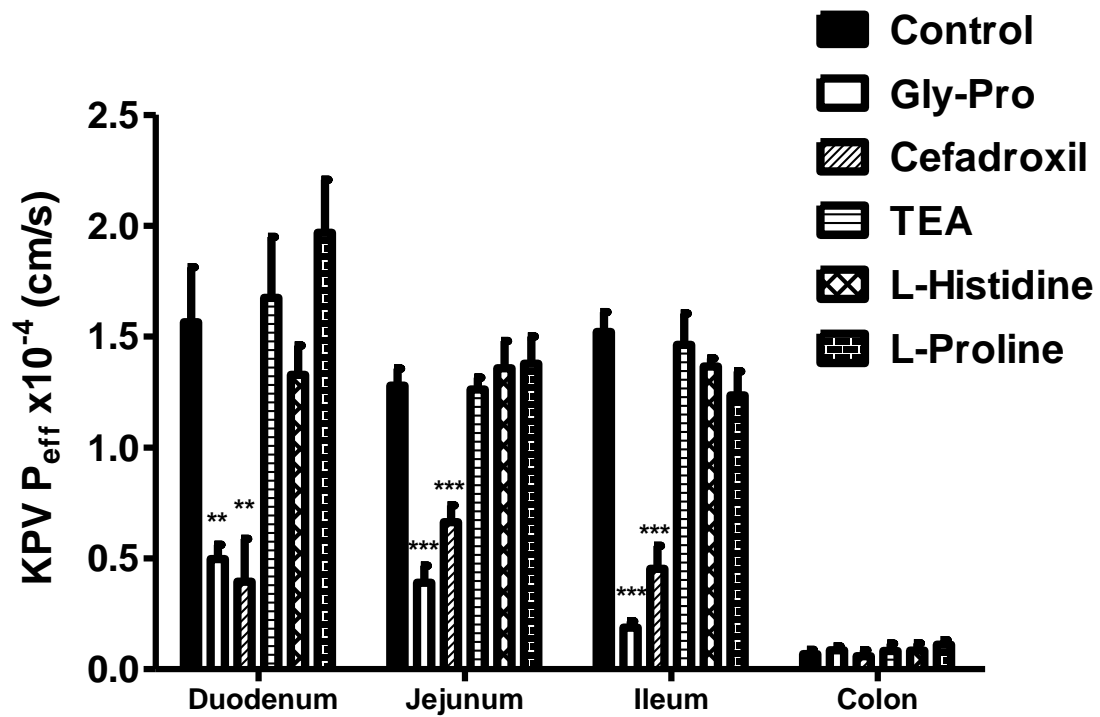


Figure 4.3. PEPT1 substrates (Gly-Pro and Cefadroxil) inhibited the effective permeability of Lys-Pro-Val in three small intestinal segments, but not in colon. Substrate of PHT1/2, L-histidine, substrate of organic cation transporter, TEA, and substrate of PAT1 transporter, L-Proline showed no inhibition in all intestinal segments (Mean \pm SE, n=4). The concentration of all inhibitors was 25 mM. Statistical analyses were performed by one-way ANOVA with Dunnett's comparison against control within each segment.

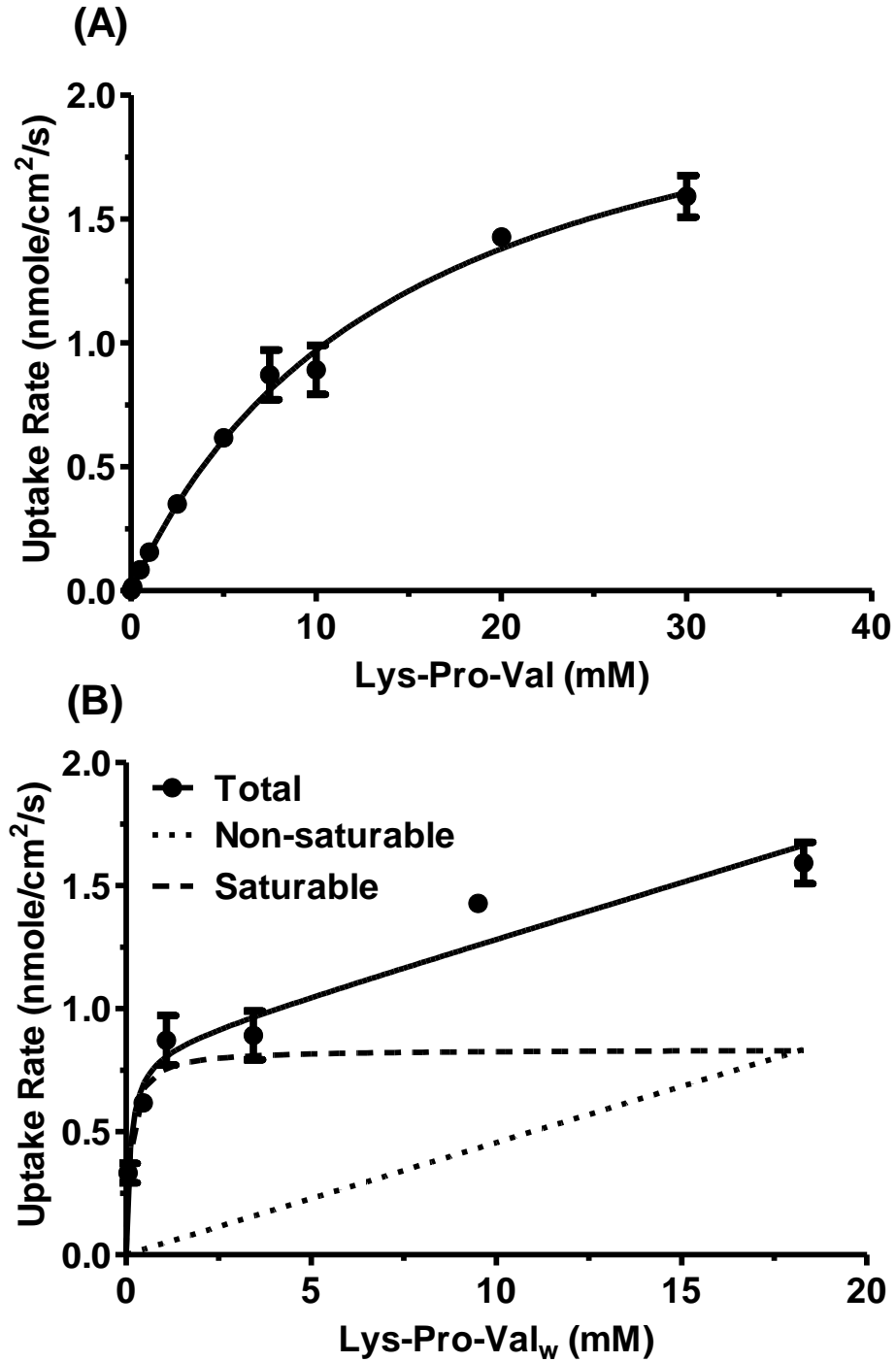


Figure 4.4. Concentration dependency of Lys-Pro-Val uptake in the jejunum of wild-type mice (Mean \pm SE, $n=3-4$). (A) as reference to the inlet concentration which modeled by a single Michaelis-Menten equation. (B) as reference to the estimated concentration at intestinal wall which modeled by a single Michaelis-Menten plus a linear term.

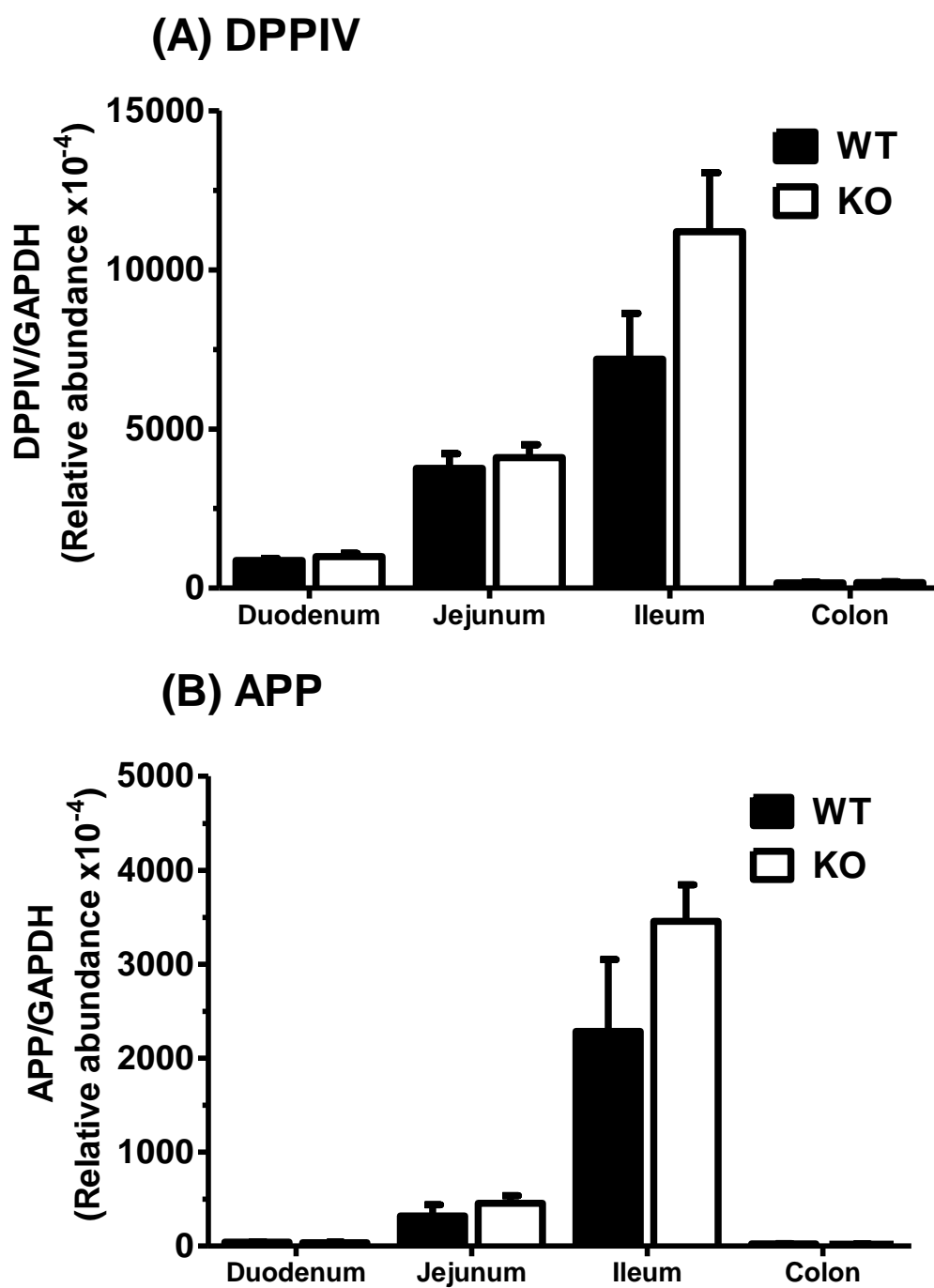


Figure 4.5. mRNA expression of DPPIV and APP in the intestinal segments in both genotypes (Mean \pm SE, n=6).

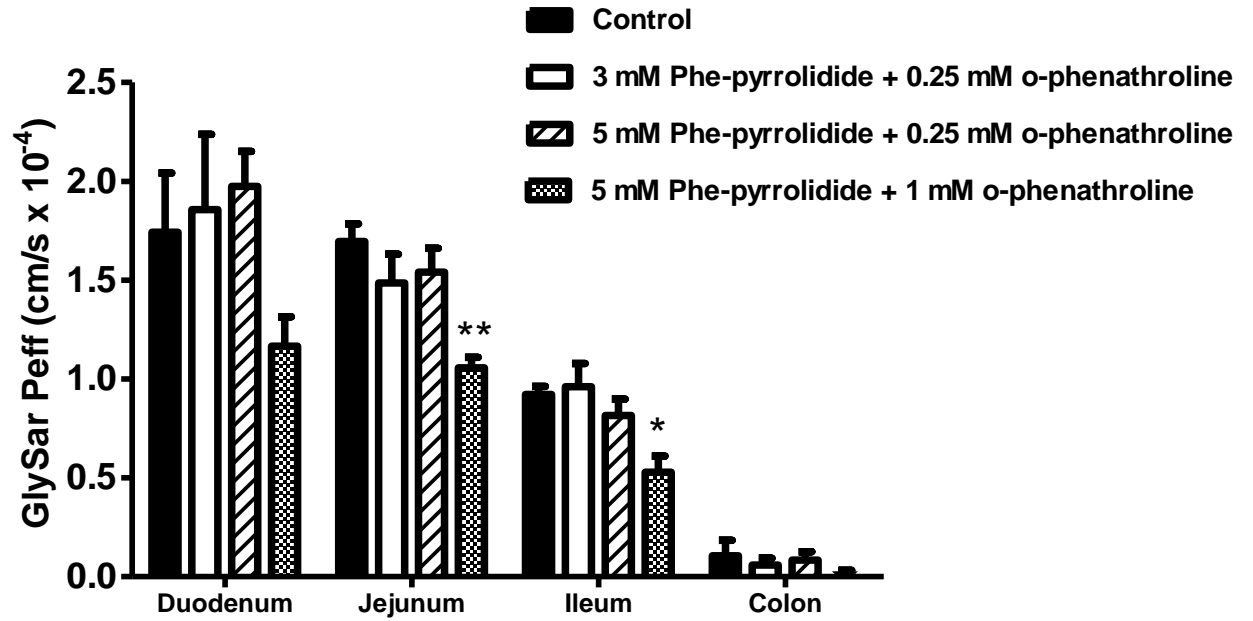


Figure 4.6. Effective permeability of GlySar was influence by peptidase inhibitors at high concentrations (Mean \pm SE, n=4-6). Statistical analyses were performed by one-way ANOVA with Dunnett's comparison against control within each segment (* <0.05, ** <0.01).

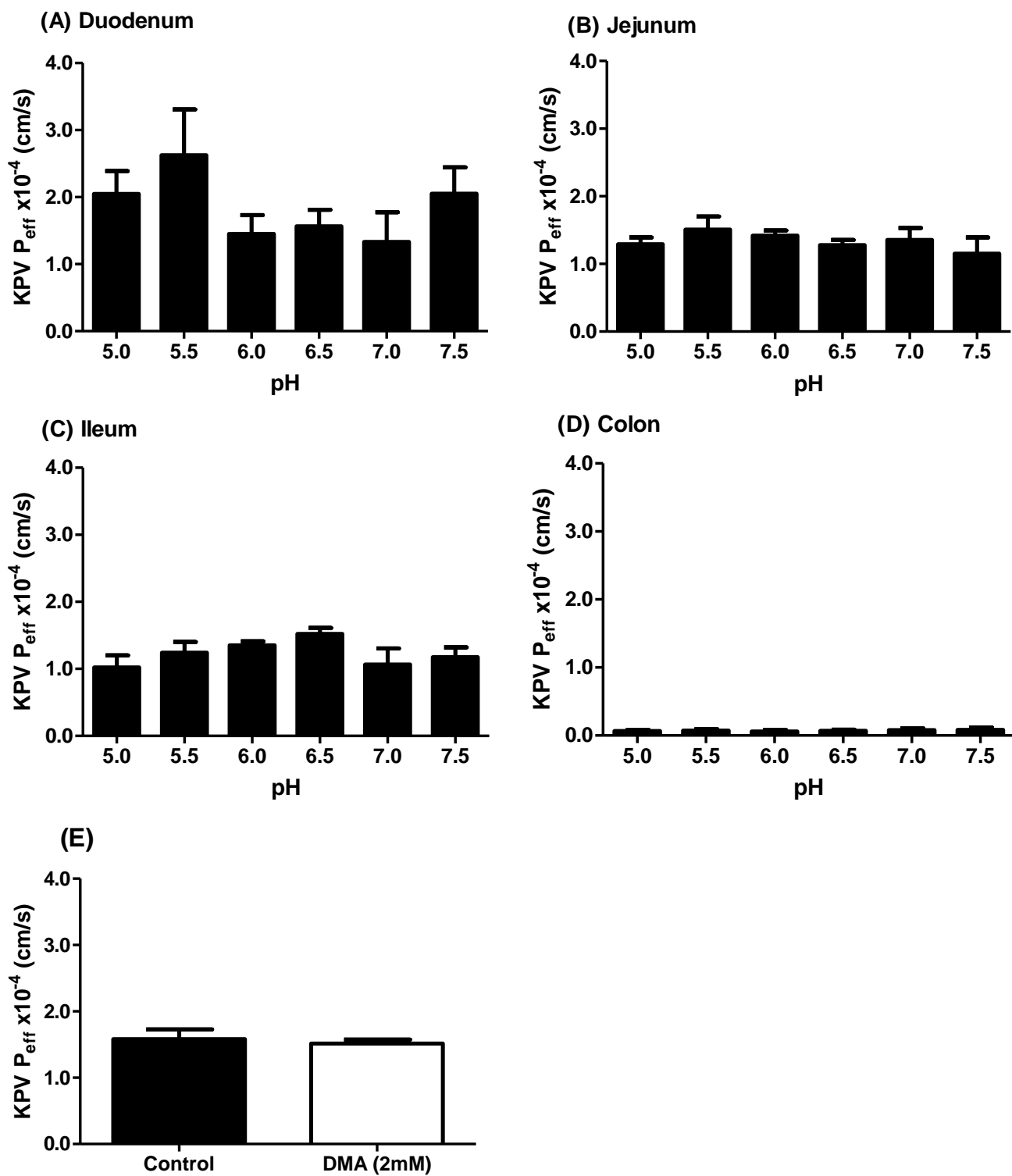


Figure 4.7. (A-D) pH dependency of Lys-Pro-Val transport in different intestinal segments (Mean \pm SE, n=4). (E) Influence of DMA to the transport of Lys-Pro-Val in the jejunum of wild-type mice (Mean \pm SE, n=4).

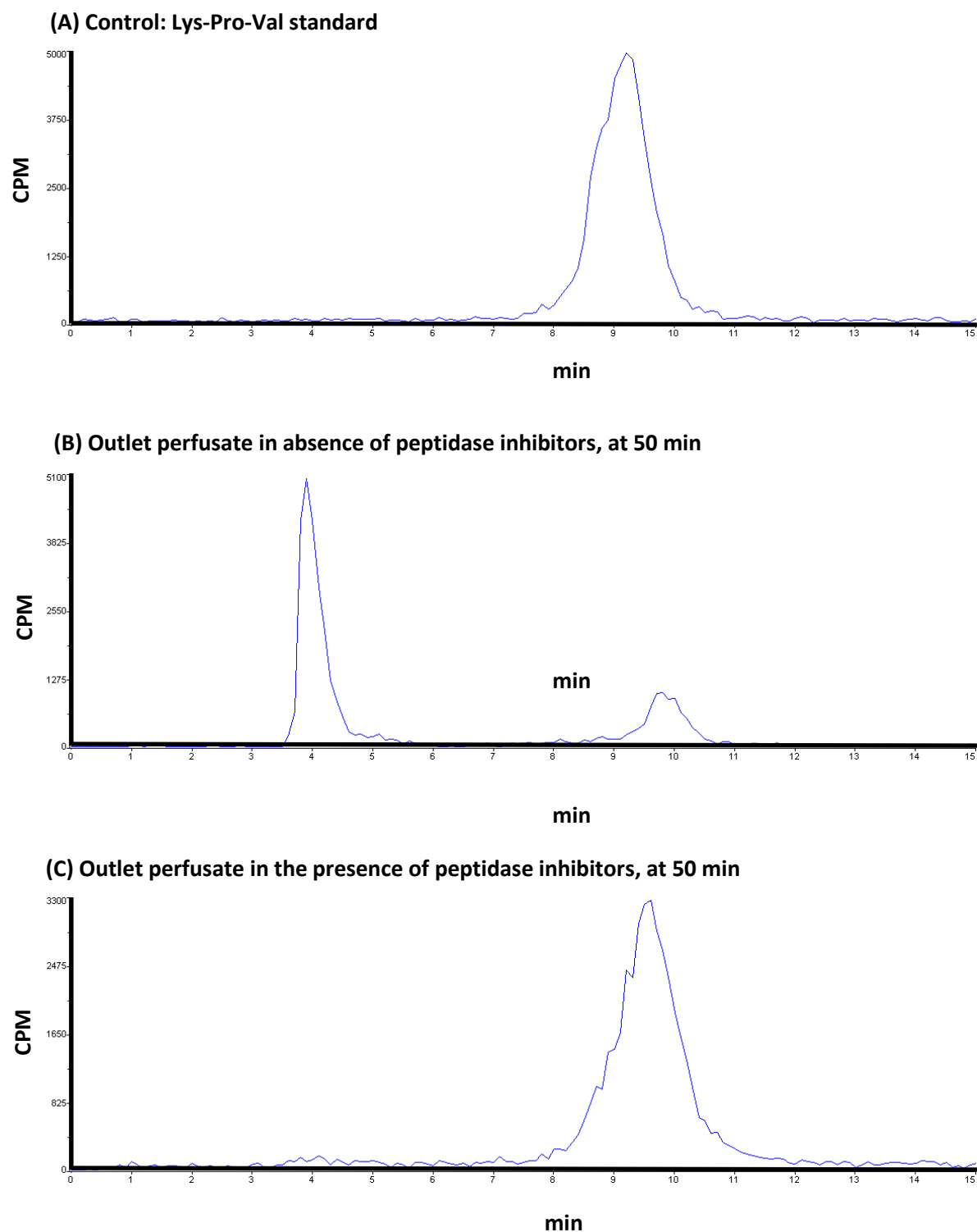


Figure 4.8. Chromatogram of [^3H -Pro]Lys-Pro-Val during the perfusion of jejunum in wild-type mice. (A) Control, (B) Outlet perfusate without peptidase inhibitors, (C) Outlet perfusate with peptidase inhibitors.

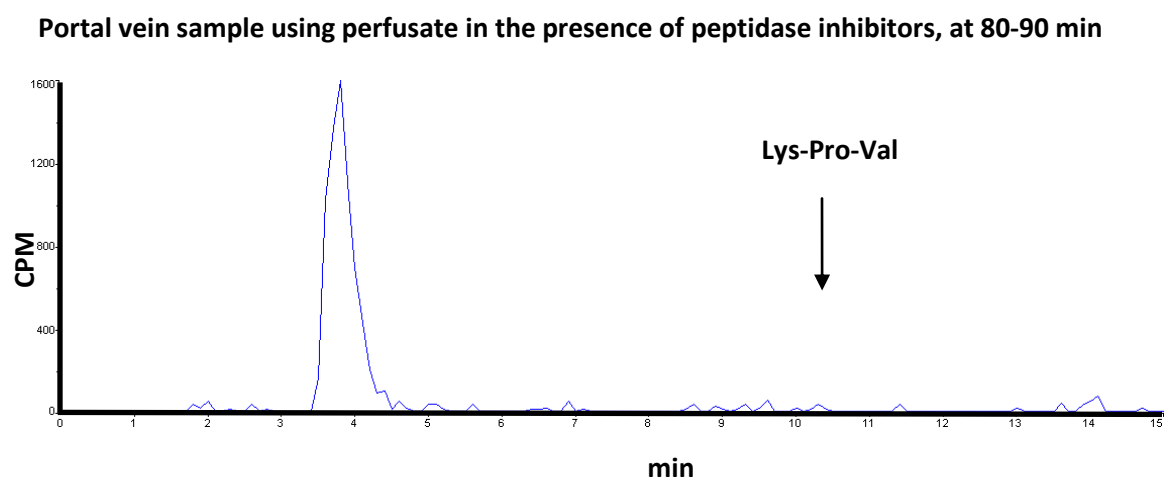


Figure 4.9. Chromatogram of [^3H -Pro]Lys-Pro-Val in portal vein plasma during the perfusion of jejunum in wild-type mice.

REFERENCES

- Agu R, Cowley E, Shao D, Macdonald C, Kirkpatrick D, Renton K, Massoud E (2011). Proton-coupled oligopeptide transporter (POT) family expression in human nasal epithelium and their drug transport potential. *Mol Pharm* **8**: 664-672.
- Bai JP (1994). Distribution of brush-border membrane peptidases along the rat intestine. *Pharm Res* **11**: 897-900.
- Bhardwaj RK, Herrera-Ruiz D, Eltoukhy N, Saad M, Knipp GT (2006). The functional evaluation of human peptide/histidine transporter 1 (hPHT1) in transiently transfected COS-7 cells. *Eur J Pharm Sci* **27**: 533-542.
- Brandsch M, Knutter I, Leibach FH (2004). The intestinal H⁺/peptide symporter PEPT1: structure-affinity relationships. *Eur J Pharm Sci* **21**: 53-60.
- Dalmaso G, Charrier-Hisamuddin L, Nguyen HT, Yan Y, Sitaraman S, Merlin D (2008). PepT1-mediated tripeptide KPV uptake reduces intestinal inflammation. *Gastroenterology* **134**: 166-178.
- Fei YJ, Kanai Y, Nussberger S, Ganapathy V, Leibach FH, Romero MF, Singh SK, Boron WF, Hediger MA (1994). Expression cloning of a mammalian proton-coupled oligopeptide transporter. *Nature* **368**: 563-566.
- Foltz M, Meynen EE, Bianco V, van Platerink C, Koning TM, Kloek J (2007). Angiotensin converting enzyme inhibitory peptides from a lactotripeptide-enriched milk beverage are absorbed intact into the circulation. *J Nutr* **137**: 953-958.
- Furukawa O, Bi LC, Guth PH, Engel E, Hirokawa M, Kaunitz JD (2004). NHE3 inhibition activates duodenal bicarbonate secretion in the rat. *Am J Physiol Gastrointest Liver Physiol* **286**: G102-109.
- Ganapathy ME, Huang W, Wang H, Ganapathy V, Leibach FH (1998). Valacyclovir: a substrate for the intestinal and renal peptide transporters PEPT1 and PEPT2. *Biochem Biophys Res Commun* **246**: 470-475.
- Ganapathy V, Gupta N, Martindale RG (2006). Protein Digestion and Absorption. . In: *Physiology of the Gastrointestinal Tract*, Fourth Edition, pp. p. 1667-1692.: Academic Press, Burlington.

Getting SJ, Schioth HB, Perretti M (2003). Dissection of the anti-inflammatory effect of the core and C-terminal (KPV) alpha-melanocyte-stimulating hormone peptides. *J Pharmacol Exp Ther* **306**: 631-637.

Hiltz ME, Catania A, Lipton JM (1991). Anti-inflammatory activity of alpha-MSH(11-13) analogs: influences of alteration in stereochemistry. *Peptides* **12**: 767-771.

Hogerle ML, Winne D (1983). Drug absorption by the rat jejunum perfused in situ. Dissociation from the pH-partition theory and role of microclimate-pH and unstirred layer. *Naunyn Schmiedebergs Arch Pharmacol* **322**: 249-255.

Ichiyama T, Sakai T, Catania A, Barsh GS, Furukawa S, Lipton JM (1999). Systemically administered alpha-melanocyte-stimulating peptides inhibit NF-kappaB activation in experimental brain inflammation. *Brain Res* **836**: 31-37.

Jappard D, Wu SP, Hu Y, Smith DE (2010). Significance and regional dependency of peptide transporter (PEPT) 1 in the intestinal permeability of glycylsarcosine: in situ single-pass perfusion studies in wild-type and Pept1 knockout mice. *Drug Metab Dispos* **38**: 1740-1746.

Johnson DA, Amidon GL (1988). Determination of intrinsic membrane transport parameters from perfused intestine experiments: a boundary layer approach to estimating the aqueous and unbiased membrane permeabilities. *J Theor Biol* **131**: 93-106.

Komiya I, Park JY, Kamani A, Ho NFH, Higuchi WI (1980). Quantitative mechanistic studies in simultaneous fluid flow and intestinal absorption using steroids as model solutes. *International Journal of Pharmaceutics* **4**: 249-262.

Kou JH, Fleisher D, Amidon GL (1991). Calculation of the aqueous diffusion layer resistance for absorption in a tube: application to intestinal membrane permeability determination. *Pharm Res* **8**: 298-305.

Laroui H, Dalmasso G, Nguyen HT, Yan Y, Sitaraman SV, Merlin D (2010). Drug-loaded nanoparticles targeted to the colon with polysaccharide hydrogel reduce colitis in a mouse model. *Gastroenterology* **138**: 843-853 e841-842.

Mandrika I, Muceniece R, Wikberg JE (2001). Effects of melanocortin peptides on lipopolysaccharide/interferon-gamma-induced NF-kappaB DNA binding and nitric oxide production in macrophage-like RAW 264.7 cells: evidence for dual mechanisms of action. *Biochem Pharmacol* **61**: 613-621.

Manna SK, Aggarwal BB (1998). Alpha-melanocyte-stimulating hormone inhibits the nuclear transcription factor NF-kappa B activation induced by various inflammatory agents. *J Immunol* **161**: 2873-2880.

Meredith D, Temple CS, Guha N, Sword CJ, Boyd CA, Collier ID, Morgan KM, Bailey PD (2000). Modified amino acids and peptides as substrates for the intestinal peptide transporter PepT1. *Eur J Biochem* **267**: 3723-3728.

Ogihara H, Saito H, Shin BC, Terado T, Takenoshita S, Nagamachi Y, Inui K, Takata K (1996). Immuno-localization of H⁺/peptide cotransporter in rat digestive tract. *Biochem Biophys Res Commun* **220**: 848-852.

Okano T, Inui K, Takano M, Hori R (1986). H⁺ gradient-dependent transport of aminocephalosporins in rat intestinal brush-border membrane vesicles. Role of dipeptide transport system. *Biochem Pharmacol* **35**: 1781-1786.

Reid RC, Prausnitz JM, Sherwood TK (1977). In: *The Properties of Gases and Liquids, 3rd*, 3rd, pp. 573. McGraw-Hill Book Company, New York.

Satake M, Enjoh M, Nakamura Y, Takano T, Kawamura Y, Arai S, Shimizu M (2002). Transepithelial transport of the bioactive tripeptide, Val-Pro-Pro, in human intestinal Caco-2 cell monolayers. *Biosci Biotechnol Biochem* **66**: 378-384.

Tan KM, Candlish JK (1998). Carnosine and anserine as modulators of neutrophil function. *Clin Lab Haematol* **20**: 239-244.

Thwaites DT, Cavet M, Hirst BH, Simmons NL (1995). Angiotensin-converting enzyme (ACE) inhibitor transport in human intestinal epithelial (Caco-2) cells. *Br J Pharmacol* **114**: 981-986.

Tomita Y, Katsura T, Okano T, Inui K, Hori R (1990). Transport mechanisms of bestatin in rabbit intestinal brush-border membranes: role of H⁺/dipeptide cotransport system. *J Pharmacol Exp Ther* **252**: 859-862.

Vig BS, Stouch TR, Timoszyk JK, Quan Y, Wall DA, Smith RL, Faria TN (2006). Human PEPT1 pharmacophore distinguishes between dipeptide transport and binding. *J Med Chem* **49**: 3636-3644.

Weitz D, Harder D, Casagrande F, Fotiadis D, Obrdlik P, Kelety B, Daniel H (2007). Functional and structural characterization of a prokaryotic peptide transporter with features similar to mammalian PEPT1. *J Biol Chem* **282**: 2832-2839.

APPENDIX A

COMPARISON OF THE SUSCEPTIBILITY TO DEXTRAN SODIUM SULFATE BETWEEN WILD-TYPE AND *PEPT1* KNOCKOUT MICE

OBJECTIVE

In order to examine the impact of the speculated colonic PEPT1 under intestinal inflammation situation, DSS colitis model was used to study the influence of colonic PEPT1 in the progress of colitis.

MATERIALS AND METHODS

Dextran sodium sulfate (DSS) (Avg. MW = 40,000; MP biomedical, Solon, OH) colitis model was used to investigate the difference of susceptibility after genetic PEPT1 knockout. Colitis was induced by two different treatment schedules: (1) adding 3% DSS (wt/vol) in the drinking water for 8 days in both wild-type and *Pept1* knockout mice; (2) adding 3% DSS (wt/vol) in the drinking water for 5 day following by recovery for 1 or 2 weeks in both wild-type and *Pept1* knockout mice. The progress of colitis will be monitored by daily examination of weight loss, gross bleeding, and the presence of loose stools or diarrhea for the calculation of the disease activity index (DAI) (Cooper *et al.*, 1993) (Table A.1). After treatment, colon samples were collected and divided into parts. One part is for the determination of the myeloperoxidase activity as previous described (Chapter 2) and the other part was for the measurement of mRNA expression of cytokines, chemokines, and the mRNA and protein expression of PEPT1.

RESULTS

Acute 8 day Treatment of 3%DSS

Both wild-type and *Pept1* knockout mice started to show significant weight loss as compared to their tap water control groups on day 5 after the DSS challenge (Fig. A.1). Comparing between genotypes, the weight loss showed statistical difference after 5-day treatment of 3% DSS, however, the disease activity index (DAI), which calculated by the clinical outcome criteria showed in Table A.1, showed difference on day 5, day 6, and day 8 (Fig. A.2). When comparing the indicators of intestinal inflammation, the myeloperoxidase activity (MPO) increased 6-8 fold after 8 day treatment of DSS in colon. However, there was no significant difference between genotypes (Fig. A.3). In contrast, the MPO activity showed no increase in the jejunum of wild-type and *Pept1* knockout mice (Table A.3). All of the mice (6/6 in both genotypes) treated with DSS developed clinical sign of colitis, such as diarrhea and bloody stool, and none of them died on day 8 of treatment (Table A.3). For the mRNA expression of pro-inflammatory cytokines, such as TNF- α , IL-1 β , IL-12B, IL-6, showed increase to various degrees (some would not reach statistical difference, however the increase was apparent). Only IFN- γ showed no increase in both wild-type and *Pept1* knockout mice. Most importantly, there were no significant differences observed between two genotypes in any of the pro-inflammatory cytokine expression after day 8 of DSS treatment, suggesting that the severity of inflammation was not different between two genotypes (Fig. A.4). Same kind of trends were also observed in either chemokines or anti-inflammatory cytokines after DSS treatment in both genotypes, which were induction of chemokines (Cxcl2 and KC) and pro-inflammatory cytokine, IL-10 within genotypes but no significant difference between

genotypes (Fig. A.5 and A.6). Taken as a whole, colitis was successfully induced by the treatment of DSS in both wild-type and *Pept1* knockout mice. However, there was no significant difference of degree of severity observed between two genotypes.

PEPT1 Expression after 8 day Treatment

The mRNA and protein level of PEPT1 were checked by real-time PCR and western blot. The results showed that under the colitis situation, the mRNA of PEPT1 in colon decrease significantly (Fig. A.12A). The protein of PEPT1 was not detectable after the induction of colitis (Fig. A.12B), suggesting that PEPT1 might not be induced under this treatment.

5 day 3%DSS Treatment with Recovery

According to previous paper (Radeva *et al.*, 2007), which demonstrated by immunohistochemistry that PEPT1 ectopically expressed in distal colon after DSS treatment, the treatment consisted of challenge phase and recovery phase. Both wild-type and *Pept1* knockout mice were then treated in similar schedule, which was 5 day treatment of 3% DSS following by 1 or 2 weeks recovery. In this kind of treatment, both wild-type and *Pept1* knockout mice started to show significant weight loss on day 6 after the DSS challenge and started to gain weight after day 9 (reached the trough on day 9). Comparing between genotypes, the weight loss patterns showed no significant difference over the recovery phase although *Pept1* knockout mice showed a little more decrease in average, but not reach statistical significance (Fig. A.7). When comparing the indicators of intestinal inflammation, the myeloperoxidase activity (MPO) stay slightly higher than control after 1 week recovery and return to normal on week 2 in wild-type mice (Fig. A.8). Surprisingly, in *Pept1* knockout mice, after 2 week recovery, the MPO activity was

still higher than control (Fig. A.8). Although it might indicate more severe colitis occurred in *Pept1* knockout mice, the mRNA expression of pro-inflammatory cytokines, chemokines, and anti-inflammatory cytokines did not support the result. The mRNA expression of TNF- α , IL-1 β , IL-12B, IL-6, and IFN- γ showed increase to various degrees (some would not reach statistical difference, however the increase was apparent) after week 1 and remained high after week 2, indicating that although the weight of mice fully recovered, the colon was still under inflammatory status. Most importantly, there were no significant differences observed between two genotypes in any of the pro-inflammatory cytokine expression after week 1 and 2, suggesting that the severity of inflammation was not different between two genotypes (Fig. A.9). Similar trends were also observed in both chemokines and anti-inflammatory cytokines after DSS treatment in both genotypes, which were induction of chemokines (Cxcl2 and KC) and pro-inflammatory cytokine, IL-10 within genotypes at week 1 and 2, but no significant difference between genotypes (Fig. A.10 and A.11). To summarize, inflammation was persistent after 1 or 2 weeks recovery although the challenge of 3% DSS was removed on day 5 in both wild-type and *Pept1* knockout mice, however, the no significant difference of degree of severity has been shown between two genotypes in the recovery phase.

Pept1 Expression during the Recovery Phase

In order to check the presence of the ectopically expressed of PEPT1 in colon during the recovery phase, mRNA and protein of PEPT1 were examined. The results showed that neither mRNA nor protein changed during the recovery phase (Fig. A.13). The mRNA remained similar level as compared to control and the protein was still

undetectable, which suggesting that the little (or undetectable by western blot) ectopically expression of PEPT1 did not contributed significant enough for the inflammation.

DISCUSSION

Although the aberrant expression of PEPT1 has been suggested to be involved in the pathogenesis of inflammatory bowel disease because of the ability to transport the bacterially-produced peptides (Charrier *et al.*, 2006), there was no significant difference on the susceptibility to DSS between wild-type and *Pept1* knockout mice. Both genotypes mice developed colitis after treatment of 3% DSS in both schedules. The expression of mRNA and protein might suggested that the lack of difference between genotypes was because the ectopic expression of PEPT1 (if any) was not accumulated significantly enough to contribute to the inflammation and therefore different colitis models might be needed.

FIGURES

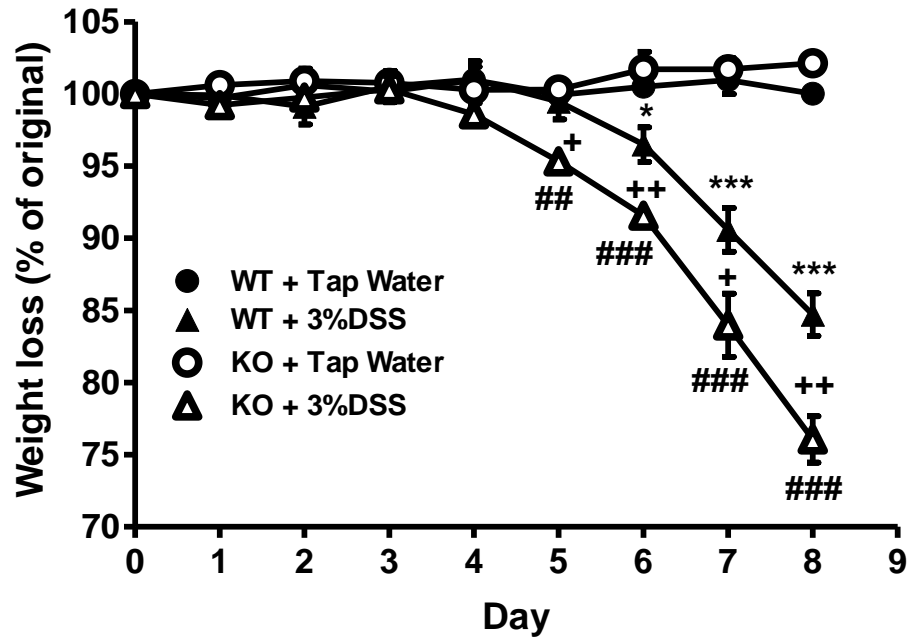


Figure A.1. Percentage of body weight loss after 3% DSS treatment in wild-type and *Pept1* knockout mice over time (Mean \pm SE, n=6). Statistical analyses were performed by student's t-test (* denoted DSS vs. control of wild-type; # denoted DSS vs. control of *Pept1* knockout mice; + denoted DSS between genotypes; * p< 0.05, ** p< 0.01, *** p < 0.001, etc.).

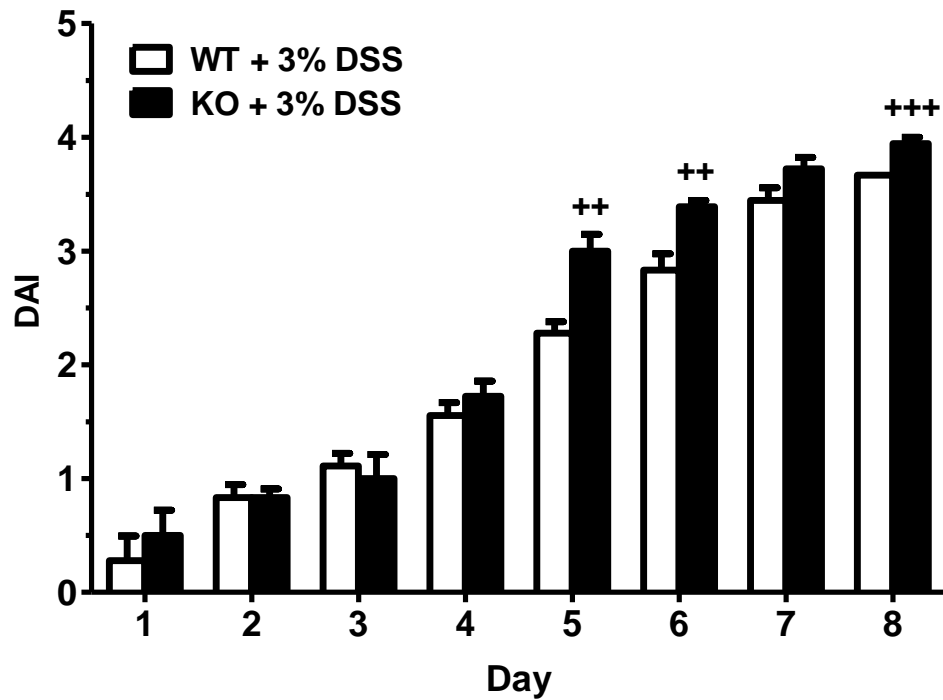


Figure A.2. The disease activity index (DAI) after treatment of 3% DSS in wild-type and *Pept1* knockout mice over time (Mean \pm SE, n=6). Statistical analyses were performed by student's t-test (++ $p < 0.01$; +++ $p < 0.001$ between genotypes).

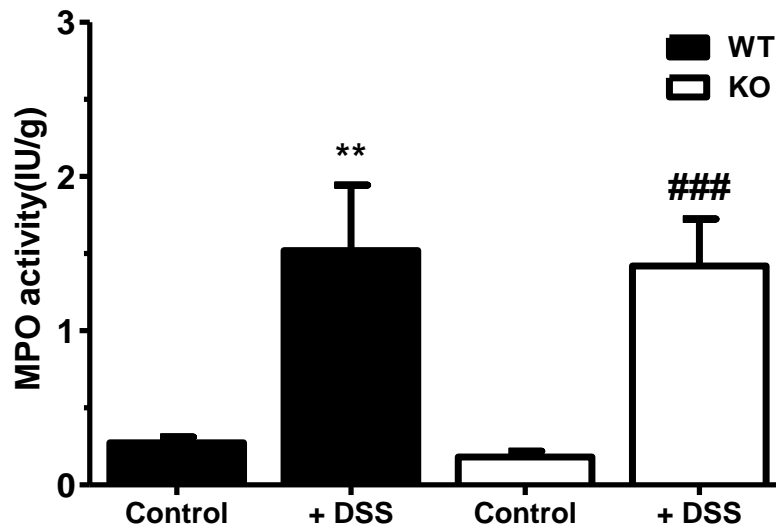


Figure A.3. The myeloperoxidase (MPO) activity after 3% DSS treatment for 8 days in wild-type mice and *Pept1* knockout mice (Mean \pm SE, n=5). Statistical analyses were performed by student's t-test (* denoted DSS vs. control of wild-type; # denoted DSS vs. control of *Pept1* knockout mice).

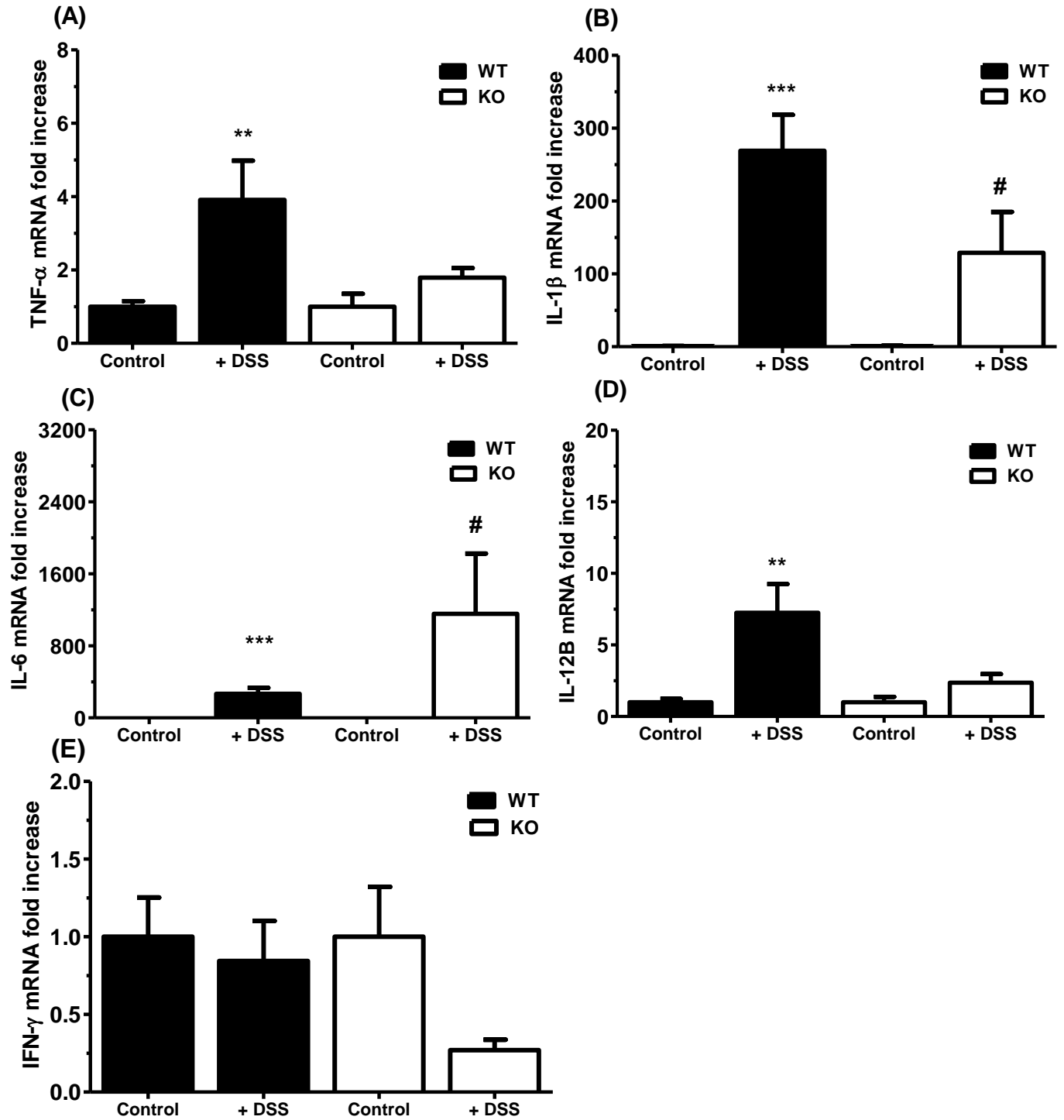


Figure A.4. mRNA expression of different cytokines in wild-type and *Pept1* knockout mice treated with 3% DSS for 8 days (Mean \pm SE, n=3-6). Statistical analyses were performed by student's t-test. (A) TNF- α , (B) IL-1 β , (C) IL-6, (D) IL-12B, (E) IFN- γ (* denoted DSS vs. control of wild-type; # denoted DSS vs. control of *Pept1* knockout mice).

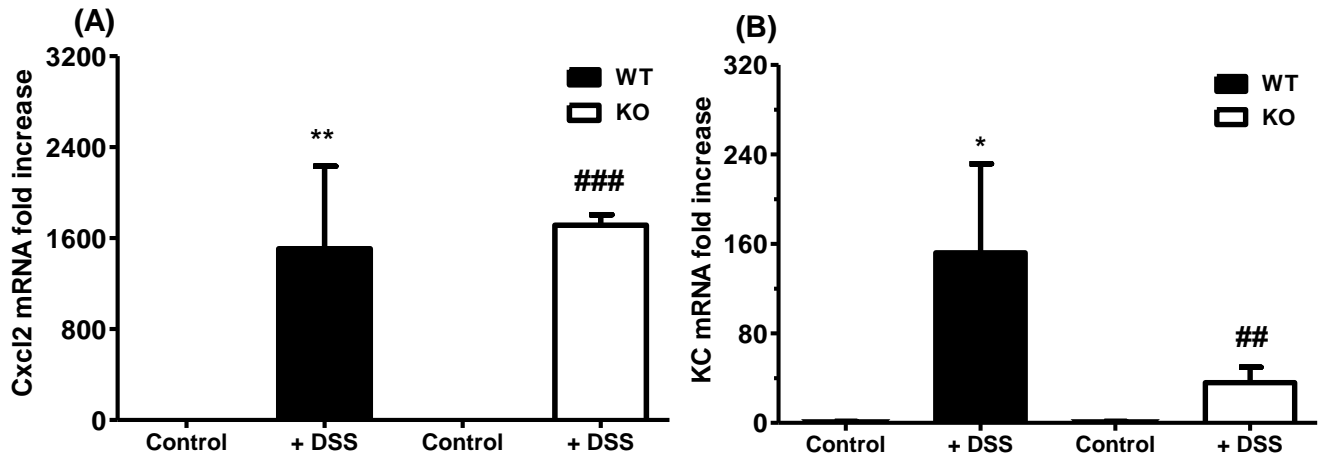


Figure A.5. mRNA expression of different chemokines between wild-type and *Pept1* knockout mice after treatment of 3% DSS for 8 days (Mean \pm SE, n=3-6). Statistical analyses were performed by student's t-test. (A) Cxcl2, (B) KC (* denoted DSS vs. control of wild-type; # denoted DSS vs. control of *Pept1* knockout mice).

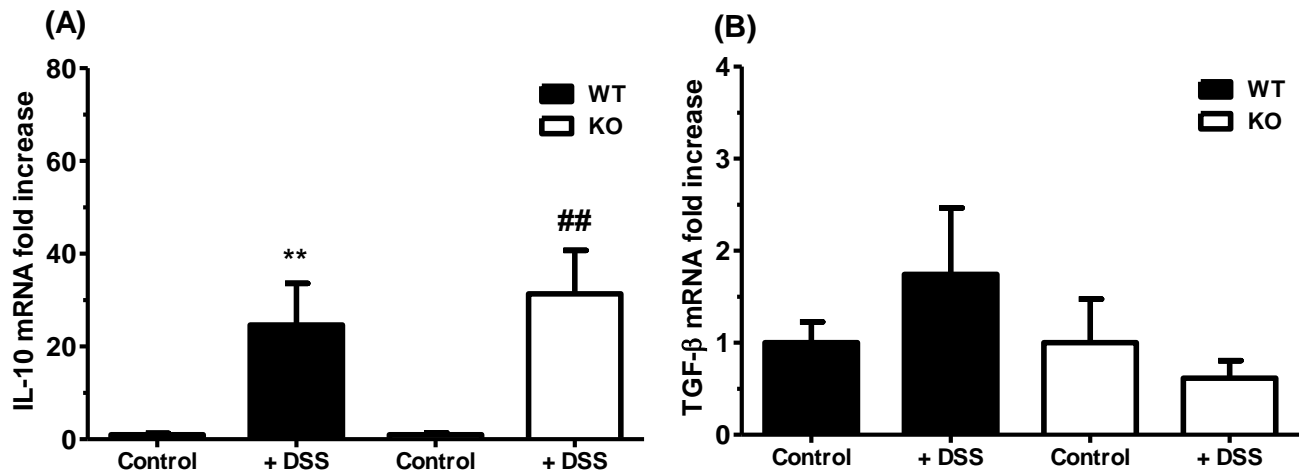


Figure A.6. mRNA expression of different anti-inflammatory cytokines between wild-type and *Pept1* knockout mice after treatment of 3% DSS for 8 days (Mean \pm SE, n=3-6). Statistical analyses were performed by student's t-test. (A) IL-10, (B) TGF- β (* denoted DSS vs. control of wild-type; # denoted DSS vs. control of *Pept1* knockout mice).

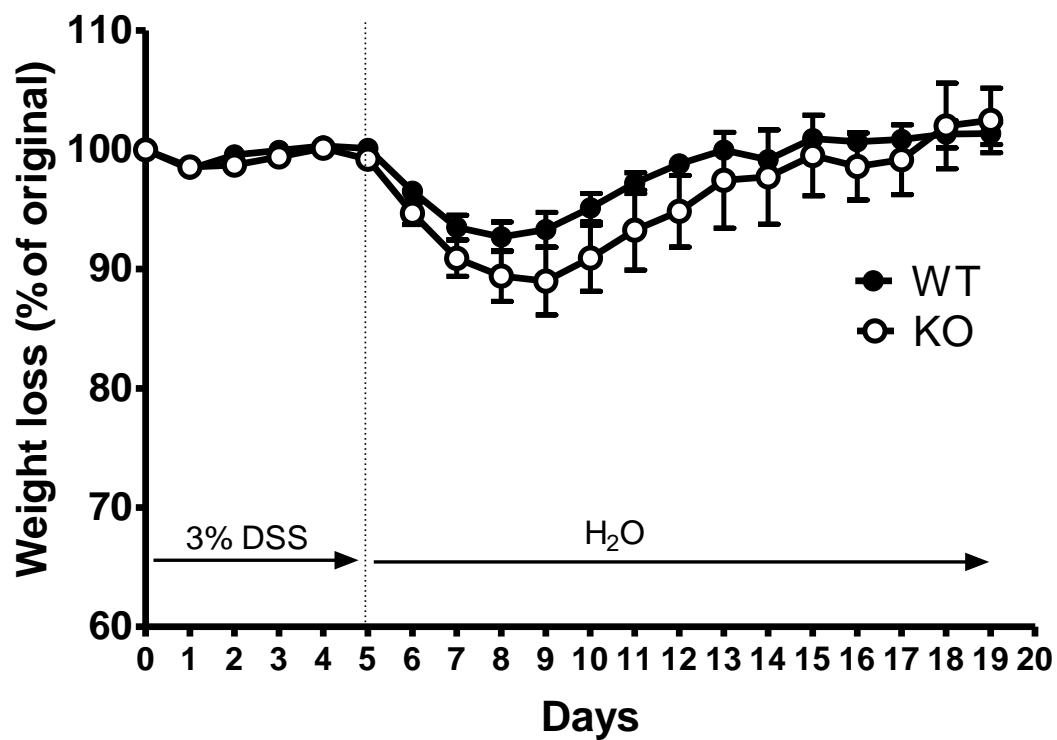


Figure A.7. Percentage of weight loss after 5-day 3% DSS treatment and recovered for 1 or 2 weeks in wild-type mice (solid circle: control, slide triangle: DSS) and *Pept1* knockout mice (open circle: control, open triangle: DSS) (Mean \pm SE, n=6-12 in each group).

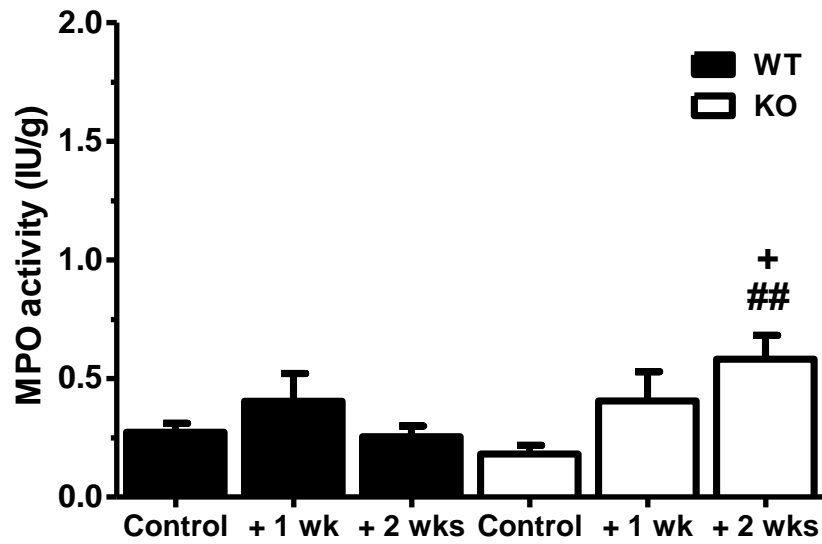


Figure A.8. The MPO activity of mice treated with 3% DSS for 5 days and recovered for 1 or 2 weeks (Mean \pm SE, n=5-6). Statistical analyses were performed by one-way ANOVA with Dunnett's comparison against each genotype control (# denoted DSS vs. control of *Pept1* knockout mice; + denoted DSS between genotypes).

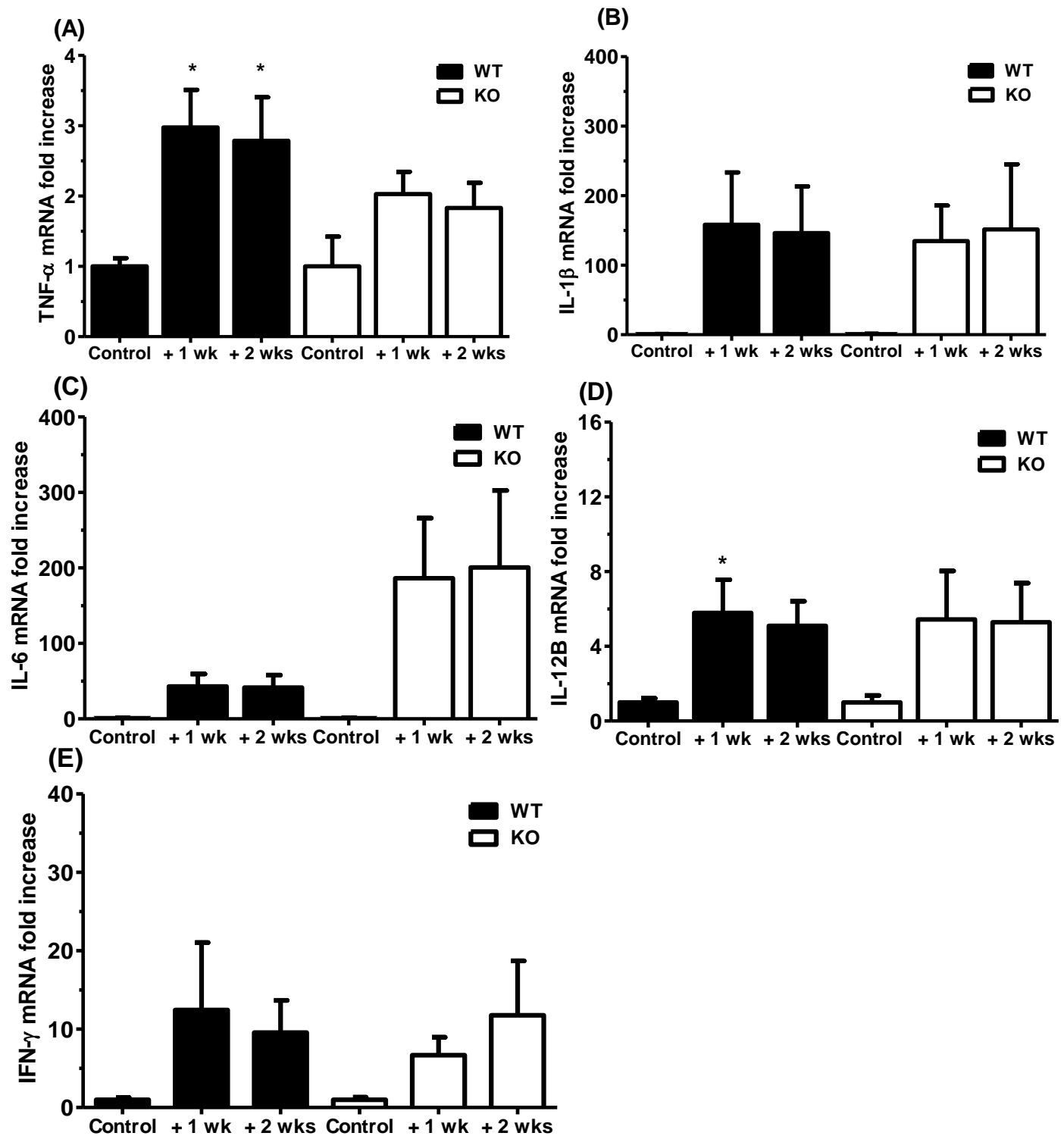


Figure A.9. mRNA expression of different cytokines in wild-type and *Pept1* knockout mice at the recovery phase after treated with 3% DSS for 5 days and recovered for 1 or 2 weeks (Mean \pm SE, n=6). Statistical analyses were performed by one-way ANOVA with Dunnett's comparison against each genotype control. (A) TNF- α , (B) IL-1 β , (C) IL-6, (D) IL-12B, (E) IFN- γ (* denoted DSS vs. control of wild-type mice).

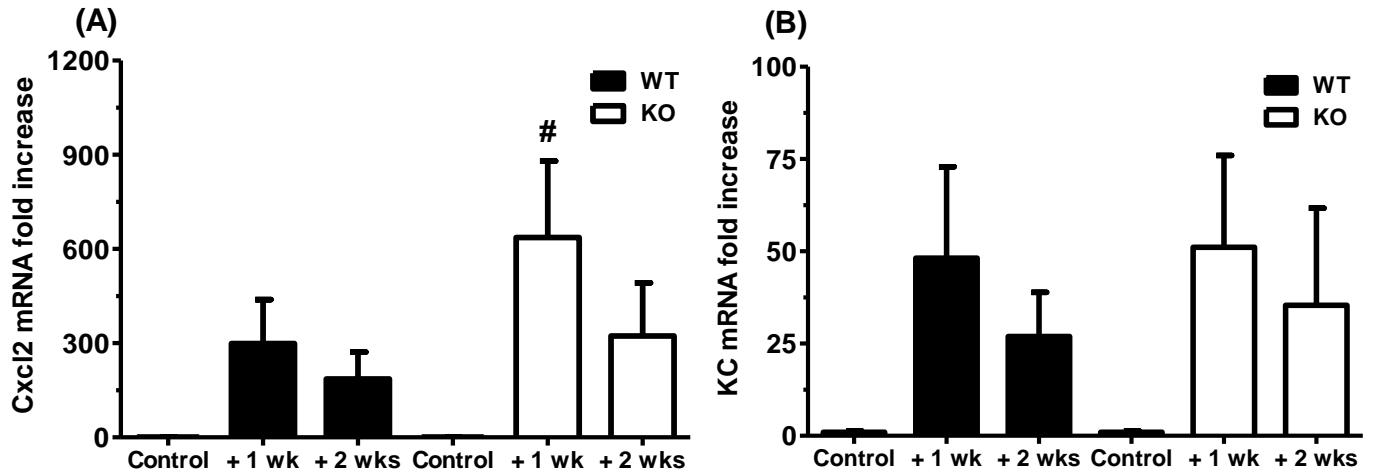


Figure A.10. mRNA expression of different chemokines in wild-type and *Pept1* knockout mice at the recovery phase after treated with 3% DSS for 5 days and recovered for 1 or 2 weeks (Mean \pm SE, n=6). Statistical analyses were performed by one-way ANOVA with Dunnett's comparison against each genotype control. (A) Cxcl2, (B) KC (# denoted DSS vs. control of *Pept1* knockout mice).

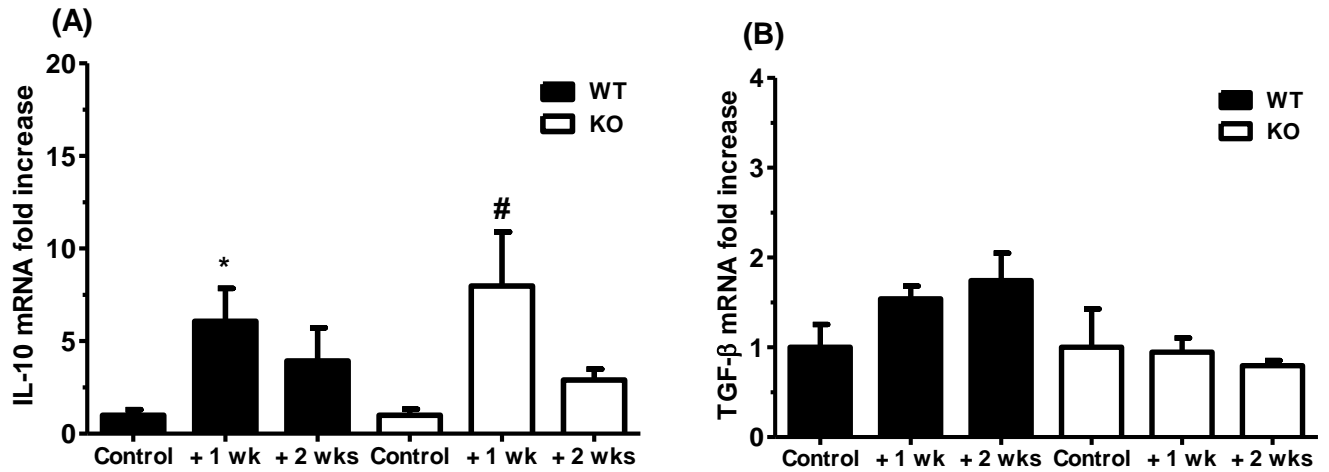


Figure A.11. mRNA expression of different anti-inflammatory cytokines in wild-type and *Pept1* knockout mice at the recovery phase after treated with 3% DSS for 5 days and recovered for 1 or 2 weeks (Mean \pm SE, n=6). Statistical analyses were performed by one-way ANOVA with Dunnett's comparison against each genotype control (A) IL-10, (B) TGF- β . (* denoted DSS vs. control of wild-type mice; # denoted DSS vs. control of *Pept1* knockout mice).

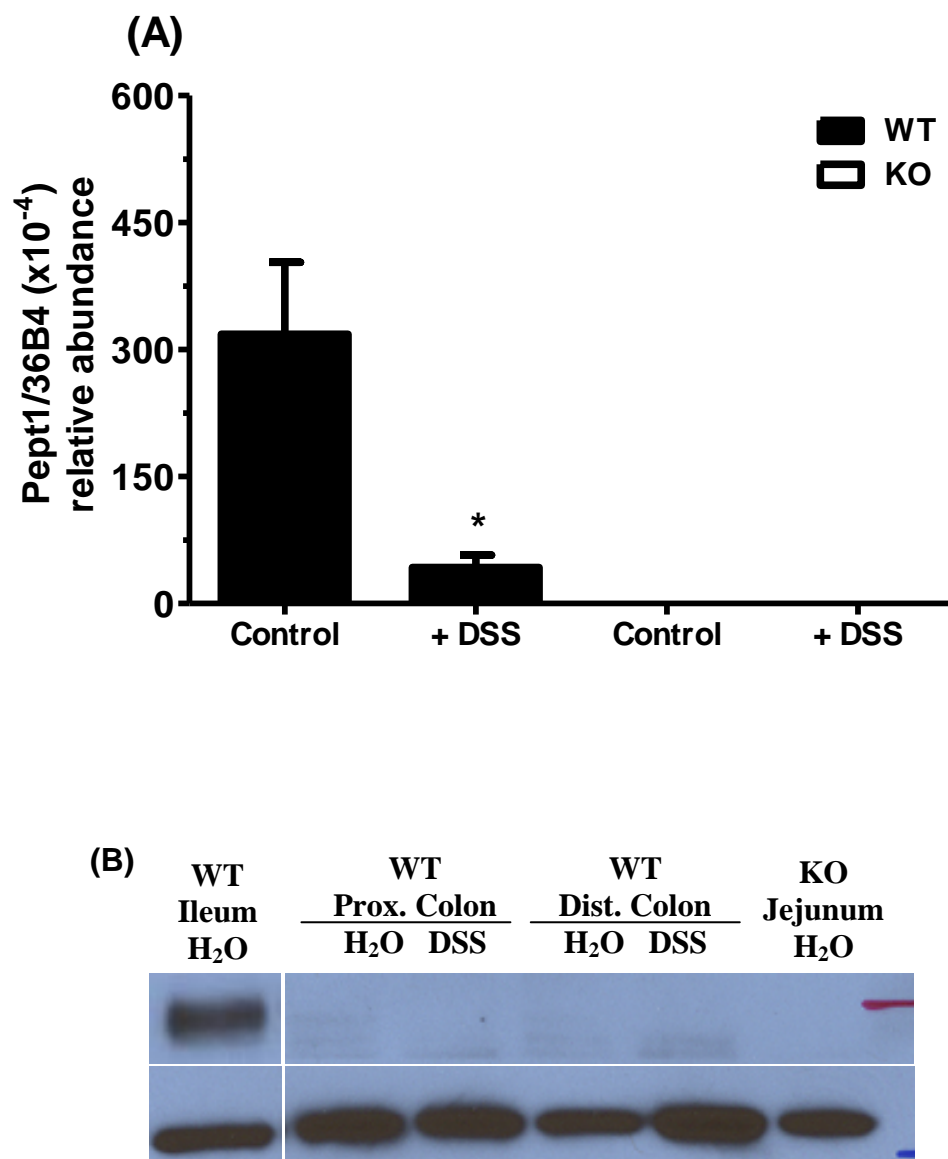


Figure A.12. PEPT1 expression in colon after 3% DSS treatment for 8 days. (A) mRNA expression showed decrease after 8 days DSS treatment (Mean \pm SE, n=3-6). Statistical analyses were performed by student's t-test. (B) PEPT1 protein expression showed no increase in either proximal or distal colon after 8 days DSS treatment.

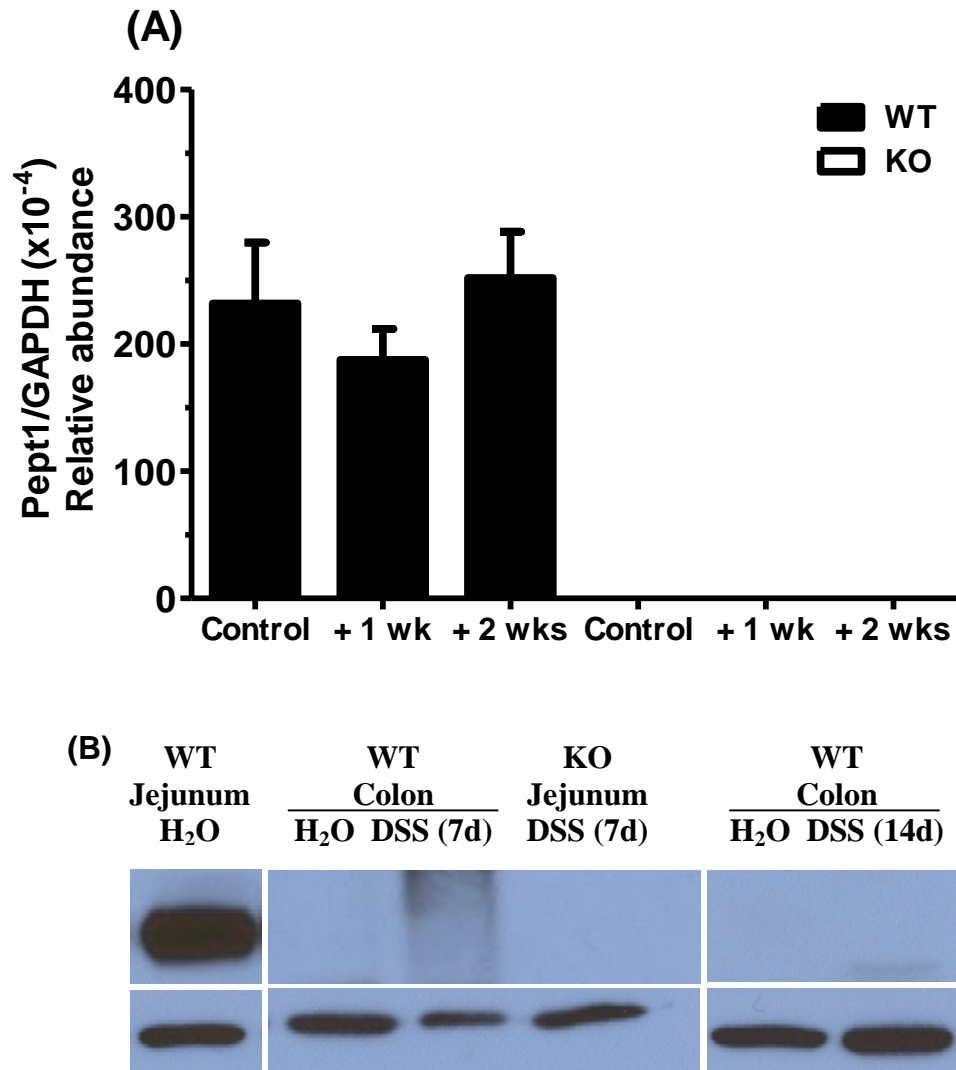


Figure A.13. PEPT1 expression in colon at the recovery phase after 3% DSS treatment for 5 days. (A) mRNA expression show slight decrease at 1 week recovery, but return to normal after 2 weeks of treatment (Mean \pm SE, n=6). (B) PEPT1 protein expression showed no up-regulation at 1 or 2 weeks recovery after treatment of 5 days DSS.

Score	Weight loss	Stool consistency	Occult/gross bleeding
0	None	Normal	Normal
1	1-5%		
2	5-10%	Loose stools	Hemoccult +
3	10-20%		
4	> 20%	Diarrhea	Gross bleeding

The Disease Activity Index (DAI) is the combined scores of weight loss, stool consistency, and bleeding divided by 3

Table A.1. The clinical criteria of scoring system for colitis progress (Adopted from Cooper HS et al., 1993).

Primers used for real-time PCR

Genes		Oligonucleotide sequences
36B4	sense	5'-TCC AGG CTT TGG GCA TCA-3'
36B4	antisense	5'-CTT TAT CAG CTG CAC ATC ACT CAG A-3'
GAPDH	sense	5'-GAG ACA GCC GCA TCT TCT TGT-3'
GAPDH	antisense	5'-CAC ACC GAC CTT CAC CAT TTT-3'
TNF- α	sense	5'-AGG CTG CCC CGA CTA CGT-3'
TNF- α	antisense	5'-GAC TTT CTC CTG GTA TGA GAT AGC AAA-3'
IL-1 β	sense	5'-TCG CTC AGG GTC ACA AGA AA-3'
IL-1 β	antisense	5'-CAT CAG AGG CAA GGA GGA AAA-3'
IL-6	sense	5'-ACA AGT CGG AGG CTT AAT TAC ACA-3'
IL-6	antisense	5'-TTG CCA TTG CAC AAC TCT TTT C-3'
IL-12B	sense	5'-GGA AGC ACG GCA GCA GAA TA-3'
IL-12B	antisense	5'-AAC TTG AGG GAG AAG TAG GAA TGG-3'
IFN- γ	sense	5'-CAG CAA CAG CAA GGC GAA A-3'
IFN- γ	antisense	5'-CTG GAC CTG TGG GTT GTT GAC-3'
IL-10	sense	5'-CAG CCG GGA AGA CAA TAA CTG-3'
IL-10	antisense	5'-CGC AGC TCT AGG AGC ATG TG-3'
TGF- β	sense	5'-GAG GTC ACC CGC GTG CTA-3'
TGF- β	antisense	5'-TGT GTG AGA TGT CTT TGG TTT TCT C-3'
CCL5	sense	5'-GCA GTC GTG TTT GTC ACT CGA A-3'
CCL5	antisense	5'-GAT GTA TTC TTG AAC CCA CTT CTT CTC-3'
KC	sense	5'-TTG TGC GAA AAG AAG TGC AG-3'
KC	antisense	5'-TAC AAA CAC AGC CTC CCA CA-3'

Table A.2. Primers for the real-time PCR analysis of cytokines and chemokines.

	WT + Water	WT + 3% DSS	KO + Water	KO + 3% DSS
Clinical signs				
Diarrhea	0/6	6/6	0/6	6/6
Bloody stools	0/6	6/6	0/6	6/6
Dead	0/6	0/6	0/6	0/6
MPO activity (IU/g; mean \pm SE)				
	**		**	
Colon	0.27 \pm 0.04	1.52 \pm 0.42	0.18 \pm 0.04	1.42 \pm 0.30
Jejunum	0.71 \pm 0.21	0.99 \pm 0.27	0.64 \pm 0.05	0.78 \pm 0.12

Table A.3. Clinical signs of DSS-induced colitis and MPO activity in wild-type and *Pept1* knockout mice at day 8 of DSS treatment (Mean \pm SE, n=6 in each group; Mean \pm SE, n=5 for MPO activity).

REFERENCES

Charrier L, Merlin D (2006). The oligopeptide transporter hPepT1: gateway to the innate immune response. *Lab Invest* **86**: 538-546.

Cooper HS, Murthy SN, Shah RS, Sedergran DJ (1993). Clinicopathologic study of dextran sulfate sodium experimental murine colitis. *Lab Invest* **69**: 238-249.

Radeva G, Buyse M, Hindlet P, Beaufils B, Walker F, Bado A, Farinotti R (2007). Regulation of the oligopeptide transporter, PEPT-1, in DSS-induced rat colitis. *Dig Dis Sci* **52**: 1653-1661.

APPENDIX B

UP-REGULATION OF COLONIC PEPT1 EXPRESSION BY OTHER ALTERNATIVE COLITIS MODELS

OBJECTIVE

In order to search for a better model for the study of impact of the aberrant colonic PEPT1 to intestinal inflammation, two alternative colitis models were studied, which were *Citrobacter rodentium* infection model and IL-10 knockout mice model.

MATERIALS AND METHODS

For *Citrobacter rodentium* infection model, around 6×10^{10} cfu/ 100 μ l bacteria was given to animal (FVB) by oral gavage and sterile LB was given for control animals. On day 10 of infection, the animals were scarified and small intestine and colon were collected for study. For the IL-10 knockout mice model, animals (C57BL/6) were housed under SPF environment until the age of 3⁺ months (14 weeks). Wild-type mice were used as control (12 weeks). No special diet restriction was applied. Animals were free to both food and water and colon of both wild-type and IL-10 knockout mice were collected for study.

RESULTS

***Citrobacter rodentium* Infection Model**

Although up-regulation has been shown by infection of *Citrobacter rodentium* in mice *ex vivo* and *in vivo* (Nguyen et al., 2009), similar result was not observed in current

study. No detectable expression of PEPT1 was observed after infection of *Citrobacter rodentium* for 10 days (Fig. B.1).

IL-10 knockout Mice Model

Comparing to wild-type mice, both mRNA (not reach statistical difference but the increase was apparent) and protein expression were increased in the colon of IL-10 knockout mice (Fig. B..2). This result was consistent with previous finding in IL-10 knockout mice in different strain of mice (129/SvEv), where the up-regulation of PEPT1 in the colon of IL-10 knockout mice was demonstrated (Chen *et al.*, 2010).

DISCUSSION

From appendix A, one potential reason for the lack of difference between wild-type and *Pept1* knockout mice was no enough ectopically expressed PEPT1 accumulated in colon. Two other alternative colitis models have been demonstrated to up-regulate colonic PEPT1 expression to the detectable level by western blot (Nguyen *et al.*, 2009; Chen *et al.*, 2010). Although there were some different experimental settings between current study and previous studies, such as the inoculation dose, the sampling time, the strain of animals, etc., the IL-10 knockout mice model showed consistent result as previously. The colonic PEPT1 expression clearly increased in both mRNA (not reach statistical significance) and protein. Therefore, IL-10 knockout would be a better model to use to study the impact of the aberrant colonic PEPT1 in the pathogenesis of intestinal inflammation or inflammatory bowel disease in the future.

FIGURES

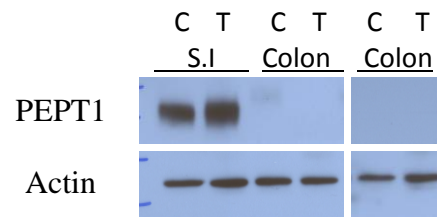


Figure B.1. The protein expression of PEPT1 after *Citrobacter rodentium* infection. (C: control, T: *Citrobacter rodentium* infection, SI: small intestine).

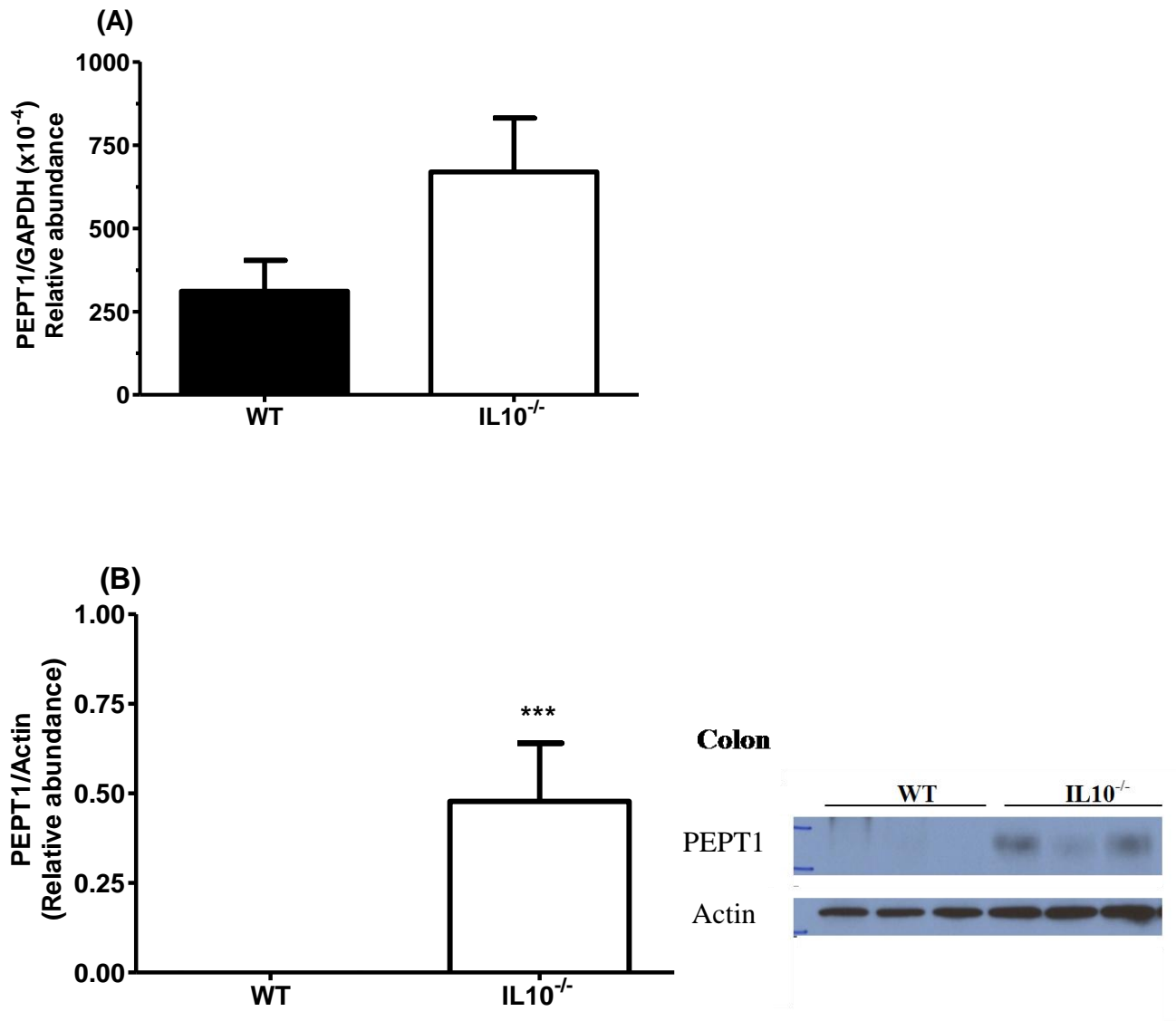


Figure B.2. PEPT1 expression in wild-type and IL-10 knockout mice. (A) mRNA expression showed increase but not reached statistical difference between genotypes (Mean \pm SE, n=3). (B) Protein expression showed significantly increase in IL-10 knockout mice as compared to wild-type mice (Mean \pm SE, n=3).

REFERENCES

- Chen HQ, Yang J, Zhang M, Zhou YK, Shen TY, Chu ZX, Hang XM, Jiang YQ, Qin HL (2010). Lactobacillus plantarum ameliorates colonic epithelial barrier dysfunction by modulating the apical junctional complex and PepT1 in IL-10 knockout mice. *Am J Physiol Gastrointest Liver Physiol* **299**: G1287-1297.
- Nguyen HT, Dalmasso G, Powell KR, Yan Y, Bhatt S, Kalman D, Sitaraman SV, Merlin D (2009). Pathogenic bacteria induce colonic PepT1 expression: an implication in host defense response. *Gastroenterology* **137**: 1435-1447 e1431-1432.